Fisheries New Zealand
Tini a Tangaroa

Genetic connectivity of deep-sea corals in the New Zealand region

New Zealand Aquatic Environment and Biodiversity Report No. 245

L.P. Holland,
A.A. Rowden,
J.Z. Hamilton,
M.R. Clark,
S.M. Chiswell,
J.P.A. Gardner

ISSN 1179-6480 (online)
ISBN 978-1-99-002598-3 (online)

September 2020

New Zealand Government

Requests for further copies should be directed to:

Publications Logistics Officer
Ministry for Primary Industries
PO Box 2526
WELLINGTON 6140

Email: brand@mpi.govt.nz
Telephone: 0800 00 83 33
Facsimile: 04-894 0300

This publication is also available on the Ministry for Primary Industries websites at:
http://www.mpi.govt.nz/news-and-resources/publications
http://fs.fish.govt.nz go to Document library/Research reports

TABLE OF CONTENTS

EXECUTIVE SUMMARY

Holland, L.P.; Rowden A.A.; Hamilton, J.Z.; Clark, M.R.; Chiswell, S.M.; Gardner, J.P.A. (2020). Genetic connectivity of deep-sea corals in the New Zealand region.

New Zealand Aquatic Environment and Biodiversity Report No. 245. **88 p.**

Deep-sea corals are diverse and abundant in the New Zealand region, where they represent indicator taxa for Vulnerable Marine Ecosystems (VMEs). VMEs, such as coral reefs, are at risk from fishing activity due to physical or functional vulnerability of their component habitats, communities or populations, and as such may require conservation and management measures.

In this project we assessed the connectivity of populations of two stony and two black coral species, which are VME indicator taxa in the New Zealand region. *Desmophyllum dianthus* is a cup coral, and *Enallopsammia. rostrata* is a matrix forming stony coral species, whereas *Bathypathes. patula* and *Leiopathes* spp. are black corals. Quantifying connectivity (i.e., gene flow) can contribute to an understanding of the interdependence and vulnerability of deep-sea coral populations, which can inform their management and protection. This study adds to research conducted under a wider study of VMEs in the South Pacific Ocean.

To assess connectivity and understand observed genetic patterns, we: 1) measured population structure and connectivity using genetic methods, 2) applied seascape genetics, and 3) used models of larval dispersal to test our estimates of genetic connectivity. We partitioned our samples into a geospatial analysis framework consistent with biogeographic provinces, regions and geomorphic features (e.g., seamounts) to assess connectivity at spatial scales commensurate with environmental drivers, and also relevant for management.

For *D. dianthus*, population differences did not occur at the geomorphic feature scales, but we did find genetic structure at the regional scale, with high connectivity between the Kermadec Ridge region and the Louisville Seamount Chain. Populations on the Chatham Rise showed little connectivity with those in other areas, and Chatham Rise may harbour unique genetic diversity. Overall, genetic diversity was highest in the Kermadec Ridge region. For the other three study species, population structuring was less pronounced and distant populations were genetically indistinguishable, except for Antarctic *B. patula* which had distinct populations north and south of the Antarctic Circumpolar Current.

Seascape genetics analyses indicated that population structure was related to certain environmental variables. For *D. dianthus*, indices of benthic topology (such as Benthic Position Index, aspects of slope) correlated with genetic data, suggesting that physical seafloor habitat characteristics are important delimiters of genetic boundaries for this species. Primary productivity, as well as topological characteristics, potentially influence the genetic structure of *E. rostrata* populations. These observations suggest that the patterns of genetic connectivity in each coral species may be explained by different environmental variables which may require species-specific consideration.

Overall, patterns of genetic connectivity were generally consistent with directional predictions of where larvae with different pelagic larval durations could be carried by ocean currents. However, dispersal models did not always predict the extent of connectivity between distant sites, and the models suggest that connectivity between distant sites was more likely to occur via shallow than deep water currents. Prevailing currents that converge on the Chatham Rise from both north and south are likely to explain the unique genetic diversity found there, and the relative isolation of stony coral populations on this feature. In the absence of genetic connectivity data, simulated larval dispersal could in some cases be a useful proxy to infer likely regional connectivity patterns of coral populations.

Preliminary exploration of spatial management options suggests that the current deep-sea spatial closures in the New Zealand region could be improved to better encompass the extent of the genetic diversity present in some deep-sea corals, and potentially sustain the extent of genetic connectivity among regions.

1. INTRODUCTION

1.1 The importance of connectivity and genetic diversity

Assessing population connectivity is one way to understand the extent of movement between geographically separated populations. For sessile species such as corals, this occurs primarily through the dispersal and recruitment of planktonic larvae (and not through adult movement). The concept of genetic connectivity describes the extent of the exchange of genes between populations (Palumbi 2003). The basic premise is that high levels of connectivity lead to genetically uniform populations across a species' range, and low levels of connectivity lead to genetically differentiated populations (which can also be described as weak versus strong genetic structure, respectively).

Because connectivity influences the exchange of genetic material, it also underpins biodiversity, which is governed by underlying genetic variation. High levels of biodiversity are important to facilitate adaptation to a changing environment and to maintain ecosystem function and resilience after disturbance (Hughes et al. 2008, Sgro et al. 2011, Underwood et al. 2009), whereas low genetic diversity is detrimental to the long-term survival likelihood of a population or species. This negative effect is because low diversity can be associated with a reduction in survival and growth rates, an increased extinction risk, and increased inbreeding allowing for the expression of deleterious mutations that would otherwise not be expressed (Reed & Frankham 2003, Bradshaw & Holzapfel 2008, Wright et al. 2008).

Maintaining high genetic diversity through connectivity can be especially important for vulnerable ("at risk") species. Such species (or populations) must be maintained at numbers sufficient to preserve current levels of genetic diversity whilst minimising extinction risks and mitigating threats to prevent further loss (Reed & Frankham 2003). Furthermore, a reduction of genetic diversity at local and regional scales may occur within a metapopulation (i.e., all populations of a species that exchange genes) if only a single sub-population is lost (Feral 2002). Therefore, determining the extent of genetic variation amongst populations and assessing genetic connectivity is important for predicting how they will fare in a changing environment, and to assist in developing management plans (e.g., Johannesson & Andre 2006, Zeng et al. 2017, 2019).

1.2 Assessing genetic connectivity and diversity

Genetic diversity can be quantified in several ways depending on the marker type in question. For DNA sequence data, this may include measuring the number of different haplotypes, or the number of different variable sites (DNA bases) within a DNA sequence. For co-dominant marker types such as microsatellites, this may include comparing the average number of genetic variants (alleles, that vary by DNA base pair composition and/or length) at a particular genetic location (locus; plural loci), measuring the total number of genotypes within a population (allelic and genotypic richness, respectively), or measuring the average proportion of loci that have two different alleles at a single locus within an individual (Hughes et al. 2008). The greater the number of haplotypes or alleles, the greater the genetic diversity. In summary, genetic diversity measurements offer a snapshot of population health and may identify populations that are vulnerable to stress as they may not have the genetic diversity necessary to cope with anthropogenic disturbances such as fishing-induced mortality or rapid climate change, or with natural (longer term) environmental change.

1.3 Inferring connectivity

The exchange of genetic material between many coral populations is mediated via the dispersal and subsequent recruitment of planktonic larvae. The extent of dispersal relates to species-specific reproductive traits such as the timing of reproduction, mode of larval production (e.g., internal vs. external fertilisation and development) and larval attributes (e.g., behaviour, feeding method) that determine how long larvae are in the water column. Reproductive traits are sometimes used as a proxy for connectivity, with the simple premise that the longer a larva's pelagic larval duration (PLD), the

further it may disperse from its natal population in local currents and the more likely it is that distant populations will be connected. As a generalisation across different phyla and different environments, this concept is helpful (Ross et al. 2009, Weersing & Toonen 2009, Gardner et al. 2010, Faurby & Barber 2012), but it is important to realise that the relationship between PLD and actual dispersal is both species-specific and location-specific, for reasons discussed below.

Generally, it is assumed that internally-fertilised directly-developing (brooded) and/or yolk-feeding larvae have shorter PLDs and limited dispersal, whereas gametes released from adults (broadcast spawners) that undergo external fertilisation and develop into plankton-feeding larvae have longer PLDs and greater dispersal. However, this assumption is over simplistic and has been repeatedly questioned; in reality, many factors determine the scale of larval dispersal in addition to, or instead of PLD (reviewed by Kinlan & Gaines 2003, Bradbury et al. 2008, Cowen & Sponaugle 2009). Isolation-by-distance (IBD) slopes (i.e., the correlation between geographic and genetic distances) can be useful in cases where dispersal occurs in a stepping-stone fashion and where ocean currents have uniform flow between sites (Selkoe & Toonen 2011), although correlations between PLD and gene flow may be confounded by inaccurate gene flow calculations (Faurby & Barber 2012) and/or by poor sampling design (Selkoe & Toonen 2011).

In the absence of genetic data, or when sampling is patchy, coupling reproductive attributes with physical variables in a hydrodynamic modelling (biophysical or larval dispersal modelling) or seascape genetics approach may also identify barriers to gene flow and infer the likely extent and routes of connectivity. This use of larval dispersal models, when linked to population genetic data provides a powerful approach to identifying connectivity routes (e.g., Crandall et al. 2012, Silva et al. 2019). In conjunction with other approaches, such as seascape genetics, larval dispersal models may make it possible to further refine and to better understand which factors contribute to the observed gene exchange between populations within or between regions. Seascape genetics as a discipline is reasonably young (Selkoe et al. 2008, 2016, Liggins et al. 2013, Riginos & Liggins 2013, Wei et al. 2013b) and is being increasingly applied to marine, mostly coastal, systems. Seascape genetics seeks to explain spatially explicit population genetic variation in terms of co-occurring spatially explicit variation in, for example, geomorphological features such as headlands or ridges or rises, or factors such as depth, or physico-chemical variation such as temperature, salinity, dissolved oxygen, pH, $CaCO_3$ saturation state, etc. Given the complexity of collecting spatially explicit environmental data for the deep sea, it is not surprising that deep-sea seascape genetics is very much still in its infancy (Zeng et al. 2020). However, this approach provides great promise for generating new insights into how and why genetic connectivity is reduced or enhanced in the deep sea.

1.4 Corals and Vulnerable Marine Ecosystems in the New Zealand region

Vulnerable Marine Ecosystems (VMEs) include groups of species, communities, or habitats that are vulnerable to damage caused by bottom fishing activity in areas beyond national jurisdiction (UNGA Resolutions 59/25 and 61/105). Coral reefs are one of the VMEs highlighted in the UNGA resolutions, and FAO report *International Guidelines for the Management of Deep-sea Fisheries in the High Seas* (FAO, 2009). VMEs are identified by the following criteria: the presence of unique or rare species, the functional significance of the habitat, the fragility of species or habitats, the life-history traits of species that impede recovery, and the structural complexity of the habitat (FAO 2009). Although VME is not a legally recognised term inside the New Zealand EEZ, the attributes that contribute to coral vulnerability apply equally across the EEZ boundary. Hence the VME terminology is used in this report.

VME indicator taxa possess characteristics that conform to the above listed criteria and are used to indicate the presence of a VME if caught as bycatch in fishing trawls or by longlines. In the South Pacific Ocean, coral VME indicator taxa include Scleractinia (stony corals), Antipatharia (black corals), Alcyonacea (soft corals), and Stylasteridae (hydro corals) (Parker et al. 2009). In the New Zealand Exclusive Economic Zone (EEZ), corals are widespread, with habitat for stony, black, and hydro corals predicted to occur on the continental slope, around the deep fringes of the Campbell Plateau, the

Kermadec Ridge region, the Norfolk Ridge, around the Bounty Trough and Macquarie Ridge, and the Chatham Rise (Anderson et al. 2016a). Seamount features (including knolls and hills) are also important habitat for stony corals (Tracey et al. 2011).

Areas predicted to contain corals are known to occur in all Fisheries Management Areas in New Zealand and coral abundance/diversity may coincide with fishing effort (Baird et al. 2013). The most intensive offshore trawling effort is on the Chatham Rise, on the edge of the Stewart-Snares shelf, south of the Auckland Islands, and off the west coast of the South Island (Ministry for Primary Industries 2016). Trawling for orange roughy, black cardinalfish, alfonsino, and oreos occurs primarily on seamounts. These species have been the target of deepwater fisheries in New Zealand for over 30 years, and up to 80% of known seamounts in the New Zealand EEZ have been fished by bottom trawling (Clark & O'Driscoll 2003, O'Driscoll & Clark 2005). Anderson & Clark (2003) documented very high levels of coral bycatch in the early years of a new orange roughy fishery south of Tasmania, which declined rapidly to small amounts within two years. In heavily fished areas, deep-sea coral reef habitats have been damaged, and show no sign of recovery (Althaus et al. 2009, Clark & Rowden 2009, Williams et al. 2010, Clark et al. 2019).

Within New Zealand's EEZ, corals are legally protected under the Wildlife Act (1953) and are protected spatially from trawling (along with other benthic fauna) by 17 seamount closure areas (encompassing 19 seamounts) and 17 Benthic Protection Areas (BPAs) (Brodie & Clark 2004, Helson et al. 2010). Trawling is prohibited within one hundred metres of the seabed in BPAs, whereas in seamount closure areas all trawling is prohibited. These spatial protection measures within the EEZ are monitored by Fisheries New Zealand. Internationally, implementation of protective measures for VMEs, such as fisheries closures, is undertaken by regional fisheries management organisations based on agreements amongst member states. Beyond New Zealand's EEZ in the South Pacific, VME management falls under the jurisdiction of the South Pacific Regional Fisheries Management Organisation (SPRFMO). Within the SPRFMO area, spatial closures that apply to New Zealand vessels have been implemented on an interim basis to afford specific protection to VMEs (Penney et al. 2009). The efficacy of closures within the EEZ and the SPRFMO area in protecting biodiversity, including VMEs, has been questioned (e.g., Leathwick et al. 2008, Penney & Guinotte 2013). Genetic diversity and population connectivity were not considered in determining the size and distribution of protected areas.

1.5 Research objectives

The extent of the genetic connectivity of deep-sea VME indicator taxa including corals is largely unknown, which impedes the design of protective measures that will most effectively ensure the long-term viability of geographically widespread but interdependent populations (Baco et al. 2016). For the New Zealand EEZ, and the surrounding SPRFMO area, there are on-going efforts to improve spatial management protection measures for benthic communities including VMEs (e.g., Benthic Protection Areas, Helson et al. 2010) and genetic connectivity is a key consideration for marine spatial management design (Boschen et al. 2016). Improved understanding of genetic connectivity within and amongst populations, the identification of source (from where larvae originate) and sink (to where larvae disperse) populations, and genetic diversity hotspots may therefore contribute to improved spatial management in in New Zealand's EEZ, and potentially in the SPRFMO area. Theoretical optimisation of the design of spatial management should include populations that are either net sources of individuals to other areas or are genetically isolated (Zeng et al. 2017).

Science Objectives

The primary objective of this research was to determine the genetic connectivity of deep-sea coral taxa in the New Zealand EEZ and wider South Pacific, and to quantify the factors that influence connectivity between populations in the region.

We undertook the following to achieve this objective:

1. Assessed the genetic variation of selected coral VME indicator taxa using microsatellite markers and/or DNA sequencing techniques.
2. Determined the extent of genetic connectivity among coral populations within and beyond New Zealand's EEZ.
3. Used seascape genetics and larval dispersal models in combination with genetic data to better understand observed population structure and to test hypotheses about contemporary routes of larval migration.

This study adds to research conducted under a wider study of VMEs in the South Pacific, which has assessed the genetic connectivity of other VME indicator taxa (Zeng et al. 2017, 2019, 2020).

2. STUDY SPECIES

2.1 Selection of study species

Four species were initially selected for this study; two species of scleractinian (stony) coral, *Desmophyllum dianthus* and *Enallopsammia rostrata*, and two species of antipatharian (black) coral, *Bathypathes patula* and *Leiopathes secunda*. These species were chosen because samples held in the NIWA Invertebrate Collection (NIC) were from widely dispersed locations within and beyond the New Zealand EEZ (Figure 1 and Figure 2), they had been identified to species level, they had been preserved in such a way that allowed optimal DNA yield, and they were not being used for any other similar studies by other scientists. Sample numbers for *L. secunda*, however, proved to be quite low, so we adopted a genus-level approach for this black coral, by adding samples of other *Leiopathes* species from the NIC into the *L. secunda* dataset.

2.2. Characteristics of the deep-sea corals studied

Stony corals

Desmophyllum dianthus (Esper, 1794) is a solitary cup coral that typically occurs in the upper bathyal zone with a depth range spanning 200–2500 m (Addamo et al. 2012). *D. dianthus* is one of only four scleractinian species to occur on seamounts in three oceans (Rogers et al. 2007) and it can form close associations with other bathyal fauna including reef-building corals such as *Lophelia pertusa* and *Madrepora oculata* in the North Atlantic (e.g., Reveillaud et al. 2008), and thus contribute to the formation of deep-sea coral reefs. It is therefore considered a secondary reef-constructing species (Cairns 1982, Rogers et al. 2007). *Desmophyllum dianthus* is a slow-growing coral (0.5–2 mm y^{-1}) with a lifespan of up to 200 years (Addamo et al. 2012 and references therein) and, like other cold-water corals, food supply may restrict or limit its growth at depth (Rogers et al. 2007). In New Zealand's EEZ, *D. dianthus* is prevalent on seamounts, where it may form associations with other scleractinians such as *Enallopsammia rostrata*, *Goniocorella dumosa*, and *Solenosmilia variabilis*, and where it often clusters near to or at the base of hydrocoral species (Figure 3).

Enallopsammia rostrata (Pourtalès, 1878), is one of the four dominant reef-building corals in New Zealand waters. It occurs in a depth range of about 200 to 2150 m and is found on seamounts, slopes and ridges (Tracey et al. 2011). This species also occurs in the North Atlantic Ocean and Mediterranean Sea. *Enallopsammia rostrata* has a faster extension rate than *D. dianthus* but still grows slowly at

5 mm y^{-1} and has a lifespan of over 100 years (derived from an Atlantic specimen, Adkins et al. 2004). In addition to sexual reproduction, *E. rostrata* can grow through extra-tentacular budding (Cairns 1995) (Figure 3).

Black corals

Bathypathes patula Brook, 1889 is one of at least four species of this black coral genus to have been recorded in the New Zealand region, *B. patula*, the type species for the genus, is cosmopolitan and around New Zealand is found within the EEZ and beyond, including Antarctica. This species has one of the deepest known occurrences for black corals, at 8600 m in the northwest Pacific Ocean (Wagner et al. 2012) (Figure 3).

Leiopathes secunda Opresko, 1998 is one of three species of the family Leiopathidae (the others being *L. acanthophora* and *L. bullosa*) found in the New Zealand region and off Australia. None of these species is found in the Atlantic Ocean and they are (as yet) unrecorded from the Antarctic region. *Leiopathes* sp. colonies can be extremely long-lived; some Hawai'ian specimens have been radiocarbon dated at over 4000 years old (Roark et al. 2009). To maximise sample sizes, we included individuals with reliable taxonomic identifications of the three species described above, as well as some unidentified *Leiopathes* specimens (Figure 3).

2.3. Life-history traits of the study species

Little is known about the reproductive life-history strategies employed by the stony corals in this study (*D. dianthus* and *E. rostrata*), although it is thought that, like most cold-water corals, they are probably single-sexed broadcast-spawning corals that produce yolk-feeding (rather than plankton-feeding) larvae. Broadcast spawning appears to be a more common strategy in deep-sea corals studied thus far than brooding (whereby larvae develop internally within a coral polyp, Waller et al. 2002, Waller 2005, Waller & Tyler 2005, Rogers et al. 2007, Waller & Baco-Taylor 2007). Evidence for single-sexed colonies has been observed in shallow water *D. dianthus* colonies in the Patagonian fjords (Feehan 2016). In *E. rostrata*, the large size of oocytes suggests the likely production of lecithotrophic larvae (Rogers et al. 2007 and references therein). Deep-sea coral fecundity is highly variable and is undocumented for our study species, apart from *E. rostrata*, for which it appears to be low (Burgess & Babcock 2005). The timing of reproduction for the study species around New Zealand is unknown, apart from for *E. rostrata*. For this species, fertilisation is thought to occur in April or May around New Zealand, with overlapping cohorts of oocytes (Burgess & Babcock 2005). In contrast, *E. rostrata* found off Brazil appears to have continuous reproduction (Pires et al. 2014).

Even less is known about reproduction in the black corals *Bathypathes patula* and *Leiopathes secunda*, but indications are that they are also primarily gonochoric (i.e., separate male and female colonies, Wagner et al. 2011). Observations on sexually produced larvae from shallow water species have demonstrated that they can be lecithotrophic (yolk feeding), negatively buoyant and phototactic (i.e., they sink and move away from light) and that they swim poorly, which could lead to restricted dispersal (Brugler et al. 2013 and references therein). It is reported that *B. patula* is likely to be gonochoric (Wagner et al. 2011).

3. METHODS

Detailed laboratory and analytical methods, including details of relevant software and analysis settings, are given in Appendix 2. Here an abbreviated methodology is given.

3.1 Samples

Samples were obtained from material archived in the NIC, and for *D. dianthus* and *E. rostrata* additional samples were collected during research voyages to the Louisville Seamount Chain in March 2014 (Clark et al. 2015a) and to the Chatham Rise in March 2015 (Clark et al. 2015b). Only samples from which we obtained reliable data are included in this report (Figures 1 and 2, Appendix 1).

Some *D. dianthus* and *B. patula* samples originated from outside the EEZ (the Louisville Seamount Chain and the Southern Ocean, respectively), whereas *E. rostrata* and *Leiopathes* spp. were from within the EEZ only, with the latter samples restricted to areas around the North Island, following its New Zealand region distribution (Opresko et al. 2014). For *D. dianthus* and *E. rostrata*, sampling was heavily biased towards the Chatham Rise, which is likely to reflect a higher overall sampling effort there rather than increased occurrence.

3.2 Choice of molecular markers

To maximise efficiency, we decided to use pre-existing genetic resources rather than spend time and costs developing new techniques. We therefore used DNA sequence and microsatellite primers already published in related studies.

3.3 Laboratory-based molecular methods used

DNA sequencing and microsatellite amplification

Following DNA extraction, DNA was sequenced from *D. dianthus*, *E. rostrata*, and *B. patula* (but not *Leiopathes* spp.). Microsatellites were obtained for *D. dianthus* and *Leiopathes* spp.

We sequenced and tested several genes (Table 1) but ultimately used the nuclear internal transcribed spacer, or ITS, regions for *D. dianthus* and *E. rostrata*, and mitochondrial 16S, and mitochondrial ND5 and TRP intergenic regions for *B. patula*. We obtained reasonably good ITS data (i.e., successful and reliable reads) for *D. dianthus* and *E. rostrata*. For *D. dianthus*, we obtained ITS data for approximately 150 individuals prior to microsatellite primers becoming available to us part way through our study. Therefore, for *D. dianthus*, we had two datasets, with the ITS DNA sequence dataset being about half of the size of the microsatellite dataset and obtained from different individuals in the same areas. Following microsatellite optimisation, we had 9 usable loci (i.e., unique genetic markers) for *D. dianthus*. These microsatellites did not work for *E. rostrata*; therefore, only ITS data were available for this species (Table 1).

For the black corals, we used eight microsatellites for *L. secunda*, but they did not work for *B. patula*. We therefore used DNA sequence data alone for *B. patula* (16S, ND5, and TRP).

3.4 Validating microsatellite markers

For *D. dianthus*, we tested the quality and reliability of the microsatellites as a tool in several ways. Firstly, we assessed deviation from Hardy-Weinberg Equilibrium (HWE), a genetic model in which frequencies of genetic variants, or alleles, will remain constant between generations in the absence of other evolutionary influences such as migration, mutation, or selection. Deviations from HWE can indicate that genetic markers are susceptible to genotyping error. Loci showing evidence of poor amplification during the polymerase chain reaction (PCR) amplification process (null alleles) were discarded, as were microsatellites with more than 60 alleles per locus, because highly variable loci (i.e., many fragments of different sizes obtained from the same genetic location) may cause spurious results (specifically, downward biases in fixation indices (F_{ST}) estimates, Olsen et al. 2004, O'Reilly et al. 2004). Fixation indices are used to measure the extent of genetic structure based upon variation in allele

frequencies between populations; so low values would potentially falsely indicate little genetic difference.

Next, we tested for linkage disequilibrium (LD), which determines whether patterns of allele frequencies observed could be due to two or more alleles not being inherited independently, which could also cause spurious results. No loci were discarded based on LD. We then tested the neutrality of the loci, to make sure that they were not under evolutionary selection (which can violate some statistical assumptions in downstream tests). Based upon these results, the *D. dianthus* dataset was split into a 'neutral' dataset (5 loci) and an 'all loci' dataset (9 loci), meaning that some analyses were carried out twice, to determine to what extent the connectivity patterns we observed were a function of the markers considered. Generally, because results were similar between the two, only the all loci dataset results are reported (significant differences are indicated).

For *Leiopathes* spp., microsatellite amplification was successful in a total of only 53 individuals. Further validation testing was not continued further.

3.5 Spatial division of samples

Prior to genetic analyses, we divided samples at three levels according to their collection location. This division scheme reflects spatial scales relevant to marine spatial planners, allows us to address the effect of various environmental features on connectivity, and allows comparisons with complementary research (Zeng et al. 2017). The three levels were; firstly, the lower-bathyal biogeographic provinces (henceforth provinces) identified by Watling et al. (2013), with samples assigned to BY6 (New Zealand-Kermadec, including the Chatham Rise and the Louisville Seamount Chain), BY10 (sub-Antarctic), and in the case of *B. patula*, BY9 (Antarctic); henceforth 'northern', 'southern' or 'Antarctic' provinces. These provinces represent environmental conditions that could influence the distribution of species and populations. Secondly, a regional division to recognise the currents and fronts associated with the Chatham Rise, and which could act as barriers to larval dispersal and/or result in mixing of populations; 'North' (north of the Chatham Rise), 'Central' (the Chatham Rise) and 'South' (south of the Chatham Rise) with boundaries at latitudes 42° S and 45° S. Finally, samples were assigned to geomorphic features that comprise parts of the seascape of the New Zealand region, and which can possess particular bathymetrically-forced hydrographic conditions that can influence larval dispersal (Appendix 1).

Following Zeng et al. (2017) we defined a 'population' as a minimum of four individuals from the same site or from sites within close proximity. The dispersed distribution of *B. patula* samples meant that this stipulation could not be met under any scheme except the provincial level, so the data were analysed as northern, (including the Chatham Rise), southern (Campbell Plateau, Macquarie Ridge, Tasmania) and Antarctic (south of mainland New Zealand but north of the Ross Sea) provincial scales, as outlined above. For the *Leiopathes* dataset, microsatellite amplification was successful for only 53 individuals, which comprised a mix of *L. secunda, L. bullosa* and some specimens identified only to genus level. *Leiopathes* specimens were collected from waters around the North Island only, so analyses of these populations were based on geomorphic features only. To meet the population size threshold of four individuals after assigning samples to a geomorphic feature, the dataset was further reduced to 46 individuals when all *Leiopathes* species were combined, and 28 individuals when considering *L. secunda* alone.

3.6 Population genetic analyses

The *D. dianthus* microsatellite and ITS datasets were by far the largest numerically. Analyses conducted are therefore more comprehensive for this species. The following section always refers to *D. dianthus*, and to the other three species only where indicated.

3.6.1 Population differentiation

Analysis of Molecular Variance (AMOVA, Arlequin v3.5, Excoffier & Lischer 2010) was used to test for population differences associated with each spatial scale (province, region, geomorphic feature) and the p-values (significance levels) were obtained for the neutral and all loci microsatellite datasets, and from the ITS sequence data. Subsequently, to assess the extent of population differentiation between/amongst populations within this scheme, we calculated conventional pairwise F_{ST} values for microsatellites (Wright 1951, Weir & Cockerham 1984) and its analogue, Φ_{ST}, for ITS sequence data. These F_{ST} values are estimates of genetic distance and they vary between zero and one, with zero signifying no differentiation and one representing completely disparate populations (Balloux & Lugon-Moulin 2002).

Φ_{ST} was calculated from ITS DNA sequence data for *E. rostrata* and from concatenated 16S-ND5-TRP DNA sequence data respectively, whereas *Leiopathes* data were derived from microsatellites (and therefore F_{ST} was calculated). In the case of *E. rostrata*, the patchy distribution of samples resulted in difficulty meeting the minimum population size threshold of four individuals, so to permit analysis of data from this species minimum population sizes less than 4 have been used on some occasions (e.g., three geomorphic features were represented by only two individuals; the Kermadec Ridge region, the Norfolk Ridge, and the Challenger Plateau). Therefore, a very cautious interpretation of these data is warranted at the geomorphic features scale.

3.6.2 Genetic diversity

We used allelic richness (the average number of alleles at a given locus) as a measure of genetic diversity for microsatellite data, and nucleotide and haplotypic diversity (the average number of nucleotide differences per site between any two sequences and the probability that two randomly chosen haplotypes are different, respectively) from the DNA sequence data. Rarefied allelic richness (which accounts for different sample sizes) and private allelic richness (the number of unique alleles in a population, Kalinowski 2004) were also calculated.

3.6.3 Identifying genetic clusters

Discriminant analysis of principle components (DAPC) was performed to identify population clusters based on microsatellite variation. This multivariate analysis first partitions sample variance into between-group and within-group components based upon an initial principal component analysis (PCA), after which a discriminant analysis (DA) identifies clusters using the PCA factors as variables to maximise the intergroup component of variation, making no assumptions about the evolutionary structure of the samples.

To identify clusters at spatial levels deemed significant in AMOVA analyses, microsatellite data were tested using STRUCTURE, a model-based Bayesian clustering approach in which individuals are probabilistically assigned to a known or unknown population (K) based upon shared allele frequencies. Reliability of each model run was verified after which optimal K values from all simulations were derived. STRUCTURE assumes HWE, but not LD, and works best when population sample sizes are similar. Adjustment for different population sample sizes is possible (Wang 2017), and has been employed here, where appropriate. For comparison, cluster analyses were also performed using a non-parametric approach without any prior assumptions about HWE or LD.

3.6.4 Inferring demographic population changes

We used several approaches to test for population growth. We compared observed vs. expected sequence distributions of ITS sequence data (the mismatch distribution) under both constant population size (at equilibrium) and growing/declining population models. We used the Ramos-Onsins and Rozas R2 test, which detects recent pronounced population growth, and examined the raggedness statistic r

(Harpending 1994), which relates to the shape of the mismatch distribution and differs between constant size and growing populations.

The neutral microsatellite dataset was used to test for evidence of genetic bottlenecks (a drastic reduction in population size which can adversely affect genetic diversity, and potentially, the genetic resilience of a population). Samples from the Campbell Plateau and Macquarie Ridge were not analysed in the geomorphic features dataset because the program requires at least 10 individuals per population. Finally, the relative distribution of allele frequencies (mode-shift indicator) was tested, because a reduction in alleles occurring at low frequencies distorts allele frequency distributions in recently bottlenecked populations (Luikart et al. 1998).

3.6.5 Assessing contemporary and historical connectivity, and effective population size

We used two approaches to determine the extent and direction of gene flow between populations associated with geomorphic features, using the *D. dianthus* microsatellite neutral (n=5) and all loci (n=9) datasets. We focussed on these datasets only, due to higher sample sizes obtained from each geomorphic feature, and to explore the temporal and directional patterns of migration between the Kermadec Ridge region and the Louisville Seamount Chain indicated in prior analyses (AMOVA results revealed no significant difference at the province and/or at the regional spatial scales, therefore these spatial scales were not tested in the analyses described below). We used two Bayesian approaches to assess historical and contemporary (i.e., over the last few generations) gene flow. We also estimated contemporary effective population sizes (i.e., numbers of individuals contributing genetic material to subsequent generations, with estimates applying to the time-period encompassed by the sampling period, *Ne*) at the regional and geomorphic features scales (but not at the province scale because the AMOVA was statistically insignificant). Parametric confidence intervals were estimated.

3.7 Seascape genetics

To determine the effect of environmental factors (Table 2) on genetic differentiation, we examined correlations between environmental variables at sample sites and F_{ST} (for *D. dianthus*) and Φ_{ST} (for *E. rostrata*). The spatial testing framework was not used for seascape analyses, primarily because the geographic extent of sampling at province and regional scales was larger than the scale of differences between environmental variables (i.e., a wide range of variables applied to areas within the bounds of each province or region, and thus choosing one set over another could lead to confounding results). Instead, samples were assigned to a population if collected from the same site or from sites in close proximity, with a minimum sample size set at four individuals, samples were not pooled as before. Seascape genetics analyses focussed on the stony corals only, due to inadequate sample distribution for the black corals. For *D. dianthus*, twenty putative (i.e., hypothetical) populations were obtained across the sampled range (i.e., from the EEZ to the Louisville Seamount Chain, Appendix 3). For *E. rostrata*, only four putative populations met the minimum sample size threshold and these were all on the Chatham Rise, although each had different environmental variable values (see Table 2 and Appendix 3 for environmental variables for each dataset).

We used a generalised linear model (GLM) to assess associations between the mean multilocus F_{ST} or Φ_{ST} for each population and a combined set of biological, topographical and physicochemical environmental variables (Appendix 3).

3.8 Larval dispersal models

To compare genetic connectivity patterns revealed by the genetic analyses, and to better understand the environmental factors potentially contributing to the patterns revealed by the seascape genetics analyses, we predicted likely larval dispersal routes using oceanographic current modelling. Predicting potential routes of larval movement on a site-by-site basis is a useful approach to determine potential connectivity pathways between or amongst specific regions or geomorphic features. We modelled float

trajectories from the Global Drifter Program (GDP) (http://www.aoml.noaa.gov/phod/dac/gdp_information.php) and from the ARGO program (http://www.argo.ucsd.edu/), to predict (respectively) potential larval dispersal distances via surface and deep (1000 m) currents, for a range of hypothetical PLDs specified for 'virtual' larvae. In this approach, coral larvae are treated as passive particles for dispersal, with no ability to influence the direction or rate of dispersal. We initially used seven PLD periods between 0 and 70 days (in ten-day increments), but after preliminary runs, we changed this to four PLD periods of 0–10 days, 30–40 days, 90–100 days and 150–200 days, given the high connectivity observed in our preliminary genetic data and the possibility that stony coral larvae may survive for as long as 195 – 244 days (Graham et al. 2008).

4. RESULTS

4.1 Molecular marker utility

The microsatellite markers used in this study for *D. dianthus* were developed for the confamilial *S. variabilis* by Zeng (2016) and by Miller & Gunasekera (2017). These microsatellites amplified successfully in *D. dianthus*, supporting observations that microsatellites can cross-amplify within families of scleractinians (Addamo et al. 2015) and octocorals (Holland et al. 2013). Conserved microsatellite flanking regions are therefore thought to reflect slowly evolving coral nuclear genomes (e.g., Shearer et al. 2002).

We found evidence of selection at four of nine loci, and subsequently split our dataset accordingly to test patterns of connectivity with (all 9 loci) and without (5 neutral loci) putatively selected loci. We found generally concordant results for both datasets (refer to separate sections below and individual tables and figures); hierarchical AMOVA tests suggested that genetic information was partitioned at both regional and geomorphic features scales (but not at the province scale), F_{ST} analyses with both datasets indicated divergence between populations of the Chatham Rise and all other areas in the geomorphic features data, and BayesAss-derived contemporary gene flow estimates were almost identical between the two datasets. Differences between the two datasets were apparent in the regional scale analysis of F_{ST} values, where the North and South regions were divergent for all loci but not for neutral loci. Because we had general agreement in results for both datasets, we retained all loci in subsequent clustering analyses (e.g., STRUCTURE and DAPC). A further reason for retaining all loci in subsequent analyses is that there is some evidence that populations undergoing range expansions (of which we found evidence, see below) may show false positive outliers in neutrality tests (Lotterhos & Whitlock 2014). There is also increased recognition of the value of using both selected and neutral loci, whether microsatellites or not, in inferring genetic connectivity (Johannesson & Andre 2006). Non-neutral loci may reveal signatures of genetic structure otherwise hidden in large effective populations where the effect of genetic drift is weak and where populations appear to be homogeneous despite little migration (Wei et al. 2013a, Gagnaire et al. 2015, Zeng et al. 2017), which could also be the case here for *D. dianthus*.

During the course of this research, 24 novel loci not used in this study were characterised in *D. dianthus* via next-generation sequencing (Addamo et al. 2015). Due to their high amplification success rate in other coral genera, these novel loci should provide a useful resource for connectivity studies of deep-sea corals. However, it is noteworthy that in our study, the genotypic diversity encompassed within our relatively large dataset was recoverable with 6 loci, suggesting that the addition of more microsatellite loci would not necessarily have increased the resolution of our dataset (Appendix 3).

4.2 Genetic diversity

Desmophyllum dianthus
Analysis of the ITS data indicated high genetic diversity for populations of the Kermadec Ridge region (Table 3), which had high nucleotide and haplotype diversity, although the highest values for these metrics were for populations in the South region and from the Campbell Plateau. Although it is worth noting that π and *h* calculated from ITS data are not rarefied like Ar and are thus are more sensitive to sample size variation, and that there were only 8 polymorphic sites and 9 haplotypes overall in this 441 bp alignment.

Based on microsatellite variation (Table 4), overall genetic diversity for this species was high for populations at the geomorphic features scale, with an average of 22.1 alleles per locus. Observed heterozygosity (H_E) ranged between 0.248 (Macquarie Ridge) and 0.558 (Louisville Seamount Chain) and was lower than expected in populations from every region and at every geomorphic feature. Allelic richness and private allelic richness were greatest in the north at the regional scale, which is underpinned by populations associated with the Kermadec Ridge region and the Louisville Seamount Chain having the highest and second highest allelic richness (Ar) values in the geomorphic features analysis, respectively (Table 4). Surprisingly, populations on the Campbell Plateau had a higher Ar value than those on the Chatham Rise, despite much smaller sample numbers, which is nonetheless taken into account in the rarefied Ar calculation (Kalinowski 2004). Samples from both the Louisville Seamount Chain and Chatham Rise had the largest private allele (Ar private) values, suggesting that even though overall genetic diversity was slightly lower in these populations relative to those of the Kermadec Ridge region, some degree of isolation has led to the accumulation of unique genetic diversity there.

For *D. dianthus*, we found a very low proportion of duplicate multilocus microsatellite genotypes amongst individuals from each population (less than 2% of the total dataset) and found that even individuals from the same cluster were genetically distinct from each other (Figure 3A). These results support the suggestion that this species is highly likely to reproduce sexually (Miller & Gunasekera 2017) and also indicates that our samples were separate colonies and not fragments of the same colony.

Enallopsammia rostrata
From the ITS sequence data, haplotypic diversity for this species was greatest at the North regional scale, which is underpinned by populations of the northernmost geomorphic features (Norfolk Ridge, Kermadec Ridge region, and Challenger Plateau) also having the greatest haplotypic diversity (Table 5). Populations on the Chatham Rise, as a geomorphic feature, and when representing the Central region, had the lowest genetic diversity despite having the highest representative number of samples (i.e., DNA sequences). The range in haplotypic diversity values probably stems from the varied number of individuals sequenced from each province, region or feature. For example, high haplotypic values for populations from the Norfolk Ridge, Kermadec Ridge region, and Challenger Plateau features arise because each of the sequences derived from populations of these features are different to each other. Therefore, the Chatham Rise cannot be taken unquestionably as an area with populations of lower genetic diversity than populations of *E. rostrata* from other sampled regions and features.

Bathypathes patula
Genetic diversity was calculated for this species from three provinces (northern, southern, and Antarctic) separately for three genes and together in a concatenated assembly of them (Table 6). The greatest diversity values based upon both nucleotide and haplotypic diversity for all datasets were found to be for populations in the northern province, which may be expected given that twice as many samples were included from there. The southern and Antarctica population samples had similar numbers of individuals, and nucleotide and haplotypic diversity values indicated that diversity was marginally lower in Antarctica than in the southern province for TRP, but was higher there for the ND5, 16S and concatenated data. If the three genes are considered separately, ND5 had the greatest number of polymorphic sites and therefore (although still based upon small sample sizes) is the most informative gene that is likely to provide the most robust diversity estimates. Conversely, the 16S gene was mostly invariable (containing only one and two polymorphic sites for the southern and Antarctica provinces,

respectively). Despite both marker and sample size limitations, overall this analysis suggested that Antarctic populations of *B. patula* were more diverse than those from around southern New Zealand.

***Leiopathes* spp.**
Allelic richness measures were generally similar for both the *Leiopathes secunda* and the *Leiopathes* spp. datasets (Table 7). When the mixed species dataset was considered, allelic richness was greatest for the Chatham Rise population, followed by the Kermadec Ridge region population, with the lowest Ar value found for the Challenger Plateau population. For the *L. secunda* dataset, the opposite was found; Ar for the Challenger Plateau population was greater than that for the Chatham Rise population.

4.3 Population genetic structure

Desmophyllum dianthus
Microsatellite-based DAPC scatter plots, AWclust and STRUCTURE cluster analyses all indicated subdivision into multiple groups for this species, although the number of indicative populations was incongruent amongst tests and between datasets. Considering all individuals together, non-parametric multidimensional scaling plots indicated the presence of 2 clusters, although both groups were poorly defined (data not shown). AWclust gap analyses for the regional and geomorphic features datasets suggested the likely existence of K (where K is the number of likely different groups) equals 2 and 3 groups, respectively (Figure 4). At the regional level, DAPC plots indicated K = 3 (North, Central, and South regions, Figure 5), and STRUCTURE HARVESTER delta K (ΔK) analysis indicated K = 2 (Figure 6A). For the geomorphic features analysis, DAPC plots indicated K = 4 (with distinct Louisville Seamount Chain, Kermadec Ridge region, Campbell Plateau, and Macquarie Ridge/Chatham Rise clusters), whereas geomorphic ΔK STRUCTURE-based analysis suggested that K = 3, with two principal clusters containing the Louisville Seamount Chain/Kermadec Ridge region and Chatham Rise samples (Figure 6B), with further subdivision in the latter. This analysis also showed affinity between populations on the Macquarie Ridge and the Chatham Rise and between those on the Campbell Plateau and the Louisville Seamount Chain/Kermadec Ridge region, supporting F_{ST} analyses that indicated that there is some level of connectivity between these features (see below). A lack of clear division between samples from the Louisville Seamount Chain and the Kermadec Ridge region in the AWclust and STRUCTURE analyses (and to some extent in DAPC scatter plots) highlighted the high levels of allelic affinity and the corresponding high levels of connectivity between these populations.

AMOVA results based upon all loci indicated that populations from the regional and geomorphic features sampling division, but not the province division, showed evidence of genetic differentiation (Table 8). ITS sequence-based AMOVAs were concordant with a geomorphic features-based, but not regionally based, hierarchy. As such, subsequent analyses did not partition samples by province but were based upon either regional or geomorphic features-based populations.

Based on microsatellite variation, pairwise F_{ST} results at the regional scale varied depending upon dataset (Table 9). When all loci were considered, each region was divergent from the others, whereas neutral loci alone suggested that the North and South regions were not significantly different. At the geomorphic features scale, both datasets were concordant and indicated that the Chatham Rise population is divergent from both the Louisville Seamount Chain and Kermadec Ridge region populations, but that all other putative populations are not genetically differentiated. Based upon ITS sequence data, pairwise Φ_{ST} results indicated that there were more significant differences between populations from different geomorphic features, with the Chatham Rise population being divergent from the Louisville Seamount Chain, Kermadec Ridge region, and the Campbell Plateau populations. Furthermore, these results also highlight that the Campbell Plateau and the Louisville Seamount Chain populations are different (Table 10).

Enallopsammia rostrata
E. rostrata results are based on ITS data only and on small sample sizes; as such, they must be interpreted with caution. At the geomorphic features scale, very high and significant pairwise Φ_{ST} differences were found between populations on the Chatham Rise and the Campbell Plateau and the

Norfolk Ridge, and between the Norfolk Ridge and the Campbell Plateau, but not between anywhere else. Non-significant results suggest high connectivity (gene flow) between populations at distant sites such as the Kermadec Ridge region and the Campbell Plateau (Table 11). Non-significant AMOVA results indicated an absence of genetic division amongst populations from the provincial, regional, and geomorphic features scale, suggesting that partitioning populations based upon these spatial scales would not account for any observed differences between populations (Table 12).

Bathypathes patula

B. patula results are based on concatenated mitochondrial DNA sequences (16S-ND5-TRP) and pairwise tests of population differentiation were calculated between provinces only (due to limited sample distribution as outlined in 3.5 above). Significant Φ_{ST} differences were found between all pairwise comparisons of the northern, southern, and Antarctic provinces (Table 13), suggesting that population connectivity may be limited between them.

***Leiopathes* spp.**

Leiopathes spp. (combined species) and *L. secunda* F_{ST} analyses are based upon microsatellite data and the geomorphic features scale only. No significant differences were observed between any populations when only *L. secunda* samples were considered (Table 14). These results are indicative of high levels of connectivity between these populations. For the *Leiopathes* spp. dataset, significant divergence was observed between the Kermadec Ridge region population and both the Challenger Plateau and Hikurangi Trough populations, but not between Kermadec Ridge region or Chatham Rise populations (suggesting that the Kermadec Ridge region population is not isolated from everywhere else). The Challenger Plateau population was not significantly different to elsewhere, with the exception of the Kermadec Ridge region population, suggesting the possibility of gene flow between westerly and easterly areas off the North Island. These results must be interpreted with caution given the small sample sizes (N=28 for *L. secunda* and N=46 for *Leiopathes* spp.).

The geomorphic feature ΔK STRUCTURE-based analysis suggested that K = 2 for the *Leiopathes* spp. or that K = 3 for the *L. secunda* datasets (Figure 7). Although only three or four geomorphic features were considered in these analyses (one geomorphic feature was omitted from the analysis because it did not meet the minimum population size criterion), the observed clusters did not correspond to each feature and each K (i.e., putative population) had a widespread distribution. Therefore, populations from these geomorphic features were not genetically distinct for *L. secunda* or *Leiopathes* spp. Clusters resulting from STRUCTURE analyses did not correspond to species-level taxonomic identities, suggesting that microsatellites cannot outline MOTUs representative of biological species within *Leiopathes*.

4.4 Population demographic change

Desmophyllum dianthus

From the ITS sequence data for both the Louisville Seamount Chain and Chatham Rise populations of *D. dianthus*, we obtained unimodal mismatch distributions, which are indicative of past demographic expansions (Slatkin & Hudson 1991, Rogers & Harpending 1992, Figure 8). Low R2 values are also indicative of an expansion scenario (Ramos-Onsins & Rozas 2002) and the Chatham Rise population also had the lowest R2 value, although it was not statistically significant (Table 15). The Campbell Plateau population had a multimodal distribution and the Kermadec Ridge region population also had a distribution that was not unimodal. A multimodal distribution can be interpreted in terms of new genetic variation being generated as a function of time, and can be representative of a population at equilibrium or that has been stationary for a long time (Harpending 1994); a population in equilibrium occurs where genetic drift, the stochastic element of the genetic process that can lead to allele loss between generations, is balanced by gene flow driven by incoming migrants to the population (Greenbaum et al. 2014). The Campbell Plateau population also had a positive Tajima's D test result. This result signifies low levels of both low and high frequency polymorphisms indicative of a reduction in population size and/or balancing selection (Balding et al. 2008), whereas a negative result, as seen for the Kermadec Ridge region population, signifies an excess of low frequency polymorphisms relative

to expectation and is indicative of a population size expansion (e.g., after a bottleneck or a selective sweep) and/or purifying selection. A relatively low raggedness statistic calculated for the Kermadec Ridge region population suggests a previous expansion of this population (Harpending 1994).

When testing for a population bottleneck using the microsatellite data (Table 16), no significant heterozygosity excess was detected in any of the *D. dianthus* populations (as determined using a Wilcoxon signed rank test) and no evidence was found for shifted modes of allele distribution, suggesting that no populations had undergone bottlenecks and that they may be at mutation-drift equilibrium (Luikart & Cornuet 1996, Luikart et al. 1998). However, significant heterozygote deficiencies were detected under the three mutation models in the Central region/Chatham Rise populations (i.e., the same data); heterozygote deficiencies are indicative of a population expansion (Girod et al. 2011, Luikart & Cornuet 1996). Wilcoxon signed rank tests also suggested that all other populations have a heterozygote deficiency indicative of an expansion under the SMM, and that the North region also has under the TPM (but not the IAM). Several caveats must be considered when interpreting these data: allele frequency mode-shift calculations may be sensitive to small numbers of loci and we only tested 5 loci (Luikart et al. 1998); BOTTLENECK assumes mutation-drift equilibrium, and we do not know if our loci conform to IAM, TPM and SMM mutation models. However, when all available evidence is considered, it is unlikely that any bottlenecks are occurring or have recently occurred, and the population on the Chatham Rise, at least, can be considered as an expanding population.

Bathypathes patula

Mismatch distributions were obtained from three genes for the northern, southern and Antarctic provinces for this species (Figure 9 and Table 15). The results were consistent for each gene. Samples from the northern and Antarctic provinces had a multimodal distribution, which can be indicative of a stable population (Harpending 1994). Multimodal distributions were also obtained for both the ND5 and TRP genes, but not for 16S, for the southern province samples. The 16S is the least variable gene used in this analysis, lending slightly more weight to the assertion that this population is also likely to be stable. Overall, there is no strong indication that the northern, southern or Antarctic populations of *B. patula* have undergone population expansion.

4.5 Contemporary and historical connectivity

Comparisons between contemporary and historical connectivity and calculations of effective population size (*Ne*) were limited to *D. dianthus* geomorphic features datasets only, as they had the largest sample sizes and most genetic structure (Figure 10 and Table 17).

Both neutral (i.e., excluding genetic markers potentially under selection) and all loci datasets were tested. The results differed slightly between datasets for historical gene flow estimation, but when considered together, noteworthy patterns indicate that historically; most populations had a high proportion of self-recruitment (as shown by larval migration pathways returning back to natal populations), gene flow occurred from the Louisville Seamount Chain to the Kermadec Ridge region (although the relative proportion varies by dataset) and to the Chatham Rise, and that the Macquarie Ridge population was not a source for any other population. These analyses also indicate that the Campbell Plateau was a source, rather than a sink, population. High levels of connectivity between populations from the Louisville Seamount Chain and the Kermadec Ridge region were in concordance with our previous analyses.

Contemporary migration pathways were identical between the neutral and all loci datasets, and also indicate a high proportion of self-recruitment. However, unlike historical gene flow pathways, neither the population on the Chatham Rise nor the Louisville Seamount Chain were sources for elsewhere. This analysis showed that populations on the Macquarie Ridge, Campbell Plateau, and Kermadec Ridge region were all source rather than sink populations, with the Kermadec Ridge region acting as a larval source for the Louisville Seamount Chain.

Estimates of contemporary *Ne* were very high for all populations for both datasets, except for the South region which had a low *N*e value (albeit with large confidence intervals, Table 18). In both cases, populations of the Louisville Seamount Chain and Chatham Rise had the lowest *Ne* (although *Ne* values for the former were still large), with *Ne* calculated from the all loci dataset being substantially smaller than the neutral dataset *Ne* in the case of the Louisville Seamount Chain (but vice versa for the Chatham Rise). Because the mutational rate of the microsatellites is unknown, these *Ne* results cannot be interpreted directly as numerical values but rather as a proportional indication of the variation in *Ne* among sampled areas. All appear to be large except for historical *Ne* for populations on the Chatham Rise, which were apparently smaller than at present, supporting evidence for a population expansion in this area (see Section 4.4).

4.6 Seascape genetics analyses

4.6.1 Independence testing of environmental variables

For *D. dianthus*, data for 17 environmental variables were available for sites where more than four individuals had been sampled (i.e., a population, Figure 11). Several of these variables were not independent and were removed from subsequent analyses, resulting in 11 environmental variables being tested: bathymetric position indices (BPI; both broad and fine), aragonite, particulate organic carbon flux (POC), salinity, silicate, slope, seamount, standard deviation (SD) of slope, temperature, and phosphate (Appendix 5).

For *E. rostrata*, data were available for 30 environmental variables for the four putative populations. As above, strongly correlated variables were reduced to a set of seven environmental variables that were tested: broad and fine BPI, depth, POC, slope percent, dynamic topography, and surface water primary productivity (Appendix 5).

4.6.2 Generalised Linear Models

For *D. dianthus*, the top 200 best fitting GLMs were all significant at $p < 0.01$ when testing F_{ST} against 11 environmental variables. For the top twenty models (Appendix 6), the Akaike Information Criterion (AIC) values ranged between -63.7 and -59.0 (with a range from -63.7 to -44.0 in the top 200), suggesting that multiple combinations of these variables were similarly plausible as a means to explain genetic variation, and that no single model in particular stood out as being more applicable than the others. Most models in the top 20 included eight or nine of the 11 environmental variables. fine BPI, POC, salinity, slope, and SD of slope occurred in all 20, broad BPI in 19, aragonite in 12, temperature in 11, seamount and silicate in ten, and phosphate in nine. Three of these variables were significant according to the ML test of individual effects, which, in descending order of their contribution to the model, were fine BPI, SD of slope, and slope (Table 19).

For *E. rostrata*, only the top nine models of the top 200 were significant at the $p < 0.05$ level, with very large AIC values that varied by several orders of magnitude amongst the top models, suggesting that only the highest ranked models contained the variables that could most plausibly explain the genetic structure (Appendix 6). Of the seven variables, a maximum of five were included in the top 20 models, with two or three of them occurring most frequently (seven and eight cases, respectively). Of the included variables, none occurred in all models, with dynamic topography being the most frequent in 13 of the top 20 models, followed by depth (11), and fine BPI (ten). Dynamic topography was the only variable to occur in all nine of the significant models, although according to the ML test, fine BPI was the only significant variable with a high contribution to the model (Table 19).

4.7 Larval dispersal models

Larval dispersal trajectories based upon a maximum PLD of 200 days were inferred from 43 sites representing all four study species, using GDP drifter (surface currents) and ARGO float (deeper currents) data (Figure 12). Generally, the surface current models indicated that greater larval dispersal was possible, and that more connectivity could be achieved amongst sites than was indicated by the deeper current models. Despite the fact that our samples originated from depths generally closer to ARGO float data, the dispersal routes inferred by GDP data (i.e., surface currents) are more concordant with our genetic data that show evidence for high connectivity over large spatial scales (e.g., between the Kermadec Ridge region and the Louisville Seamount Chain, Figure 12).

In terms of potential connectivity amongst populations of the provinces, regions, and geomorphic features, simulated dispersal trajectories both supported and contrasted with genetic data. For *D. dianthus*, neither surface nor deepwater current models suggested that larval migration occurred from the Louisville Seamount Chain to the southern part of the Kermadec Ridge region (from where our samples were obtained), although some GDP-based trajectories with longer PLDs reached further north into the Kermadec Ridge region and the Hikurangi Trough to the south. This result contrasts with analyses of historical connectivity, where a high proportion of unidirectional westerly migration occurred between these sites (neutral loci). Conversely, easterly migration from the Kermadec Ridge region towards the northern part of the Louisville Seamount Chain was feasible according to both GPD and ARGO data, which agrees with analyses of contemporary connectivity for *D. dianthus* and which could underpin the overall high connectivity (i.e., little genetic differentiation) observed between these features (although a PLD of 200 days isn't quite sufficient to reach the Louisville Seamount Chain using a model based on ARGO data).

According to both the GPD and ARGO data-based larval dispersal models, the Chatham Rise population received no larval input from the Louisville Seamount Chain population, although substantial easterly migration from western, mid and eastern Chatham Rise sites was feasible according to GDP drifters, which showed that dispersal was possible to all areas of the Louisville Seamount Chain. Historical genetic connectivity analyses for *D. dianthus* suggested that there was a small amount of migration from the populations of the Louisville Seamount Chain to those of the Chatham Rise, but contemporary analyses did not support this, and agreed more with the GDP current model (i.e., that there was no migration from populations of the Louisville Seamount Chain to the Chatham Rise). Connectivity assessments from the ARGO-based model suggest that larvae would not reach the Louisville Seamount Chain from the Chatham Rise but would instead disperse at greater depths in a southeasterly direction. Generally, unidirectional migration towards the Chatham Rise from areas to both the north and south of it, coupled with easterly flow from the Chatham Rise according to both GDP and ARGO data are likely to explain the unique genetic diversity and divergence of populations sampled there, as indicated by the *D. dianthus* F_{ST} values and the *E. rostrata* Φ_{ST} values. Conversely, the apparently high connectivity we observed amongst populations of *L. secunda* and *Leiopathes* spp. from three and five geomorphic features, respectively, implies that larval migration is theoretically possible between all pairs of features from which samples were collected (although given our combined data for *Leiopathes* spp. it is impossible to ascertain which, or if all, species are responsible for this result), although according to both GDP and ARGO models, migration between northern (e.g., the Hikurangi Trough) and southern (e.g., Campbell Plateau) features is unlikely.

No dispersal trajectories between the northern and southern extremes of the sampled range for *D. dianthus* were observed that could explain absence of differentiation between these areas as indicated by genetic clustering analyses (e.g., STRUCTURE). However, widespread migration in a northeasterly and easterly direction was indicated by GDP and ARGO data-based models from the Campbell Plateau, suggesting that dispersal distances within this area can be considerable and that such dispersal may follow the direction of major currents in the area (Figure 13). For *B. patula*, our genetic data indicated strong population divergence amongst provinces, which agrees with the larval dispersal modelling showing little evidence of migration between the Southern Ocean and southern areas of New Zealand. Larval dispersal from our sampling sites in the Southern Ocean is governed by easterly current flows

(shown by both GDP- and ARGO-based models) from which northerly migration appears to be prohibited.

5. DISCUSSION

This research examined population genetic structure and connectivity of four coral VME indicator taxa in the New Zealand region, the cup coral *Desmophyllum dianthus,* the matrix-forming coral *Enallopsammia rostrata,* and the black corals *Bathypathes patula* and *Leiopathes* spp. The dataset for *D. dianthus* was the most robust due to its larger sample size and greater number of markers, and as such was the basis for most analyses. Despite the more limited data for the other three species, the combined results could be useful for the design of spatial management measures for the protection of benthic fauna in the New Zealand EEZ and parts of the SPRFMO area.

5.1 Limitations - choice of markers and sample numbers

We had a choice of using existing genetic resources (i.e., markers) to characterise a few regions (loci) of the genome, or to develop new markers using NGS to assess population structure. Both options have advantages and disadvantages, and represent a trade-off between time, cost, and utility.

Using existing methods (i.e., genetic markers) is quicker and cheaper, and cnidarian genomes are conserved enough that some pre-existing markers will cross-amplify DNA across several species. The downside is that existing coral markers are generally limited in resolution, i.e., they cannot always resolve evolutionary relationships at low taxonomic levels such as between populations, so differentiation amongst populations reflects a property of the markers themselves rather than the populations (Shearer et al. 2002, Hellberg 2006).

Using NGS methods primarily has the advantage that much more of the genome can be compared amongst individuals and populations. The downside is that this approach is expensive, requires more bioinformatics input, and the resultant markers are usually species-specific. In marine invertebrates, NGS methods do not always yield better results; for example, NGS-generated markers could not differentiate seamount barnacle populations (Herrera & Shank 2016b), and microsatellites generated from NGS methods were still low in number in a coral (e.g., 9 useable loci from 173 candidate loci, Davies et al. 2013). NGS methods have, however, shown promise for Cnidaria as a means to elucidate population genetic structure (e.g., of an anemone, Rietzel et al. 2013 and of an octocoral, Everett et al. 2016) and for molecular-based taxonomy (e.g., of an octocoral, Herrera & Shank 2016a).

To maximise efficiency, to be sure we would obtain usable results, and to examine several taxa, we chose to use existing methods to obtain DNA sequence data and microsatellites. We sequenced the nuclear ITS region based on its previous utility in differentiating coral populations by depth, amplification success in preserved coral material, and the availability of similar data from the New Zealand region (Miller et al. 2010, Miller et al. 2011, Zeng et al. 2017). Duplicate ITS variants are known to occur even within the same individual, which therefore warrants a cautious approach to the interpretation of ITS data (Le Goff-Vitry et al. 2004). Nonetheless, we found this marker useful as a quick means to gain an overview of the geographic spread of haplotypic diversity that supported our conclusions drawn from higher-resolution microsatellite data.

We found evidence of microsatellite loci under selection, although this result needs to be treated with caution given the abundance of null alleles (i.e., non-amplifying alleles) within marine invertebrates generally. Null alleles themselves do not indicate the likelihood of selection, but they may result in markers with the same allelic characteristics as loci that are actually under selection. For future work, greater numbers of polymorphic loci via NGS could improve the overall resolution in our dataset; however, for *D. dianthus*, the genotypic diversity encompassed within our relatively large dataset was

recoverable with only six loci, suggesting that the addition of more loci would not necessarily have improved our results.

Obtaining large sample numbers and uniformly-spaced populations was challenging in this study, so we consolidated samples in a framework to assess spatially meaningful genetic boundaries and used metrics, such as rarefied allelic richness, which account for uneven sample sizes. Our results, based upon several markers and several diversity, clustering and migration analyses can be interpreted as an overview of genetic connectivity for our study species in the New Zealand region, with the caveat that only very small areas of some features were sampled (e.g., the Campbell Plateau). For *D. dianthus*, relatively large numbers of individuals were collected at several sites (e.g., N = 67 at 39 South Seamount on the Louisville Seamount Chain). Although not every population met a suggested minimum of 25-30 individuals for microsatellite analyses (Hale et al. 2012), and more samples from southern areas would have been informative, our samples from the Kermadec Ridge region, Louisville Seamount Chain, and Chatham Rise did meet this number and hence can be considered robust.

Sample numbers for *E. rostrata* and for both black corals were small (*E. rostrata*, N=79; *B. patula*, N=55–58; *L. secunda*, N=28–46), but represent all the material available in New Zealand. More reliable and robust estimates of connectivity could undoubtedly be derived from greater sample numbers. Furthermore, not all of the markers available amplified successfully in all taxa; microsatellite markers that amplified in *D. dianthus* did not amplify in *E. rostrata*, microsatellite markers that amplified in *Leiopathes* did not amplify reliably in *B. patula*, and sequence-based markers assessed for *B. patula* did not yield reliable data for *Leiopathes* spp. Taking these limitations into account, connectivity patterns nonetheless appeared to contrast quite markedly amongst the corals tested. Based on DNA sequence data, *B. patula* was the only species to show population divergence at the largest spatial scale (provincial scale in the sense of Watling et al. 2013), whereas no structure was observed for *Leiopathes* spp. at the geomorphic features scale based upon faster-evolving (and typically more informative) microsatellite markers.

All datasets would benefit from the inclusion of more samples and from examination of multiple marker types to validate our findings. Nonetheless, the results and interpretations here are the most robust that could be achieved based on existing material in New Zealand.

5.2 Genetic diversity

For *D. dianthus*, genetic diversity was lowest in populations on the Macquarie Ridge and highest in those of the Kermadec Ridge region, although private allelic richness (i.e., unique genetic content) was greatest for populations on the Chatham Rise and the Louisville Seamount Chain. Genetic diversity for *Leiopathes* spp. largely followed this trend as the Chatham Rise and Kermadec Ridge region populations had the greatest relative diversity, and for *E. rostrata*, the Kermadec Ridge region populations also had amongst the greatest values (although in this case the Chatham Rise had the least). Taken together (and considering sampling size caveats associated with some of our data), the Kermadec Ridge region and the Chatham Rise are areas of high genetic diversity.

High levels of genetic diversity are essential to allow for adaptive evolution (see Introduction). For *D. dianthus*, our results suggest that northern (i.e., at and above the Chatham Rise) populations would be more resilient to anthropogenic and climatic perturbation than those in the southern province. For *B. patula*, although only assessed at provincial scales, there also seems to be a north-to-south gradient in reducing genetic diversity. It is highly likely that we have not sampled the genetic limits of the range of *D. dianthus* (or any of our study species) in the New Zealand region, and that our sampling sites represent a subset of populations from a larger metapopulation (i.e., all populations of a species that exchange genes), because we did not find substantially lower diversity or a higher incidence of clonality at any particular site, both of which would indicate peripheral sites (Ayre & Hughes 2004, Johannesson & Andre 2006). *D. dianthus* is a cosmopolitan species found in all oceans, with the exception of the northern boreal Pacific Ocean and continental Antarctic Ocean (Försterra & Häussermann 2003), and our study has shown that population connectivity can occur over large spatial scales. However, we

cannot assume that all *D. dianthus* populations in the New Zealand region have high diversity and/or are not isolated; for example, isolated populations of *D. dianthus* have been identified at different depths within the region (Miller et al. 2011).

We also found comparable measures of genetic diversity and a very similar low proportion of duplicate genotypes (less than 2%) to that reported in previous research on *D. dianthus* populations on a Southern Ocean seamount Miller et al. *(*2011). This result supports the likelihood that this species reproduces sexually (Miller & Gunasekera 2017), an advantageous trait for maintaining population diversity and evolutionary resilience in corals (Harrison 2011).

5.3 Population structure, genetic connectivity, and the influence of historical and contemporary gene flow

The mechanisms of gene flow are important considerations for marine management. Distinguishing between historical (evolutionary, several or many generations ago) and contemporary (ecological, over the last few generations) connectivity is useful, as both types of information can be used differently. Historical connectivity can be useful to managers interested in biological conservation, taxonomy or detecting when lineages split (i.e., as a measure of biodiversity), whereas understanding contemporary connectivity may be more valued for ensuring sustainable fisheries or for futureproofing MPA networks (i.e., measuring demographic exchange, Sale et al. 2010).

For *D. dianthus*, we found evidence of weak genetic structure that reflects regional boundaries to connectivity (i.e., North, Central, and South), but which do not correspond to biogeographic provinces (in the sense of Watling et al. 2013). Little genetic differentiation between populations of the Louisville Seamount Chain and the Kermadec Ridge region stems from historical and contemporary migration, suggesting that oceanographic barriers do not preclude connectivity between these regions despite the distance between them (about 1500 km). The Chatham Rise populations are distinct from those of both the Kermadec Ridge region and the Louisville Seamount Chain, and from the South region and southern geomorphic features (for the latter, in some, but not all, analyses). This observation suggests that there is limited gene flow between populations of *D. dianthus* on the Chatham Rise and other areas. *E. rostrata* population genetic structure is similar in some characteristics to that of *D. dianthus*; the most northern and southern features appear to be connected (Challenger Plateau and Campbell Rise), the Chatham Rise has a degree of divergence from some (but not all) populations, and the Kermadec Ridge region populations have high levels of diversity.

Our *D. dianthus* and *E. rostrata* results are concordant in some respects with prior coral population genetics research in the New Zealand region. For example, diverse and/or divergent populations on the Chatham Rise and differences between the Kermadec Ridge region and the Chatham Rise (for *D. dianthus* but not *E. rostrata*) were observed also by Zeng et al. (2017) for the stony coral *G. dumosa*, although in contrast to the findings of Zeng et al. (2017), we did not find evidence of barriers between the populations of the Louisville Seamount Chain and the Kermadec Ridge region.

Of the two black corals in this study, *B. patula* has the most southerly distribution, extending to Antarctica. We found pronounced genetic differences between populations in the northern, southern and Antarctic provinces, suggesting limited gene flow between these areas and supporting previous assertions that the Antarctic Circumpolar Current (ACC) is likely to form a dispersal barrier to VME indicator taxa between the Antarctic region and southern New Zealand (Dueñas et al. 2016). Geomorphic features-based patterns of population structure for *Leiopathes* varied depending upon the dataset considered, with no discernible differences between *L. secunda* populations but some separation between a few populations in the mixed-species *Leiopathes* spp. dataset. The latter dataset comprised individuals of *L. secunda* and specimens as yet unidentified at the species level. Given that our microsatellites amplify in all species of *Leiopathes* tested to date, it is uncertain whether the increased divergence in the mixed dataset is due to increased resolution from the inclusion of more specimens of the same species, or to the inclusion of novel diversity from additional species. Although we cannot

resolve these options, we did not see evidence of geomorphic-specific endemism, supporting previous assessments of the general absence of seamount black coral population structure (Thoma et al. 2009).

Our data suggest that contemporary gene flow of *D. dianthus* is characterised by high self-recruitment and occasional long-distance recruitment. Primarily self-seeding populations with rare dispersal events linking them have also been inferred for seamount octocorals (*Corallium lauuense* in Hawai'i, Baco & Shank 2005). Although these events may occur infrequently, small numbers of high-dispersing larvae may propagate beneficial genes, may mitigate negative inbreeding effects, and may ensure that subpopulations share the majority of diversity observed in the metapopulation (Lowe & Allendorf 2010, Hare et al. 2011). Such benefits can derive from as little as one migrant per generation (Mills & Allendorf 1996, but see Beger et al. 2014, Greenbaum et al. 2014). Genetic signatures suggesting sufficient migration to offset geographic differentiation include low F_{ST} values, which we observed across our *D. dianthus* dataset (e.g., of less than 0.2, Dawson & Hamner 2008). It is worth noting that as generation times of *D. dianthus* are likely to be hundreds of years, such analyses offer a snapshot rather than an ongoing representation of connectivity.

5.4 Effective population size

Historical and contemporary estimates of effective population size (*Ne*, the number of individuals contributing genetic material to the next generation), calculated for *D. dianthus* only, were generally very high, consistent with those in an Australian study of *D. dianthus* from seamounts (Miller & Gunasekera 2017). These results contrast strongly with those of Zeng et al. (2017) for the deep-sea corals *Goniocorella dumosa*, *Madrepora oculata*, and *Solenosmilia variabilis* in the New Zealand EEZ, who reported that in most cases, contemporary effective population size was very small and in the range of only about 20 to 60 individuals. Overall, these multi-study results strongly suggest that *Ne* values are species-specific.

Effective population sizes can be used as an indicator of adaptive potential; small *Ne* indicates low adaptive resilience and low population fitness, which can increase extinction risk (Baums et al. 2006, Hare et al. 2011, Pinsky & Palumbi 2014, Reed & Frankham 2003). Therefore, low values of *Ne* are a cause for concern, and populations with small or decreasing *Ne* values may require protection and monitoring. *Ne* estimates are sensitive to sample size and the number of loci considered, they can vary depending on the genomic region examined and can be more reliable if compared between discrete generations (Charlesworth 2009, Waples & Do 2010, Hare et al. 2011). As such, interpretation of our *D. dianthus* data requires caution. Nonetheless, preserving areas containing populations with apparently large *Ne* values would be one way to maximise the possibility of protecting populations with a favourable resilience outlook. Monitoring *Ne* changes through time, although challenging for deep-sea corals given their longevity, overlapping generations and sampling constraints, could be a useful indicator of population resilience and a useful management tool. Reduced *Ne* values have indicated, for example, a mass mortality event (Costantini & Abbiati 2016), a possible bottleneck (Quattrini et al. 2015) and can be a comparative measure between sympatric species facing similar threats (Miller & Gunasekera 2017, Zeng et al. 2017).

5.5 Seascape genetics

Environmental correlates have previously been used as a means to predict habitat suitability for some protected corals and VME indicator taxa in the New Zealand region (e.g., Baird et al. 2013, Anderson et al. 2014, 2016a, 2016b), but they have not been applied to deep-sea seascape genetics analyses, with the exception of the work of Zeng et al. (2020). In the present study, a seascape genetics approach showed similar and contrasting results for *D. dianthus* and *E. rostrata* and revealed that species-specific genetic structure may be attributed to different environmental variables. It is of note that different locations were sampled at different spatial scales and that alternative molecular markers were used for both species, making direct comparison between the two species challenging. Furthermore, pronounced correlations between several pairs of environmental variables, and the subsequent exclusion of such variables from the seascape analyses, limits determining the relative importance of all environmental

factors for which data are available. However, sampling and analysis constraints notwithstanding, significant model results found in our study highlight that particular environmental correlates (and/or other environmental variables strongly correlated with the retained variable) may drive genetic structure in both coral species.

For *D. dianthus*, spatial genetic variation is mostly explained by environmental variation related to habitat topological characterisation: fine BPI, SD of slope, and slope. Previous research has highlighted the importance of slope as a means to predict overall coral distributions in the New Zealand region based on habitat suitability mapping (Baird et al. 2013) and our results suggest that topographical characteristics may shape genetic structure in *D. dianthus*. For example, topological characteristics may influence local current patterns that impact upon dispersal and larval settlement habitat (D'Aloia et al. 2015, Treml et al. 2015), which in turn may influence population genetic structure. Of the other variables frequently occurring in our analyses, salinity and POC (which both occurred in all top 20 models) and broad BPI (which occurred in 19 models) also provide large contributions to habitat suitability models for other stony corals in New Zealand (Baird et al. 2013, Anderson et al. 2016b). Salinity ranges and gradients are indicative of water masses and large-scale current distributions that may influence species distributions (Watling et al. 2013), and by extension such masses/currents could theoretically foster demarcations in genetic structure. Broad BPI is a variable that is likely to reflect the influence of large topographic features (e.g., Chatham Rise, Campbell Plateau) on current flow at large spatial scales (e.g., topographically steered currents/fronts such as the Subtropical Front and the Deepwater Western Boundary Current), and thus genetic structure. It is harder to make a direct link between POC (typically considered a proxy for particulate food availability) and controls on genetic structure, but it is possible that POC might be acting as a surrogate for other variables that influence the dispersal of larval and thus the species' genetic structure. For example, POC generally decreases with water depth, and factors associated with water depth may be responsible for depth-related genetic structure previously observed in New Zealand and Australian *D. dianthus* populations (Miller et al. 2010, Miller & Gunasekera 2017). Concordance between variables that are predictive of suitable habitat, and that are also potentially related to genetic structure, further highlight those particular environmental conditions previously observed to influence the distribution of *D. dianthus* populations around New Zealand (Anderson et al. 2016b). In contrast, other factors thought to predict the distribution of solitary corals specifically did not appear to be relevant drivers of genetic structure of *D. dianthus*, for example, dynamic topography (Baird et al. 2013).

For *E. rostrata*, dynamic topography, along with primary productivity, were the variables most likely to explain genetic structure. Both high primary productivity and dynamic topography have previously been shown to correlate positively with predictions of habitat suitability for coral distribution on seamounts globally (Tittensor et al. 2009) and in New Zealand specifically (Baird et al. 2013). Our data suggest that populations on the Chatham Rise may be delineated by factors related to large-scale current patterns (dynamic topography is a proxy for such patterns), which could influence genetic structure through controls on gene flow via limited larval dispersal. Primary productivity, typically used in habitat suitability models as a proxy for food availability, also reflects the broad-scale temperature characteristics of the water masses that control variations in planktonic biomass. Temperature influences reproductive timing of marine organisms, and *E. rostrata* off New Zealand is thought to broadcast larvae in April or May, which coincides with pelagic biomass accumulations after the Austral summer (Burgess & Babcock 2005). Thus, it is possible that primary productivity as a proxy for variation in temperature across the EEZ could explain patterns of generic structure. Habitat suitability models have previously identified salinity, POC and broad BPI as good environmental predictors of the distribution of *E. rostrata* (Anderson et al. 2016b). Broad BPI also occurred in the best fit model in our data for *E. rostrata*, although salinity and POC were less likely to determine genetic structure for *E. rostrata* than for *D. dianthus*.

Our research suggests that environmental variables that explain coral genetic variation are species-specific. Despite limited comparative data, previous research also indicates that environmental variables relevant to genetic structure or to habitat suitability predictions vary by species or by family for stony corals (Zeng 2016) and octocorals (Bryan & Metaxas 2006).

5.6 Larval dispersal models

Some of the patterns of genetic connectivity amongst populations of deepwater corals found in this study illustrate how larval dispersal may be profoundly influenced by currents in the region. The Chatham Rise is an area of mixing between warmer northern and cooler southern waters, which at surface and intermediate depths (1000 m) meet at the rise and flow east (Chiswell & Sutton 2015, Chiswell et al. 2015). These currents are likely to form a barrier between the north and south and may isolate Chatham Rise populations, explaining the high F_{ST} and Φ_{ST} values, private allelic richness, and high levels of self-recruitment and/or separation indicated by cluster analyses for *D. dianthus* and *E. rostrata*. Similar findings for deep-sea VME indicator sponges have been reported by Zeng et al. (2019). The surface currents also form the Subtropical Front, which flows in an easterly direction from the Chatham Rise towards the Louisville Seamount Chain, although at 1000 m depth the current turns south at the eastern end of the rise (Chiswell & Sutton 2015, Chiswell et al. 2015). The latter may thus form a barrier to connectivity between populations on the Chatham Rise and the Louisville Seamount Chain at depth, which is supported by the ARGO-based larval dispersal models between these sites. Modelled larval dispersal results from our study based upon a range of PLD times were generally in agreement with the direction of these currents. However, the Subtropical Front does not appear to be a barrier to dispersal and simulated larval dispersal at the longer end of the modelled PLD spectrum (i.e., 200 days) suggests that migration between the Chatham Rise and Louisville Seamount Chain is possible, especially from sites on the mid-Chatham Rise. Our samples of *D. dianthus* on the Chatham Rise were collected at depths between 500 and 700 m. We do not know if the larvae of these populations are transported in shallow or deeper currents, but limited connectivity between populations on the Chatham Rise and Louisville Seamount Chain makes deeper entrainment more plausible.

High genetic connectivity between populations of the Kermadec Ridge region and Louisville Seamount Chain may be explained partly by the direction of currents between these geomorphic features. Kermadec-bound currents at 1000 m from the northern end of the Louisville Seamount Chain (samples from these seamounts were collected deeper than 900 m) would support the finding that a large proportion of larvae have migrated there historically. Migration in the opposite direction, from the Kermadec Ridge region to the Louisville Seamount Chain, as suggested by contemporary genetic migration analyses, is most plausible when considering longer PLDs and surface current (GDP-derived data) models. Overall, from the modelled dispersal, we could expect to see stronger genetic divergence between the Louisville Seamount Chain and Kermadec Ridge region populations.

For *B. patula*, genetic data provide evidence of restricted larval migration between the seas around New Zealand and the Southern Ocean, adding further support to the suggestion that the ACC is a barrier to dispersal. We have not determined to what extent this barrier is semi-permeable for *B. patula*, as has been suggested for octocorals in the same region using migration analyses (Dueñas et al. 2016), but modelled dispersal for both short and long PLD times suggest that northerly dispersal is highly unlikely.

6. POTENTIAL APPLICATION OF THE RESULTS

Our study was conducted within the context of developing an evidence base for spatial management designs that takes genetic source into account. Below we discuss some of the possible applications of our results, in particular with respect to the efficacies of seamount closures and BPAs (within the EEZ), and SPRFMO's interim fishing closures (High Seas) as conservation measures in the New Zealand region.

6.1 New Zealand EEZ

In the New Zealand EEZ, benthic habitats including deep-sea corals are protected spatially from trawling by 17 seamount closure areas (encompassing 19 seamounts) and 17 BPAs (Brodie & Clark 2004, Helson et al. 2010) (Figure 1).

The results of our analyses suggest that *D. dianthus* comprises three genetically distinct 'regional stocks' within the EEZ – North (Louisville Seamount Chain/Kermadec Ridge region), Central (Chatham Rise) and South (Campbell Plateau and Macquarie Ridge), with occasional connectivity between/amongst them. The limited regional connectivity between the stocks within the EEZ could usefully be factored in when considering spatial management to protect *D. dianthus* and other vulnerable corals with similar patterns of connectivity (Zeng et al. 2017). That is, ideally there should be spatial closures in each of the regions. Although there are seamount closures and BPAs in each of the three regions, there are fewer closures over a proportionately smaller area in the Central region. This disparity could mean that the genetic structure of corals in the Central region (i.e., on the Chatham Rise) is potentially not as well protected as it probably is in the North and South regions (see also Bors et al. 2012, Zeng et al. 2017, Zeng et al. 2019). The relative lack of protection for the Chatham Rise may need to be considered because it is one of the most heavily trawled areas of the New Zealand EEZ (Baird et al. 2013).

The Kermadec Ridge region is another area where the genetic diversity of *D. dianthus* was high. Genetic diversity in this area may be protected by the large Kermadec BPA and Tectonic Reach BPA, assuming that the population we sampled from areas to the south of the boundaries of these BPAs, has a similar genetic structure.

The southern 'stock' of *D. dianthus* was not isolated within the EEZ, and based upon genetic data and larval dispersal models, is likely to be a source population for areas to the north and east. The Macquarie Ridge and Campbell Plateau, the regions where our sample sites are located, have few seamount closures or BPAs even though it is an area of high bottom trawling activity (Baird et al. 2013). It is an area that could therefore benefit from protection of source populations of *D. dianthus* (and potentially other corals) and their ability to provide larvae for regions to the north.

The sparse distribution of black coral samples and the occurrence of single records over large geographic areas make it difficult to define 'stocks'. *Leiopathe*s spp. from the northern geomorphic features are generally panmictic, and therefore it is not possible to define 'stocks' at regional scales. Genetic structure for *B. patula* was partitioned at provincial scales, with a clear barrier between the Antarctic and southern provinces, also supported by the dispersal models. The finding that the ACC is apparently a barrier to dispersal between the two southernmost populations included in our study is consistent with similar findings for deep-sea octocorals (Dueñas et al. 2016) and other marine invertebrates (e.g., Hunter & Halanych 2008, Thornhill et al. 2008). Hence, it is important to have separate protection measures for benthic habitats in both New Zealand's EEZ and the Ross Sea territory in Antarctica.

6.2 High Seas

In recent years, there have been a number of area closures in the SPRFMO Convention Area that have applied to New Zealand vessels. Current interim closures (as of the writing of this report) comprise 62 lightly trawled blocks closed to fishing, 69 moderately trawled blocks in which a move-on rule is applied, and 20 further closed blocks in moderately and heavily trawled areas designated to provide representative protection. The blocks are centred primarily on the Louisville Seamount Chain, the Three Kings and West Norfolk ridges, the Lord Howe Rise and the Challenger Plateau (Penney et al. 2009).

D. dianthus is the only coral species from the Louisville Seamount Chain that was sampled by our study. Thus, the efficacy of genetic structure and population connectivity across the full extent of the SPRFMO region cannot be assessed at this stage.

Our results suggest limited differentiation between populations in the New Zealand EEZ and the Louisville Seamount Chain. Our study also suggests that it is feasible that migration from southern Louisville Seamount Chain populations may occur occasionally towards the Chatham Rise, and from the northern populations towards both the Kermadec Ridge region and the Chatham Rise. Genetically indistinguishable populations in the Kermadec Ridge region and the Louisville Seamount Chain suggest

strongly that these populations are connected by long-distance gene flow, and that they may be dependent upon each other for recruitment. Both northern and southern areas of the Louisville Seamount Chain appear to be important sources and sinks for coral populations within the New Zealand EEZ. This evidence, together with the findings of Zeng et al. (2017) suggests that MPA networks spanning national and international management areas would provide a better protection solution than just one or the other.

We did not obtain samples of *D. dianthus* from the full geographic extent of the Louisville Seamount Chain, which limits any suggestions on placement of protection. In the absence of such information, it would be prudent to consider distributing protection throughout the chain and not concentrate closures in one part of the area. This would maximise the possibility of encompassing representative, connected, and replicated populations as per international recommendations for MPA closures (e.g., Gjerde et al. 2016) and should include areas in which fishing has not already occurred.

7. FUTURE INFORMATION NEEDS

The present study adds to a growing body of literature concerning genetic connectivity of corals in the New Zealand region. Patterns of population genetic structure and/or genetic connectivity have now been established with reasonable geographic coverage for most of New Zealand's common stony corals (this study, Zeng et al. 2017, Miller et al. 2010) and to a lesser extent for other coral taxa (this study, Miller et al. 2010, Dueñas et al. 2016), as well as sponges (Zeng et al. 2019).

Despite recognition that connectivity is an integral part of an 'ecologically coherent' MPA network, integrating genetic data into final network designs, especially for invertebrates, is rare (McInerney et al. 2012, Laikre et al. 2016). It is, however, recognised that management of VMEs would benefit from increased consideration of genetic connectivity data for VME indicator taxa (Clark et al. 2012, Baco et al. 2016, Boschen et al. 2016), especially that derived from multiple species with overlapping ranges (e.g., Baco et al. 2016, Yan et al. 2020).

In conclusion, information that could potentially improve the management of deep-sea VME indicator and associated taxa in the New Zealand region are as follows:

1) Consolidate genetic data for deep-sea taxa found in the New Zealand EEZ, and wider South Pacific

Genetic connectivity data are now available for a range of deep-sea taxa with a range of life-history traits, from within and beyond the New Zealand EEZ. However various (and sometimes incomparable) markers have been used and samples do not originate from identical sites, and data have not been consolidated into a single dataset or database.

2) Obtain new genetic data for other VME indicator taxa

Further study of genetic connectivity for certain taxa (e.g., black corals and non-stony coral VME indicator taxa) could be usefully included in future habitat suitability modelling efforts, and/or be used in decision-support tools for spatial management.

3) Develop a platform through which genetic data/results can be made available and presented to stakeholders, modellers, working groups etc.

It would be useful to have a shared platform through which national and international geneticists, modellers, and stakeholders could access genetic connectivity data for incorporation into habitat suitability models, benthic classification schemes, biophysical models, etc. This platform could be developed, for example, through workshops or databases.

4) Data collation and gap analysis

An inventory of samples and genetic analyses would be an expected output from recommendation 2 and would facilitate a detailed evaluation of the distribution of samples, gaps in coverage, or analytical method. Such gaps could potentially be filled opportunistically (e.g., if research vessels are passing a particular location, or if a certain species is captured by a commercial vessel with an observer onboard).

8. ACKNOWLEDGMENTS

This research was funded by the Ministry for Primary Industries (ZBD2013-02 'Vulnerable Marine Ecosystems Project – Genetic Connectivity'). We are grateful to staff of the NIWA Invertebrate Collection (Kareen Schnabel, Sadie Mills, and Diana Macpherson) for their assistance in sample acquisition from the collections and for providing advice and input into species short-listing during the initial stages of the project. We are grateful to NIWA staff and crew involved in the TAN1402 and TAN1503 research voyages to the Louisville Seamount Chain and Chatham Rise (respectively) during which we acquired fresh material. These voyages were funded by MBIE through NIWA's South Pacific VME Project (C01X1229), Vulnerable Deep-Sea Communities (contract CO1X0906) and by MPI through the Chatham Rise Seamounts project (project code BEN2014-02). We are grateful to Di Tracey (NIWA) for specimen identification, coordination of sample acquisition, discussion, and for facilitating the attendance of LPH at NOAA's Next Generation Sequencing Technologies for Coral Workshop (September 2014, partially funded by the New Zealand/United States Joint Commission on Science and Technology Cooperation Marine and Ocean Theme), and a Black Coral Identification workshop held at NIWA in June 2015. Dennis Opresko and Mercer Brugler assisted with *Leiopathes* specimen identifications, and Mercer provided input and marker primers for black coral molecular work. The Baums laboratory at Pennsylvania State University (baumslab.org) provided microsatellite primer sequences for *Leiopathes* prior to their publication. Karen Miller (AIMS, Australia) and Cong Zeng (VUW and NIWA) provided the primers for *D. dianthus*. Judy Sutherland (NIWA) provided a constructive review of a draft of the report, which helped improve the final report, as did input from Mary Livingston (Fisheries New Zealand).

9. REFERENCES

Addamo, A.M.; Garcia-Jimenez, R.; Taviani, M.; Machordom, A. (2015). Development of microsatellite markers in the deep-sea cup coral *Desmophyllum dianthus* by 454 sequencing and cross-species amplifications in Scleractinia Order. *Journal of Heredity 106(3)*: 322–330.

Addamo, A.M.; Reimer, J.D.; Taviani, M.; Freiwald, A.; Machordom, A. (2012). *Desmophyllum dianthus* (Esper, 1794) in the scleractinian phylogeny and its intraspecific diversity. *PloS One 7(11)*: e50215.

Adkins, J.F.; Henderson, G.M.; Wang, S.L.; O'Shea, S.; Mokadem, F. (2004). Growth rates of the deep-sea scleractinia *Desmophyllum cristagalli* and *Enallopsammia rostrata*. *Earth and Planetary Science Letters 227(3–4)*: 481–490.

Althaus, F.; Williams, A.; Schlacher, T.A.; Kloser, R.J. et al. (2009). Impacts of bottom trawling on deep-coral ecosystems of seamounts are long-lasting. *Marine Ecology Progress Series 397*: 279–294.

Anderson, O.F.; Clark, M.R. (2003). Analysis of bycatch in the fishery for orange roughy, *Hoplostethus atlanticus*, on the South Tasman Rise. *Marine and Freshwater Research 54*: 643–652.

Anderson, O.F.; Guinotte, J.M.; Rowden, A.A.; Clark, M.R.; Mormede, S.; Davies, A.J.; Bowden, D.A. (2016a). Field validation of habitat suitability models for vulnerable marine ecosystems in the South Pacific Ocean: Implications for the use of broad-scale models in fisheries management. *Ocean & Coastal Management 120*: 110–126.

Anderson, O.F.; Guinotte, J.M.; Rowden, A.A.; Tracey, D.M.; Mackay, K.A.; Clark, M.R. (2016b). Habitat suitability models for predicting the occurrence of vulnerable marine ecosystems in the seas around New Zealand. *Deep Sea Research Part I: Oceanographic Research Papers 115*: 265–292.

Anderson, O.; Tracey, D.M.; Bostock, H, Williams, M.; Clark, M.R. (2014). Refined habitat suitability modelling for protected coral species in the New Zealand EEZ. Report prepared for Marine Species and Threats, Department of Conservation, Wellington, New Zealand. DOC14302. https://www.doc.govt.nz/Documents/conservation/marine-and-coastal/marine-conservation-services/reports/protected-coral-distribution-modelling-final-report.pdf

Antao, T.; Lopes, A.; Lopes, R.J. et al. (2008). LOSITAN: A workbench to detect molecular adaptation based on a F_{ST} -outlier method. *BMC Bioinformatics 9*: 1–5.

Aurelle, D.; Ledoux, J.B.; Rocher, C.; Borsa, P.; Chenuil, A.; Féral, J.P. (2011). Phylogeography of the red coral (*Corallium rubrum*): inferences on the evolutionary history of a temperate gorgonian. *Genetica 139(7)*: 855–869.

Ayre, D.J.; Hughes, T.P. (2004). Climate change, genotypic diversity and gene flow in reef-building corals. *Ecology Letters 7(4)*: 273–278.

Baco, A.R.; Etter, R.J.; Ribeiro, P.A.; Heyden, S.; Beerli, P.; Kinlan, B.P. (2016). A synthesis of genetic connectivity in deep-sea fauna and implications for marine reserve design. *Molecular Ecology 25(14):* 3276–3298.

Baco, A.R.; Shank, T.M. (2005). Population genetic structure of the Hawaiian precious coral *Corallium lauuense* (Octocorallia: Coralliidae) using microsatellites. *In* Freiwald, A.; Roberts, J.M. (Eds.), Cold-water Corals and Ecosystems. Springer, Heidelberg. pp 663–678.

Baird, S.J.; Tracey, D.; Mormede, S.; Clark, M. (2013). The distribution of protected corals in New Zealand waters. NIWA Client Report WLG2012-43 for DOC12303/POP2011-06. 96 p. https://www.doc.govt.nz/Documents/conservation/marine-and-coastal/marine-conservation-services/pop-2011-06-coral-distribution.pdf

Balding, D.J.; Bishop, M.; Cannings, C. (2008). *Handbook of Statistical Genetics*. John Wiley & Sons. 1616 p.

Balloux, F.; Lugon-Moulin, N. (2002). The estimation of population differentiation with microsatellite markers. *Molecular Ecology 11(2)*: 155–165.

Baums, I.B.; Miller, M.W.; Hellberg, M.E. (2006). Geographic variation in clonal structure in a reef-building caribbean coral, *Acropora palmata*. *Ecological Monographs 76*(4): 503–519.

Beerli, P. (2008). Migrate version 3.0: a maximum likelihood and Bayesian estimator of gene flow using the coalescent. Distributed over the internet at http://popgen. scs. edu/migrate.

Beerli, P.; Felsenstein, J. (2001). Maximum likelihood estimation of a migration matrix and effective population sizes in *n* subpopulations by using a coalescent approach. *Proceedings of the National Academy of Sciences of the United States of America 98(8)*: 4563–4568.

Beger, M.; Selkoe, K.A.; Treml, E.; Barber, P.H.; Von Der Heyden, S.; Crandall, E.D.; Toonen, R.J.; Riginos, C. (2014). Evolving coral reef conservation with genetic information *Bulletin of Marine Science 90*: 159–185.

Behrenfeld, M.J.; Falkowski, P.G., (1997) Photosynthetic rates derived from satellite-based chlorophyll concentration. *Limnology and oceanography 42(1)*: 1–20.

Benjamini, Y.; Hochberg, Y. (1995). Controlling the false discovery rate: A practical and powerful approach to multiple testing. *Journal of the Royal Statistical Society B 57*: 289–300.

Bors, E.K.; Rowden, A.A.; Maas, E.W.; Clark, M.R.; Shank, T.M. (2012). Patterns of deep-Sea genetic connectivity in the New Zealand Region: Implications for management of benthic ecosystems. *PLOS One 7(11)*: e49474.

Boschen, R.E.; Collins, P.C.; Tunnicliffe, V.; Carlsson, J.; Gardner, J.P.A.; Lowe, J.; McCrone, A.; Metaxas, A.; Sinniger, F.; Swaddling, A. (2016). A primer for use of genetic tools in selecting and testing the suitability of set-aside sites for deep-sea seafloor massive sulfide mining. *Ocean and Coastal Management 122*: 37–48.

Bostock, H.C.; Sutton, P.J.; Williams, M.J.M.; Opdyke, B.N. (2013a). Reviewing the circulation and mixing of Antarctic Intermediate Water in the South Pacific using evidence from geochemical tracers and Argo float trajectories. *Deep Sea Research Part 1: Oceanographic Research Papers 73*: 84–98.

Bostock H.C.; Mikaloff-Fletcher, S.E.; Williams, M.J.M. (2013b). Estimating carbonate parameters from hydrographic data for the intermediate and deep waters of the Southern Hemisphere oceans. *Biogeosciences 10*: 6199–6213. http://dx.doi. org/10.5194/bg-10-6199-2013.

Bradbury, I.R.; Laurel, B.; Snelgrove, P.V.; Bentzen, P.; Campana, S.E. (2008). Global patterns in marine dispersal estimates: the influence of geography, taxonomic category and life history. *Proceedings of the Royal Society of London B: 275(1644)*: 1803–1809.

Bradshaw, W.E.; Holzapfel, C.M. (2008). Genetic response to rapid climate change: it's seasonal timing that matters. *Molecular Ecology 17(1)*: 157–166.

Brodie, S.; Clark, M.R (2004). The New Zealand seamount management strategy – steps towards conserving offshore marine habitat. *In*: Beumer, J.P.; Grant, A.; Smith, D.C. eds. Aquatic Protected Areas: what works best and how do we know? *Proceedings of the World Congress of Aquatic Protected Areas*, Cairns 2002. Australian Society for Fish Biology, Australia, pp. 664–673.

Brugler, M.R.; Opresko, D.M.; France, S.C. (2013). The evolutionary history of the order Antipatharia (Cnidaria: Anthozoa: Hexacorallia) as inferred from mitochondrial and nuclear DNA: implications for black coral taxonomy and systematics. *Zoological Journal of the Linnean Society 169*(2): 312–361.

Bryan, T.L.; Metaxas, A. (2006). Distribution of deep-water corals along the North American continental margins: Relationships with environmental factors. *Deep-Sea Research Part I: Oceanographic Research Papers 53*: 1865–1879.

Burgess, S.N.; Babcock, R.C. (2005). Reproductive ecology of three reef-forming, deep-sea corals in the New Zealand region. *In*: Freiwald, A.; Roberts, J.M. (eds) Cold-Water Corals and Ecosystems. Erlangen Earth Conference Series. Springer, Berlin, Heidelberg.

Cairns, S.D. (1982). Antarctic and sub-Antarctic Scleractinia. *Antarctic Research Series 34*: 1–74.

Cairns, S.D. (1995). The marine fauna of New Zealand: Scleractinia (Cnidaria: Anthozoa). *New Zealand Oceanography Institute Memoirs 103*: 210 p.

CANZ (2008) New Zealand Region Bathymetry. NIWA Chart, Miscellaneous Series No. 85, National Institute of Water and Atmospheric Research, Wellington, New Zealand

Charlesworth, B. (2009). Fundamental concepts in genetics: effective population size and patterns of molecular evolution and variation. *Nature Reviews Genetics 10(3)*: 195–205.

Chiswell, S.M.; Bostock, H.C.; Sutton, P.J.; Williams, M.J. (2015). Physical oceanography of the deep seas around New Zealand: a review. *New Zealand Journal of Marine and Freshwater Research 49(2)*: 286–317.

Chiswell, S.M.; Sutton, P.J. (2015). Drifter-and float-derived mean circulation at the surface and 1000 m in the New Zealand region. *New Zealand Journal of Marine and Freshwater Research 49(2)*: 259–277.

Chiucchi, J.E.; Gibbs, H.L. (2010). Similarity of contemporary and historical gene flow among highly fragmented populations of an endangered rattlesnake. *Molecular Ecology 19(24)*: 5345–5358.

Clark, M.R.; Anderson, O.F.; Bowden, D.A.; Chin, C.; George, S.G.; Glasgow, D.A.; Guinotte, J.M.; Hererra, S.; Osterhage, D.M.; Pallentin, A.; Parker, S.J.; Rowden, A.A.; Rowley, S.J.; Stewart, R.; Tracey, D.M.; Wood, S.A.; Zeng, C. (2015a). Vulnerable Marine Ecosystems of the Louisville Seamount Chain: voyage report of a survey to evaluate the efficacy of preliminary habitat suitability models. *New Zealand Aquatic Environment and Biodiversity Report No. 149*. 86 p.

Clark, M.R.; Bowden, D.A.; Rowden, A.A.; Stewart, R. (2019). Little evidence of benthic community resilience to bottom trawling on seamounts after 15 years. *Frontiers in Marine Science 6:* 63. 16 p.

Clark, M.R.; Bowden, D.A.; Tracey, D.M.; Mills, S.; George, S.; Stewart, R.; Hart, A.; Macpherson, D.; Gammon, M.; Holland, L.; Moore, K.; Frontin-Rollett, G. (2015b). Factual voyage Report of a Survey of Seamounts on the Northwest and Southwest Chatham Rise (TAN1503). (Unpublished report held by Fisheries New Zealand.) 66 p.

Clark, M.R.; O'Driscoll, R (2003). Deepwater fisheries and aspects of their impact on seamount habitat in New Zealand. *Journal of Northwest Atlantic Fishery Science 31*: 441–458.

Clark, M.R.; Rowden, A.A. (2009). Effect of deepwater trawling on the macro-invertebrate assemblages of seamounts on the Chatham Rise, New Zealand. *Deep Sea Research Part I: Oceanographic Research Papers 56(9)*: 1540–1554.

Clark, M.R.; Schlacher, T.A.; Rowden, A.A.; Stocks, K.I.; Consalvey, M. (2012). Science priorities for seamounts: research links to conservation and management. *PLoS ONE 7(1)*: e29232.

Concepcion, G.T.; Crepeau, M.W.; Wagner, D.; Kahng, S.E.; Toonen, R.J. (2007). An alternative to ITS, a hypervariable, single-copy nuclear intron in corals, and its use in detecting cryptic species within the octocoral genus *Carijoa*. *Coral Reefs 27(2)*: 323–336.

Cornuet, J.M.; Luikart, G. (1996). Description and power analysis of two tests for detecting recent population bottlenecks from allele frequency data. *Genetics 144:* 2001–2014

Costantini, F.; Abbiati, M. (2016). Into the depth of population genetics: pattern of structuring in mesophotic red coral populations. *Coral Reefs 35(1)*: 39–52.

Cowen, R.K.; Sponaugle, S. (2009). Larval dispersal and marine population connectivity. *Annual Review of Marine Science 1:* 443–466.

Crandall, E.D.; Treml, E.A.; Barber, P.H. (2012). Coalescent and biophysical models of stepping-stone gene flow in neritid snails. *Molecular Ecology 21*: 5579–5598.

D'Aloia, C.C.; Bogdanowicz, S.M.; Francis, R.K.; Majoris, J.E.; Harrison, R.G.; Buston, P.M. (2015). Patterns, causes, and consequences of marine larval dispersal. *Proceedings of the National Academy of Sciences 112*: 13940–13945.

Davies, S.W.; Rahman, M.; Meyer, E. et al. (2013). Novel polymorphic microsatellite markers for population genetics of the endangered Caribbean star coral, *Montastraea faveolata*. *Marine Biodiversity 43(2):* 167–172.

Dawson, M.N.; Hamner, W.M. (2008). A biophysical perspective on dispersal and the geography of evolution in marine and terrestrial systems. *Journal of the Royal Society Interface 5(19)*: 135–150.

Do, C.; Waples, R.S.; Peel, D.; Macbeth, G.M.; Tillett, B.J.; Ovenden, J.R. (2014). NeEstimator v2: Re-implementation of software for the estimation of contemporary effective population size (*Ne*) from genetic data. *Molecular Ecology Resources 14(1)*: 209–214.

Dueñas, L.F.; Tracey, D.M.; Crawford, A.J.; Wilke, T.; Alderslade, P.; Sánchez, J.A. (2016). The Antarctic Circumpolar Current as a diversification trigger for deep-sea octocorals. *BMC Evolutionary Biology 16(1)*: 2.

Earl, D.; vonHoldt, B.M. (2012). STRUCTURE HARVESTER: a website and program for visualizing STRUCTURE output and implementing the Evanno method. *Conservation Genetics Resources 4*: 359–361.

Evanno, G.; Regnaut, S, Goudet, J. et al. (2005). Detecting the number of clusters of individuals using the software STRUCTURE: a simulation study. *Molecular Ecology 14*: 2611–2620.

Everett, M.V.; Park, L.K.; Berntson, E.A.; Elz, A.E.; Whitmire, C.E.; Keller A.A.; et al. (2016). Large-scale genotyping-by-sequencing indicates high levels of gene flow in the deep-sea octocoral *Swiftia simplex* (Nutting 1909) on the west coast of the United States. *PLoS ONE 1(10)*: e0165279.

Excoffier, L.; Heckel, G. (2006). Computer programs for population genetics data analysis: a survival guide. *Nature Reviews Genetics 7(10)*: 745–758.

Excoffier, L.; Lischer, H.E.L. (2010). Arlequin suite ver 3.5: A new series of programs to perform population genetics analyses under Linux and Windows. *Molecular Ecology Resources 10*: 564–567.

FAO (2009). International guidelines for the management of deep-sea fisheries in the high seas. No. FAO 338.3727 D598, Roma (Italia).

Faurby, S.; Barber, P.H. (2012). Theoretical limits to the correlation between pelagic larval duration and population genetic structure. *Molecular Ecology 21(14)*: 3419–3432.

Feehan, K. (2016). Highly Seasonal Reproduction in *Desmophyllum dianthus* from the Northern Patagonian Fjords. MSc Thesis, University of Maine. Electronic Theses and Dissertations. Paper 2433.

Feral, J.P. (2002). How useful are the genetic markers in attempts to understand and manage marine biodiversity? *Journal of Experimental Marine Biology and Ecology 268*: 121–145.

Foll, M.; Gaggiotti, O.E. (2008). A genome scan method to identify selected loci appropriate for both dominant and codominant markers: A Bayesian perspective. *Genetics 180*: 977–993.

Försterra, G.; Häussermann, V. (2003). First report on large scleractinian (Cnidaria: Anthozoa) accumulations in cold-temperate shallow water of south Chilean fjords. *Zool.Verh.Leiden 345*: 117–128.

Fu, Y.X. (1997). Statistical tests of neutrality against population growth, hitchhiking and background selection. *Genetics 147*: 915–925.

Fu, Y.X.; Li, W.H (1993). Statistical tests of neutrality of mutations. *Genetics 133*: 693–709.

Gagnaire, P.A.; Broquet, T.; Aurelle, D.; Viard, F.; Souissi, A.; Bonhomme, F.; Bierne, N. (2015). Using neutral, selected, and hitchhiker loci to assess connectivity of marine populations in the genomic era. *Evolutionary Applications 8(8)*: 769–786.

Gao, X.; Starmer, J.D. (2008). AWclust: point-and-click software for non-parametric population structure analysis. *BMC Bioinformatics 9*: 77.

Garcia, H.E.; Locarnini, R.A.; Boyer, T.P.; Antonov, J.I.; (2006) World Ocean Atlas2005, volume 3: dissolved oxygen, apparent oxygen utilization, and oxygen saturation. *In*: Levitus, S.; (Ed.) NOAA Atlas NESDIS63. USA Government Printing Office, Washington DC, p. 342.

Gardner, J.P.A.; Bell, J.J.; Constable, H.B.; Hannan, D.A.; Ritchie, P.A.; Zuccarello, G.C. (2010). Multi-species coastal marine connectivity: a literature review with recommendations for further research. *New Zealand Aquatic Environment and Biodiversity Report No. 58*. 47 p.

Garza, J.C.; Williamson, E.G. (2001). Detection of reduction in population size using data from microsatellite loci. *Molecular Ecology 10*(2): 305–318.

Gérard, K.; Guilloton, E.; Arnaud-Haond, S.; Aurelle, D.; Bastrop, R.; Chevaldonné, P.; Derycke, S.; Hanel, R.; Lapegue, S.; Lejeusne, C.; Mousset, S. (2013). PCR survey of 50 introns in animals: Cross-amplification of homologous EPIC loci in eight non-bilaterian, protostome and deuterostome phyla. *Marine Genomics 12*: 1–8.

Girod, C.; Vitalis, R.; Lebois, R.; Freville, H. (2011). Inferring population decline and expansion from microsatellite data: a simulation-based evaluation of the MSvar methods. *Genetics 188*: 165–179.

Gjerde, K. M.; Reeve, L.; Harden-Davies, H.; Ardron, J.; Dolan, R.; Durussel, C.; et al. (2016). Protecting Earth's last conservation frontier: scientific, management and legal priorities for MPAs beyond national boundaries. *Aquatic Conservation: Marine and Freshwater Ecosystems 26*: 45–60.

Goudet, J. (2002). Fstat Vision (1.2): A Computer Program to Calculate F-Statistics. *Journal of Heredity 86*: 485–486.

Graham, E.M.; Baird, A.H. Connolly, S.R. (2008). Survival dynamics of scleractinian coral larvae and implications for dispersal. *Coral Reefs 27(3)*: 529–539.

Greenbaum, G.; Templeton, A.R.; Zarmi, Y.; Bar-David, S. (2014). Allelic richness following population founding events–a stochastic modeling framework incorporating gene flow and genetic drift. *PloS One 9(12)*: p.e115203.

Grohmann, C.H.; Riccomini, C.; Chamani, M.A.C. (2011). Regional scale analysis of landform configuration with base-level (isobase) maps. *Hydrology and Earth System Sciences 15:* 1493-1504 https://doi.org/10.5194/hess-15-1493-2011

Gu, Z.; Gu, L.; Eils, R.; Schelnser, M.; Brors, B. (2014). Circlize implements and enhances circular visualization in R. *Bioinformatics 30*: 2811–2812.

Hadfield, M; Uddstrom, M; Goring, D; Gorman, R; et al. (2002) Physical variables for the New Zealand Marine Environment Classification System: development and description of data layers. NIWA Client Report CHC2002-043. NIWA, Wellington

Hale, M.L.; Burg, T.M.; Steeves, T.E. (2012). Sampling for microsatellite-based population genetic studies: 25 to 30 individuals per population is enough to accurately estimate allele frequencies. *PloS One 7(9)*: e45170.

Hare, M.P.; Nunney, L.; Schwartz, M.K.; Ruzzante, D.E.; Burford, M.; Waples, R.S.; Ruegg, K.; Palstra, F. (2011). Understanding and estimating effective population size for practical application in marine species management. *Conservation Biology 25(3)*: 438–449.

Harpending, H. (1994). Signature of ancient population growth in a low-resolution mitochondrial DNA mismatch distribution. *Human Biology 66*: 591–600.
Harrison, P.L. (2011). Sexual Reproduction of Scleractinian Corals. *In*: Dubinsky Z.; Stambler N. (eds) Coral Reefs: An Ecosystem in Transition. Springer, Dordrecht. 552 p.
Hellberg, M.E. (2006). No variation and low synonymous substitution rates in coral mtDNA despite high nuclear variation. *BMC Evolutionary Biology 6*: 24.
Helson, J.; Leslie, S.; Clement, G.; Wells, R.; Wood, R. (2010). Private rights, public benefits: industry-driven seabed protection. *Marine Policy 34(3):* 557–566.
Herrera, S.; Shank, T.M. (2016a). RAD sequencing enables unprecedented phylogenetic resolution and objective species delimitation in recalcitrant divergent taxa. *Molecular Phylogenetics and Evolution 100*: 70–79.
Herrera, S.; Shank, T.M. (2016b) Comparative population structure patterns of deep-sea hydrothermal vent barnacle populations from seamounts. 14th International Deep Sea Biology Symposium, Aveiro, Portugal, 31st Aug-4th Sep 2015. Conference presentation.
Holland, L.P.; Dawson, D.A.; Horsburgh, G.J.; Krupa, A.P.; Stevens, J.R (2013). Isolation and characterization of fourteen microsatellite loci from the endangered octocoral *Eunicella verrucosa* (Pallas, 1766). *Conservation Genetics Resources 5*: 825–829.
Hughes, R.A.; Inouye, B.D.; Johnson, M.T.J.; Underwood, N.; Vellend, M. (2008). Ecological consequences of genetic diversity. *Ecology Letters 11(6)*: 609–623.
Hunter, R.L.; Halanych, K.M. (2008). Evaluating connectivity in the brooding brittle star *Astrotoma agassizii* across the Drake Passage in the Southern Ocean. *Journal of Heredity 99(2)*: 137–148.
Jarman, S.N.; Ward, R.D.; Elliott, N.G. (2002) Oligonucleotide primers for PCR amplification of coelomate introns. *Marine Biotechnology 4*: 347– 355.
Jenness, J; (2012) DEM Surface Tools. Jenness Enterprises. Available from: (http://www.jennesssent.com/arcgis/surface_area.htm)
Johannesson, K.; Andre, C. (2006). Life on the margin: genetic isolation and diversity loss in a peripheral marine ecosystem, the Baltic Sea. *Molecular Ecology 15*: 2013–2029.
Jombart, T. (2008). Adegenet: a R package for the multivariate analysis of genetic markers. *Bioinformatics 24(11)*: 1403–1405.
Jombart, T.; Devillard, S.; Balloux, F. (2010). Discriminant analysis of principal components: a new method for the analysis of genetically structured populations. *BMC Genetics 11*: 94.
Kalinowski, S.T. (2004). Counting alleles with rarefaction: Private alleles and hierarchical sampling designs. *Conservation Genetics 5(4)*: 539–543.
Kalinowski, S.T. (2005). HP-RARE 1.0: a computer program for performing rarefaction on measures of allelic richness. *Molecular Ecology Notes 5*: 187–189.
Kamvar, Z.N.; Tabima, J.F.; Grünwald, N.J. (2014). Poppr: an R package for genetic analysis of populations with clonal, partially clonal, and/or sexual reproduction. *PeerJ 2*: e281.
Kinlan, B.P.; Gaines, S.D. (2003). Propagule dispersal in marine and terrestrial environments: a community perspective. *Ecology 84*: 2007–2020.
Laikre, L.; Lundmark, C.; Jansson, E.; Wennerström, L.; Edman, M. and Sandström, A. (2016). Lack of recognition of genetic biodiversity: International policy and its implementation in Baltic Sea marine protected areas. *Ambio 45(6)*: 661–680.
Leathwick, J.; Moilanen, A.; Francis, M.; Elith, J.; Taylor, P.; Julian, K.; Hastie, T.; Duffy, C. (2008). Novel methods for the design and evaluation of marine protected areas in offshore waters. *Conservation Letters 1*: 91–102.
Leathwick, J.R.; Rowden, A.; Nodder, S.; Gorman, R.; Bardsley, S.; Pinkerton, M.; Baird, S.J.; Hadfield, M.; Currie, K.; Goh, A. (2012). A Benthic-optimised Marine Environment Classification for New Zealand waters. *New Zealand Aquatic Environment and Biodiversity Report No. 88*. 54 p.
Le Goff-Vitry, M.C.; Pybus, O.G.; Rogers, A.D. (2004). Genetic structure of the deep-sea coral *Lophelia pertusa* in the northeast Atlantic revealed by microsatellites and internal transcribed spacer sequences. *Molecular Ecology 13*: 537–549.
Li, Y.-C.; Korol, A.B.; Fahima, T.; Beiles, A.; Nevo, E. (2002). Microsatellites: genomic distribution, putative functions and mutational mechanisms: a review. *Molecular Ecology 11*: 2453–2465.

Librado, P.; Rozas, J. (2009). DnaSP v5: A software for comprehensive analysis of DNA polymorphism data. *Bioinformatics 25(11)*: 1451–1452.
Liggins, L.; Treml, E.A, Riginos, C. (2013). Taking the plunge: An introduction to undertaking seascape genetic studies and using biophysical models. *Geography Compass 7(3)*: 173–196.
Lotterhos, K.E.; Whitlock, M.C. (2014). Evaluation of demographic history and neutral parameterization on the performance of F_{ST} outlier tests. *Molecular Ecology 23(9)*: 2178–2192.
Lowe, W.H.; Allendorf, F.W. (2010). What can genetics tell us about population connectivity? *Molecular Ecology 19(15)*: 3038–51.
Luikart, G.; Allendorf, F.W.; Sherwin, W.B. (1998). Distortion of allele frequency distributions bottlenecks. *Journal of Heredity* 89: 238–247.
Luikart, G.; Cornuet, J.M. (1996). Empirical evaluation of a test for identifying recently bottlenecked populations from allele frequency data. *Conservation Biology 12*: 228–237.
Lutz, M.J.; Caldeira, K.; Dunbar, R. B.; Behrenfeld, M. J. (2007). Seasonal rhythms of net primary production and particulate organic carbon flux to depth describe the efficiency of biological pump in the global ocean. *Journal of Geophysical Research*: Oceans *112*, (C10011).
Mackay, K.A; (2007). Database documentation: SEAMOUNT. NIWA Internal Report No. 42. (Unpublished report held by NIWA library, Wellington.)
McInerney, C.E.; Allcock, A.L.; Johnson, M.P.; Prodöhl, P.A. (2012). Ecological coherence in marine reserve network design: An empirical evaluation of sequential site selection using genetic structure. *Biological Conservation 152*: 262–270.
Miller, K.J.; Gunasekera, R.M. (2017). A comparison of genetic connectivity in two deep sea corals to examine whether seamounts are isolated islands or stepping stones for dispersal. *Scientific Reports 7*: 46103.
Miller, K.J.; Rowden, A.A.; Williams, A.; Häussermann, V. (2011). Out of their depth? Isolated deep populations of the cosmopolitan coral *Desmophyllum dianthus* may be highly vulnerable to environmental change. *PloS One 6(5)*: e19004.
Miller, K.J.; Williams, A.; Rowden, A.A.; Knowles, C.; Dunshea, G. (2010). Conflicting estimates of connectivity among deep-sea coral populations. *Marine Ecology 31*: 144–157.
Mills, L.S.; Allendorf, F.W. (1996). The one-migrant-per-generation rule in conservation and management. *Conservation Biology 10(6):* 1509–1518.
Ministry for Primary Industries (2016). Aquatic Environment and Biodiversity Annual Review 2016. Compiled by the Fisheries Science Group, Ministry for Primary Industries, Wellington, New Zealand. 790 p.
Nei, M. (1987). Molecular Evolutionary Genetics. Columbia University Press, New York. 512 p.
Neigel, J.; Domingo, A.; Stake, J.; (2007). DNA barcoding as a tool for coral reef conservation. *Coral Reefs 26(3)*: 487–499.
Olsen, J.B.; Habicht, C.; Reynolds, J.; Seeb, J.E. (2004). Moderately and highly polymorphic microsatellites provide discordant estimates of population divergence in sockeye salmon, *Oncorhynchus nerka*. *Environmental Biology of Fishes 69(1–4)*: 261–273.
O'Driscoll, R.L.; Clark, M.R. (2005). Quantifying the relative intensity of fishing on New Zealand seamounts. *New Zealand Journal of Marine and Freshwater Research 39*: 839–850.
O'Reilly, P.T.; Canino, M.F.; Bailey, K.M.; Bentzen, P. (2004). Inverse relationship between F_{ST} and microsatellite polymorphism in the marine fish, walleye pollock (*Theragra chalcogramma*): implications for resolving weak population structure. *Molecular Ecology 13(7)*: 1799–1814.
Opresko, D.M. (1998). Three new species of *Leiopathes* (Cnidaria: Anthozoa: Antipatharia) from southern Australia. *Records of the South Australian Museum 31*: 99–111.
Opresko, D.M.; Tracey, D.A.; Mackay, E. (2014). Antipatharia (Black Corals) for the New Zealand Region. A field guide of commonly sampled New Zealand black corals including illustrations highlighting technical terms and black coral morphology. *New Zealand Aquatic Environment and Biodiversity Report No. 131*. 20 p.
Palumbi, S.R. (2003). Population genetics, demographic connectivity, and the design of marine reserves. *Ecological Applications 13*: S146–S158.
Parker, S.J.; Penney, A.J.; Clark, M.R. (2009). Detection criteria for managing trawl impacts on vulnerable marine ecosystems in high seas fisheries of the South Pacific Ocean. *Marine Ecology Progress Series 397*: 309–317.

Peakall, R.; Smouse, P.E. (2012). GenAlEx 6.5: genetic analysis in Excel. Population genetic software for teaching and research-an update. *Bioinformatics 28*: 2537–2539.

Penney, A.J.; Guinotte, J.M. (2013). Evaluation of New Zealand's high-seas bottom trawl closures using predictive habitat models and quantitative risk assessment. *PLoS One 8(12)*: e82273.

Penney, A.J.; Parker, S.J.; Brown, J.H. (2009). Protection measures implemented by New Zealand for vulnerable marine ecosystems in the South Pacific Ocean. *Marine Ecology Progress Series 397*: 341–354.

Pinkerton, M. H.; Moore, G.F; Lavender, S.J., Gall, M.P.; et al. (2006). A method for estimating inherent optical properties of New Zealand continental shelf waters from satellite ocean colour measurements. *New Zealand Journal of Marine and Freshwater Research 40*: 227–247.

Pinsky, M.L.; Palumbi, S.R. (2014). Meta-analysis reveals lower genetic diversity in overfished populations. *Molecular Ecology 23(1)*: 29–39.

Pires, D.O.; Silva, J.C.; Bastos, N.D. (2014). Reproduction of deep-sea reef-building corals from the southwestern Atlantic. *Deep Sea Research Part II: Topical Studies in Oceanography 99*: 51–63.

Pritchard, J.K.; Stephens, M.; Donnelly, P. (2000). Inference of population structure using multilocus genotype data. *Genetics 155*: 945–959.

Quattrini, A.M.; Baums, I.B.; Shank, T.M.; Morrison, C.L.; Cordes, E.E. (2015). Testing the depth-differentiation hypothesis in a deepwater octocoral. *Proceedings of the Royal Society B 282 (1807)*: 20150008.

R Core Team (2013). R version 3.0.2 (codename "Frisbee Sailing"): A language and environment for statistical computing. R Foundation for Statistical Computing, Vienna, Austria. URL http://www.R-project.org/

Ramos-Onsins, S.E.; Rozas, J. (2002). Statistical properties of new neutrality tests against population growth. *Molecular Biology and Evolution 19*: 2092–2100.

Raymond, M.; Rousset, F. (1995). GENEPOP (version 1.2): population genetics software for exact tests and ecumenicism. *Journal of Heredity 86*: 248–249.

Reed, D.H.; Frankham, D. (2003). Correlation between fitness and genetic diversity. *Conservation Biology 17(1):* 230–237.

Reveillaud, J.; Freiwald, A.; Van Rooij, D.; Le Guilloux, E.; Altuna, A.; Foubert, A.; Vanreusel, A.; Olu, K.; Henriet, J. (2008). The distribution of scleractinian corals in the Bay of Biscay, NE Atlantic. *Facies 54*: 317–331.

Reitzel, A.M.; Herrera, S.; Layden, M.J.; Martindale, M.Q; Shank, T.M. (2013). Going where traditional markers have not gone before: utility of and promise for RAD sequencing in marine invertebrate phylogeography and population genomics. *Molecular ecology 22(11)*: 2953–2970.

Riginos, C.; Liggins, L. (2013). Seascape genetics: Populations, individuals, and genes marooned and adrift. *Geographic Compass 7*: 197–216.

Roark, E.B.; Guilderson, T.P.; Dunbar, R.B.; Fallon, S.J.; Mucciarone, D.A. (2009). Extreme longevity in proteinaceous deep-sea corals. *Proceedings of the National Academy of Sciences of the United States of America 106(13)*: 5204–5208.

Rogers, A.D.; Baco, A.; Griffiths, H.; Hart, T.; Hall-Spencer, J.M. (2007). Corals on seamounts. *In*: Pitcher, T.J.; Morato, T.; Hart, P.J.B.; Clark, M.R.; Haggan, N.; Santos, R.S. (Eds.), pp. 141–169, *Seamounts: Ecology Fisheries and Conservation, Blackwell Fisheries and Aquatic Resources Series.*

Rogers, A.R.; Harpending, H. (1992) Population growth makes waves in the distribution of pairwise genetic differences. *Molecular Biology and Evolution 9*: 552–569.

Ross, P.M.; Hogg, I.D.; Pilditch, C.; Lundquist, C.J. (2009). Phylogeography of New Zealand's coastal benthos. *New Zealand Journal of Marine and Freshwater Research 43*: 1009–1027.

Rowden, A.A.; Oliver, M.; Clark, M.R.; Mackay, K. (2008). New Zealand's 'SEAMOUNT' database: recent updates and its potential use for ecological risk assessment. *New Zealand Aquatic Environment and Biodiversity Report No. 27*. 49 p.

Ruiz-Ramos, D.V.; Saunders, M.; Fisher, C.R.; Baums, I.B. (2015). Home bodies and wanderers: Sympatric lineages of the deep-sea black coral *Leiopathes glaberrima*. *PloS One 10(10)*: e0138989.

Sale, P.F.; Van Lavieren, H.; Lagman, M.A.; Atema, J.; Butler, M.; Fauvelot, C.; Hogan, J.D.; Jones, G.P.; Lindeman, K.C.; Paris, C.B.; Steneck, R. (2010). Preserving reef connectivity: A handbook for marine protected area managers. Connectivity Working Group. *Coral Reef Targeted Research and Capacity Building for Management Program, UNU-INWEH*.

Selkoe, K.; Toonen, R. (2011). Marine connectivity: a new look at pelagic larval duration and genetic metrics of dispersal. *Marine Ecology Progress Series 436*: 291–305.

Selkoe, K.A.; D'Aloia, C.C.; Crandall, E.D.; Iacchei, M.; Liggins, L.; Puritz, J.B.; et al. (2016). A decade of seascape genetics: Contributions to basic and applied marine connectivity. *Marine Ecology Progress Series 554*: 1–19.

Selkoe, K.A.; Henzler, C.M,. Gaines, S.D. (2008). Seascape genetics and the spatial ecology of marine populations. *Fish and Fisheries 9*: 363–377.

Sgro, C.M.; Lowe, A.J.; Hoffmann, A.A. (2011). Building evolutionary resilience for conserving biodiversity under climate change. *Evolutionary Applications 4(2)*: 326–337.

Shearer, T.L.; Van Oppen, M.J.H.; Romano, S.L.; Wörheide, G. (2002). Slow mitochondrial DNA sequence evolution in the Anthozoa (Cnidaria). *Molecular Ecology 11(12)*: 2475–2487.

Silva, C.N.S.; MacDonald, H.S.; Hadfield, M.; Cryer, M.; Gardner, J.P.A. (2019). Ocean currents predict fine scale genetic structure of a marine broadcast spawner. *ICES Journal of Marine Science 76:* 1007–1018.

Slatkin, M.; Hudson, R.R. (1991). Pairwise comparisons of mitochondrial DNA sequences in stable and exponentially growing populations. *Genetics 129*: 555–562.

Tajima, F. (1989). Statistical method for testing the neutral mutation hypothesis by DNA polymorphism. *Genetics 123*: 585–595.

Taylor, M.L.; Rogers, A.D. (2015). Evolutionary dynamics of a common sub-Antarctic octocoral family. *Molecular Phylogenetic and Evolution 84*: 185–204.

Thoma, J.N.; Pante, E.; Brugler, M.R.; France, S.C. (2009). Deep-sea octocorals and antipatharians show no evidence of seamount-scale endemism in the NW Atlantic. *Marine Ecology Progress Series 397*: 25–35.

Thornhill, D.J.; Mahon, A.R.; Norenburg, J.L.; Halanych, K.M. (2008). Open-ocean barriers to dispersal: a test case with the Antarctic Polar Front and the ribbon worm *Parborlasia corrugatus* (Nemertea: Lineidae). *Molecular Ecology 17*: 5104–5117.

Tittensor, D.P.; Baco, A.R.; Brewin, P.E.; Clark, M.R.; Consalvey, M.; Hall-Spencer, J.; Rowden, A.A.; Schlacher, T.; Stocks, K.I.; Rogers, A.D. (2009.) Predicting global habitat suitability for stony corals on seamounts. *Journal of Biogeography 36*(6): 1111–1128.

Tracey, D.M.; Rowden, A.A.; Mackay, K.A.; Compton, T. (2011). Habitat-forming cold-water corals show affinity for seamounts in the New Zealand region. *Marine Ecology Progress Series* 430: 1–22.

Tracey, D.M.; Bostock, H.; Currie, K.J.; Fletcher, S.E.M.; Williams, M.; Hadfield, M.; Neil, H.; Guy, C; Cummings, V.J. (2013). The potential impact of ocean acidification on deep-sea corals and fisheries habitat in New Zealand waters. *New Zealand Aquatic Environment and Biodiversity Report No. 117*. 101 p.

Treml, E.A.; Ford, J.R.; Black, K.P.; Swearer, S.E. (2015). Identifying the key biophysical drivers, connectivity outcomes, and metapopulation consequences of larval dispersal in the sea. *Movement Ecology 3*: 17.

Uddstrom, M.J.; Oien, N.A. (1999). On the use of high-resolution satellite data to describe the spatial and temporal variability of sea surface temperatures in the New Zealand region. *Journal of Geophysical Research Oceans 104(C9)*: 20729–20751.

Underwood, J.N.; Smith, L.D.; Van Oppen, M.J.; Gilmour, J.P. (2009). Ecologically relevant dispersal of corals on isolated reefs: implications for managing resilience. *Ecological Applications 19(1)*: 18–29.

United Nations General Assembly (2004). Sustainable fisheries, including through the 1995 Agreement for the Implementation of the Provisions of the United Nations Convention on the Law of the Sea of 10 December 1982 relating to the Conservation and Management of Straddling Fish Stocks and Highly Migratory Fish Stocks, and related instruments. General Assembly Resolution 59/25, 2004; A/RES/59/25.

United Nations General Assembly (2006). Sustainable fisheries, including through the 1995 Agreement for the Implementation of the Provisions of the United Nations Convention on the Law of the Sea of 10 December 1982 relating to the Conservation and Management of Straddling Fish Stocks and Highly Migratory Fish Stocks, and related instruments. General Assembly Resolution 61/105, 2006; A/RES/61/105.

van Oosterhout, C.; Hutchinson, W.F.; Wills, D.P.M. et al. (2004). MICRO-CHECKER: Software for identifying and correcting genotyping errors in microsatellite data. *Molecular Ecology Notes 4*: 535–538.

Wagner, D.; Luck, D.G.; Toonen, R.J. (2012). The Biology and Ecology of Black Corals (Cnidaria: Anthozoa: Hexacorallia: Antipatharia). *Advances in Marine Biology 63*: 67–132.

Wagner, D.; Waller, R.G.; Toonen, R.J. (2011). Sexual reproduction of Hawaiian black corals, with a review of reproduction of antipatharians (Cnidaria: Anthozoa: Hexacorallia). *Invertebrate Biology 130*: 211–225.

Waller, R.G. (2005). Deep-water Scleractinia (Cnidaria: Anthozoa): current knowledge of reproductive processes. *In* Freiwald, A.; Roberts, J.M. (Eds.), pp 691–700, *Cold-water Corals and Ecosystems*. Springer, Heidelberg.

Waller, R.G.; Baco-Taylor, A. (2007). Reproductive morphology of three Hawaiian deep-water precious corals. *Bulletin of Marine Science 81(3)*: 533–542.

Waller, R.G.; Tyler, P.A. (2005). The reproductive biology of two deep-water, reef-building scleractinians from the NE Atlantic Ocean. *Coral Reefs 24*: 514–522.

Waller, R.G.; Tyler, P.; Gage, J. (2002). Reproductive ecology of the deep-sea scleractinian coral *Fungiacyathus marenzelleri* (Vaughan, 1906) in the northeast Atlantic Ocean. *Coral Reefs 21(4)*: 325–331.

Walters, R.A.; Goring, D.G.; Bell, R.G. (2001). Ocean tides around New Zealand. *New Zealand Journal of Marine and Freshwater Research 35(3)*: 567–579.

Wang, J; (2017). The computer program STRUCTURE for assigning individuals to populations: easy to use but easier to misuse. *Molecular Ecology 15(5):* 981–990.

Waples, R.S.; Do, C. (2010). Linkage disequilibrium estimates of contemporary *Ne* using highly variable genetic markers: A largely untapped resource for applied conservation and evolution. *Evolutionary Applications 3(3)*: 244–262.

Watling, L.; Guinotte, J.; Clark, M. R.; Smith, C. R. (2013). A proposed biogeography of the deep ocean floor. *Progress in Oceanography 111*: 91–112.

Weersing, K.; Toonen, R.J. (2009). Population genetics, larval dispersal, and connectivity in marine systems. *Marine Ecology Progress Series 393*: 1–12.

Wei, K.J.; Wood, A.R.; Gardner, J.P.A. (2013a). Population genetic variation in the New Zealand greenshell mussel: Locus-dependent conflicting signals of weak structure and high gene flow balanced against pronounced structure and high self-recruitment. *Marine Biology 160*: 931–949

Wei, K.J.; Wood, A.R.; Gardner, J.P.A. (2013b). Seascape genetics of the New Zealand greenshell mussel: sea surface temperature explains macrogeographic scale genetic variation. *Marine Ecology Progress Series 477*: 107–121.

Weir, B.S.; Cockerham, C.C. (1984). Estimating f-statistics for the analysis of population-structure. *Evolution 38(6)*: 1358–1370.

White, T.J.; Bruns, T.; Lee. S.; Taylor, J. (1990). Amplification and direct sequencing of fungal ribosomal RNA genes for phylogenetics. *In*: *PCR protocols: a guide to methods and applications*. Academic Press, San Diego.

Williams, A.; Schlacher, T.A.; Rowden, A.A.; Althaus, F.; Clark, M.R.; Bowden, D.A.; Stewart, R.; Bax, N.J.; Consalvey, M.; Kloser, R.J. (2010). Seamount megabenthic assemblages fail to recover from trawling impacts. *Marine Ecology 31*: 183–199.

Williams, J.; Morgenstern, O.; Varma, V.; Behrens, E.; Hayek, W.; Oliver, H.; Dean, S.; Mullan, B.; Frame, D. (2016) Development of the New Zealand Earth System Model: NZESM. *Weather and Climate 36*: 25–44.

Wilson, G.A.; Rannala, B. (2003). Bayesian inference of recent migration rates using multilocus genotypes. *Genetics 163*: 1177–1191.

Wright, S. (1922). Coefficients of inbreeding and relationship. *The American Naturalist 56(645)*: 330–338.

Wright, S. (1951). The genetical structure of populations. *Annals of Eugenics 15(4)*: 323–354.

Wright, D.J.; Lundblad, E.R.; Larkin, E.M.; Rinehart, R.W.; Murphy, J.; Cary-Kothera, L.; Draganov, K. (2005). ArcGIS Benthic Terrain Modeler. Corvallis, Oregon, Oregon State University, Davey Jones Locker Seafloor Mapping/ Marine GIS Laboratory and NOAA Coastal Services Center. Accessible online at: ⟨http://www.csc.noaa. gov/digitalcoast/tools/btm⟩.

Wright, L.I.; Treganza, T.; Hosken, D.J. (2008). Inbreeding, inbreeding depression and extinction. *Conservation Genetics 9(4)*: 833–843.

Yan, R-J.; Schnabel, K.E.; Rowden, A.A.; Guo, X-Z.; Gardner, J.P.A. (2020). Patterns of population structure and genetic connectivity of squat lobsters (*Munida* Leach, 1820) associated with Vulnerable Marine Ecosystems in the southwest Pacific Ocean. *Frontiers in Marine Science*, 6: p 791.

Zeng, C. (2016). Patterns of genetic connectivity in deep-sea vulnerable marine ecosystems and implications for conservation. PhD Thesis, Victoria University of Wellington, New Zealand. 286 p.

Zeng, C.; Clark, M.R.; Rowden, A.A.; Kelly, M.; Gardner, J.P.A. (2019). Patterns of genetic connectivity amongst four deep-sea demosponges in the New Zealand region: implications for the protection of Vulnerable Marine Ecosystems. *Scientific Reports 9 (1):* 1–13.

Zeng, C.; Rowden, A.R.; Clark, M.R.; Gardner, J.P.A. (2017). Population genetic structure and connectivity of deep-sea stony corals (Order Scleractinia) in the New Zealand region: implications for the conservation and management of Vulnerable Marine Ecosystems. *Evolutionary Applications 10 (10):* 1040–54.

Zeng, C.; Rowden, A.A.; Clark, M.R.; Gardner, J.P.A. (2020). Species-specific genetic variation in response to deep-sea environmental variation amongst Vulnerable Marine Ecosystem indicator taxa. *Scientific Reports 10 (1):* 1–15.

10. TABLES AND FIGURES

Table 1: Number of individual coral colonies from which DNA of sufficient quality could be extracted and amplified for each molecular marker. The number of individuals included for *D. dianthus* microsatellite analyses varies due to splitting data into a spatial framework (e.g., according to bioprovince, region or geomorphic feature) and/or into neutral vs. selected loci, given that population size definitions in each analysis had a minimum locus and population size threshold. [nDNA – nuclear DNA, mtDNA – mitochondrial DNA].

	ITS (nDNA)	16S (mtDNA)	ND5 (mtDNA)	TRP (mtDNA)	Microsatellites (nDNA)
Desmophyllum dianthus	153	–	–	–	346–376
Enallopsammia rostrata	80	–	–	–	–
Bathypathes patula	–	60	56	60	–
Leiopathes spp.	–	–	–	–	53

Table 2: Environmental variables used for seascape genetics analyses. Y and N indicate if the variable was included in the analysis (Yes and No) and 1 km indicates the resolution of that variable.

	Variable	Abbreviation	Unit	Source	In *E. rostrata* analysis?	In *D. dianthus* analysis?
Topography	Bathymetric Position Index – Broad	*bpi-broad*		Wright et al. (2005)	Y	Y
	Bathymetric Position Index – Fine	*bpi-fine*		Wright et al. (2005)	Y	Y
	Depth	*depth*	m		Y	Y
	Depth	*bathy*	m	CANZ (2008)	Y (1 km)	N
	Seamount	*seamount*	binomial		Y	Y
	Seamount	*smt*	–	Rowden et al. (2008), Mackay (2007)	Y (1 km)	N
	Slope in percent	*slope-percent*	percent	Jenness (2012)	Y	Y
	Standard Deviation of Slope	*stdev-slope*		Grohmann et al. (2011), 3x3 window	Y	Y
Physico-chemical	Aragonite saturation state	*arag*	Ωaragonite	Bostock et al. (2013b), Tracey et al. (2013)	Y (1 km)	N
	Bottom current speed	*botspd*			Y (1 km)	N
	Bottom water temperature	*tempbot*	°C	CARS (2009) (www.cmar.csiro.au/cars)	Y (1 km)	N
	Bottom water temperature residuals	*tempres*	-	CARS (2009), Leathwick et al. (2012)	Y (1 km)	N
	Calcite saturation state	*calc*	Ωcalcite	Bostock et al. (2013b), Tracey et al. (2013)	Y (1 km)	N
	Dissolved organic matter	*disorg*			Y (1 km)	N
	Dissolved organic matter	*cdom*	*aDOM (443)* m^{-1}	Pinkerton et al. (2006)	Y (1 km)	N
	Dynamic topography	*dynoc*	m	AVISO http://www.aviso.oceanobs.com	Y (1 km)	N
	Nitrate	*woanitc*		Garcia et al. (2006)	Y	Y
	Omega Aragonite	*aragonite*	Ω_{ARAG}	Mike Williams (NIWA)	Y	Y
	Omega Calcite	*calcite*	Ω_{CALC}	Mike Williams (NIWA)	Y	Y
	Oxygen	*oxygen*	ml l^{-1}	Mike Williams (NIWA)	Y	Y
	Phosphate	*woaphosc*		Garcia et al. (2006)	Y	Y
	Salinity	*salinity*	pss	Mike Williams (NIWA)	Y	Y
	Sea surface temperature	*sst*			Y (1 km)	N
	Sea surface temperature gradient	*sstgrad*	°C km^{-1}	Uddstrom & Oien (1999), Hadfield et al. (2002)	Y (1 km)	N
	Sigma Theta	*sigma-theta*	kg m^{-3}	Mike Williams (NIWA)	Y	Y
	Silicate	*silicate*	µmol l^{-1}	Garcia et al. (2006b)	Y	Y
	Temperature	*temperature*	°C	Mike Williams (NIWA)	Y	Y
	Tidal current speed	*tidalcurr*	ms^{-1}	Walters et al. (2001), Hadfield et al. (2002)	Y (1 km)	N
Biological	Particulate organic carbon export	*POC*	mg C m^{-2} d^{-1}	Lutz et al. (2007)	Y	Y
	Surface water primary productivity	*vpgm*	mg C m^{-2} d^{-1}	Behrenfield & Falkowski (1997)	Y (1 km)	N

Table 3: Genetic diversity, population expansion, and neutrality tests for *Desmophyllum dianthus* ITS sequence data. π nucleotide diversity and haplotype diversity (Nei 1987), raggedness statistic (Harpending 1994), Tajima's D (Tajima 1989), Fu and Li's F (Fu & Li 1993), and Ramos-Onsins and Rozas R2 statistic (Ramos-Onsins & Rozas 2002). Tajima's D and Fu and Li's F statistic based upon the total number of mutations. R_2 statistic p values were obtained from coalescent simulations in DNASp (95% confidence interval with 1000 replicates) using Theta estimated from the data, with no recombination[1], an intermediate level obtained from the data[2], and free recombination[3]. All values calculated in DNASp v.5 (Librado & Rozas 2009). Significant values are shown in bold.

Population	N	No. polymorphic sites	π	Haplotype (gene) Diversity	Raggedness Statistic	Tajima's D	Fu and Li's F	R_2	est. recomb (p)	p-value [1]	p-value [2]	p-value [3]
Louisville Seamount Chain	22	2	0.001	0.177	0.4502	-1.514	-2.381	0.1437	>1000	0.699	0.69	0.66
Kermadec Ridge region	12	6	0.003	0.455	0.1864	-1.894	-2.505	0.1596	0.001	0.898	0.886	0.942
Chatham Rise	105	6	0.001	0.115	0.5596	-1.726	-2.736	0.0354	0.001	0.532	0.547	0.535
Campbell Plateau	13	3	0.004	0.538	0.7929	2.121	1.532	0.2692	2.099	1	1	1

Table 4: ***Desmophyllum dianthus*** **genetic diversity and heterozygosity based upon microsatellite variation. N: sample number, Ar: allelic richness (average number of alleles at a locus), Ar (private): number of unique alleles in a population, k (mean): average number of alleles per individual of the given population, H*o*: observed heterozygosity, H*e*: expected heterozygosity.**

	Population	N	Ar	Ar (private)	K (mean)	H_0	H*e*
Region	North	134	5.46	1.92	12.8	0.483	0.513
	Central	216	4.95	1.48	17.8	0.420	0.576
	South	26	4.5	0.85	6	0.336	0.476
Geomorphic features	Louisville Seamount Chain	107	3.16	0.85	14	0.558	0.618
	Kermadec ridge region	27	3.22	0.78	8.4	0.542	0.624
	Chatham Rise	216	2.8	0.85	16.6	0.424	0.553
	Macquarie Ridge	6	2.14	0.38	2.4	0.248	0.265
	Campbell Plateau	8	3.03	0.58	3.6	0.431	0.458

Table 5: ***Enallopsammia rostrata*** **genetic diversity based upon ITS DNA sequence variation at the bioprovince, regional, and geomorphic features scale as calculated in DNASp v.5 (Librado & Rozas 2009).**

	Number of sequences	Number of polymorphic sites	Number of haplotypes	Haplotype diversity	Average number of differences
Bioprovince					
Northern	68	9	12	0.85	2.06
Southern	12	15	7	0.88	2.77
Region					
North	6	6	5	0.93	2.67
Central	62	7	9	0.82	1.93
South	12	15	7	0.88	2.77
Geomorphic Feature					
Campbell Plateau	11	12	6	0.85	2.47
Norfolk Ridge	2	2	2	1.00	2.00
Kermadec Ridge region	2	3	2	1.00	3.00
Challenger Plateau	2	1	2	1.00	1.00
Chatham Rise	62	7	9	0.82	1.93

Table 6: DNA sequence diversity of *Bathypathes patula* calculated in DNASp v.5 (Librado & Rozas 2009). N - number of samples; π - nucleotide diversity; number of polymorphic sites refers to sites at which polymorphism, indels, or missing data occur and haplotype diversity (with gaps considered a fifth character).

Gene	Bioprovince	N	No. polymorphic sites	π	Haplotype (gene) Diversity
ND5	North	28	9	0.008	0.78
	South	14	8	0.005	0.396
	Antarctica	13	10	0.007	0.679
TRP	North	28	13	0.007	0.78
	South	17	7	0.004	0.404
	Antarctica	14	7	0.003	0.385
16S	North	30	9	0.003	0.543
	South	15	1	0	0.133
	Antarctica	13	2	0.001	0.154
Concatenated	North	23	80	0.006	0.862
sequences	South	12	15	0.002	0.576
	Antarctica	10	16	0.003	0.844

Table 7: *Leiopathes* spp. and *Leiopathes secunda* allelic richness. *Leiopathes* spp. results are based upon a minimum sample size of 2 individuals and *L. secunda* on 4 individuals as calculated in FSTAT v2.9.3.2 (Goudet 2002).

	Leiopathes spp.		*Leiopathes secunda*	
Geomorphic Feature	N	Ar	N	Ar
Bay of Plenty	7	2.147	7	2.963
Challenger Plateau	8	2.127	8	2.669
Chatham Rise	11	2.416	13	2.776
Hikurangi Trough	16	2.154		
Kermadec Ridge region	4	2.397		

Table 8: Hierarchical Analysis of Molecular Variance (AMOVA) for *Desmophyllum dianthus* microsatellite data (Top, all loci dataset) and ITS sequence data (Bottom) based upon bioprovinces, regions, and geomorphic features as calculated in Arlequin v3.5 (Excoffier & Lischer 2010). Significant values of P <0.05 are marked as *, and P < 0.01 are marked as **. Bold rows represent significant differences (at the regional and geomorphic features scales).

ALL LOCI		Sum of		Variance	Percentage
Source of Variation	d.f.	Squares		components	of variation
Between provinces	1	-5.545	Va	-0.085	-3.88
Amongst individuals within pops	374	987.558	Vb	0.379**	17.43
Within individuals	376	707.5	Vc	1.882**	86.45
Total	**751**	**1689.513**		**2.177**	**100**
Between regions	2	163.368	Va	0.393**	16.16
Amongst individuals within pops	373	818.646	Vb	0.157**	6.44
Within individuals	376	707.5	Vc	1.882**	77.4
Total	**751**	**1689.513**		**2.431**	**100**
Between geomorphic features	4	152.448	Va	0.355**	14.7
Amongst individuals within pops	359	799.524	Vb	0.166**	6.89
Within individuals	364	689.5	Vc	1.894**	78.41
Total	**727**	**1641.473**		**2.416**	**100**
ITS SEQUENCE DATA					
Between provinces	1	-5.545	Va	3.486	-70.76
Amongst individuals within pops	3	65.272	Vb	1.114**	111.8
Within individuals	148	86.935	Vc	0.587**	58.96
Total	**152**	**155.693**		**0.996**	**100**
Between regions	2	67.938	Va	0.942	62.44
Amongst individuals within pops	2	0.82	Vb	-0.020**	-1.35
Within individuals	148	86.935	Vc	0.587**	38.92
Total	**152**	**155.693**		**1.509**	**100**
Between geomorphic features	4	15.32	Va	0.161**	38.62
Amongst individuals within pops	16	8.601	Vb	0.056**	13.45
Within individuals	133	26.495	Vc	0.199**	47.93
Total	**153**	**50.416**		**0.416**	**100**

Table 9: ***Desmophyllum dianthus*** **pairwise F_{ST} values between regions (top) and geomorphic features (bottom) based upon microsatellite data, as calculated in Arlequin v3.5 (Excoffier & Lischer 2010). Both 'all loci' (left) and 'neutral loci' (right) datasets were tested. Significant values following false discovery rate correction for multiple tests (Benjamini & Hochberg 1995) are shown in bold.**

		ALL LOCI					NEUTRAL LOCI				
Regions		North	Central	South			North	Central	South		
	North	0.000					0.000				
	Central	**0.194**	0.000				**0.173**	0.000			
	South	**0.010**	**0.028**	0.000			-0.012	**0.084**	0.000		
Geomorphic Features		Louisville Seamount Chain	Kermadec Ridge region	Chatham Rise	Macquarie Ridge	Campbell Plateau	Louisville Seamount Chain	Kermadec Ridge region	Chatham Rise	Macquarie Ridge	Campbell Plateau
	Louisville Seamount Chain	0.000					0.000				
	Kermadec Ridge region	-0.012	0.000				-0.013	0.000			
	Chatham Rise	**0.203**	**0.162**	0.000			**0.178**	**0.174**	0.000		
	Macquarie Ridge	-0.036	-0.002	-0.176	0.000		-0.059	0.007	-0.135	0.000	
	Campbell Plateau	-0.164	-0.125	-0.196	-0.082	0.000	-0.075	-0.016	-0.044	-0.063	0.000

Table 10: ***Desmophyllum dianthus*** **population pairwise Φ_{ST} (sequence-based F_{ST} analog) between populations on geomorphic features based upon ITS DNA sequence data. Significant values following false discovery rate correction for multiple testing (Benjamini & Hochberg 1995) are shown in bold.**

	Fiordland	Chatham Rise	Campbell Plateau	Kermadec Ridge region	Louisville Seamount Chain
Fiordland	0.000				
Chatham Rise	0.831	0.000			
Campbell Plateau	-0.167	**0.525**	0.000		
Kermadec Ridge region	-0.909	**0.788**	0.162	0.000	
Louisville Seamount Chain	-1.000	**0.847**	**0.413**	0.26	0.00

Table 11: ***Enallopsammia rostrata*** **geomorphic features pairwise population Φ_{ST} values based upon ITS DNA sequence data as calculated in Arlequin v3.5 (Excoffier & Lischer 2010). Significant values are shown in bold.**

	Campbell Plateau	Challenger	Chatham Rise	Kermadec Ridge region	Norfolk Ridge
Campbell Plateau	0.000				
Challenger Plateau	-0.236	0.000			
Chatham Rise	**0.408**	0.366	0.000		
Kermadec Ridge region	0.120	0.000	0.254	0.000	
Norfolk Ridge	**0.515**	0.571	**0.365**	0.167	0.000

Table 12: Hierarchical Analysis of Molecular Variance (AMOVA) for *Enallopsammia rostrata* ITS DNA sequence data as calculated in Arlequin v3.5 (Excoffier & Lischer 2010). Significant values of P <0.05 are marked as *, and P < 0.01 are marked as **.

ITS DNA SEQUENCE DATA Source of Variation		d.f.	Sum of squares		Variance components	Percentage of variation
Between bioprovinces		1	10.716	Va	0.144	9.26
Amongst individuals within pops		4	9.338	Vb	0.407**	26.19
Within individuals		74	74.170	Vc	1.002**	64.55
	Total	79	94.225		1.553	100.00
Between regions		2	13.502	Va	-0.113	-7.56
Amongst individuals within pops		3	6.553	Vb	0.608	40.61
Within individuals		74	74.170	Vc	1.002**	66.95
	Total	79	94.225		1.500	100.00
Between geomorphic features		3	14.277	Va	-0.466	14.7
Amongst individuals within pops		2	5.621	Vb	0.956	6.89
Within individuals		74	72.352	Vc	0.978**	78.41
	Total	79	92.250		1.468	100.00

Table 13: *Bathypathes patula* pairwise Φ_{ST} values between bioprovinces based upon concatenated 16S, ND5, and TRP DNA sequence data, as calculated in Arlequin v3.5 (Excoffier & Lischer 2010). Significant values are shown in bold.

	North	South	Antarctica
North	0.000		
South	**0.073**	0.000	
Antarctica	**0.190**	**0.664**	0.000

Table 14: ***Leiopathes*** **spp. pairwise** F_{ST} **values between populations on geomorphic features, based upon two microsatellite datasets - either all samples of** ***Leiopathes*** **identified at the genus level (left) or upon** ***Leiopathes secunda*** **only (right), as calculated in Arlequin v3.5 (Excoffier & Lischer 2010). Bold type indicates significant values.**

All *Leiopathes*

Regions	Bay of Plenty	Challenger Plateau	Chatham Rise	Hikurangi Trough	Kermadec Ridge region
Bay of Plenty					
Challenger Plateau	0.095				
Chatham Rise	0.073	0.022			
Hikurangi Trough	0.076	-0.002	0.017		
Kermadec Ridge region	0.124	**0.174**	0.094	**0.158**	

Leiopathes secunda

	Challenger Plateau	Chatham Rise	Hikurangi Trough
Challenger Plateau			
Chatham Rise	0.040		
Hikurangi Trough	-0.013	0.009	

Table 15: Genetic diversity, population expansion, and neutrality tests for *Bathypathes patula* sequence data (16S, TRP, and ND5, analysed separately). π nucleotide diversity and haplotype diversity (Nei 1987), raggedness statistic (Harpending 1994), Tajima's D (Tajima 1989), Fu and Li's F (Fu & Li 1993), and Ramos-Onsins and Rozas R2 statistic (Ramos-Onsins & Rozas 2002). Tajima's D and Fu and Li's F statistic based upon the total number of mutations. R^2 statistic p values were obtained from coalescent simulations in DNASp (95% confidence interval with 1000 replicates) using Theta estimated from the data, with no recombination[1], an intermediate level obtained from the data[2], and free recombination[3] (no significant values found). All values calculated in DNASp v.5 (Librado & Rozas 2009).

Marker	Population	N	No. poly-morphic sites	π	Haplotype (gene) Diversity	Raggedness Statistic	Tajima's D	Fu and Li's F	R^2	est. recomb (p)	p-value [1]	p-value [2]	p-value [3]
16S	Antarctica	13	2	0.001	0.154	0.7633	1.468	-1.921	0.2665	0.001	0.667	0.700	0.740
	North	30	9	0.003	0.543	0.2348	-1.089	-0.696	0.0783	0.07	0.068	0.722	0.044
	South	15	1	0.001	0.133	0.5556	-1.159	-1.543	0.2494	>1000	0.842	0.819	0.855
TRP	Antarctica	14	7	0.003	0.385	0.3664	-0.798	0.405	0.1189	0.001	0.088	0.092	0.131
	North	28	13	0.007	0.78	0.3556	-0.077	-0.445	0.1409	2.5	0.723	0.722	0.804
	South	17	7	0.004	0.404	0.5637	-0.044	0.581	0.1417	0.001	0.468	0.442	0.533
ND5	Antarctica	13	10	0.007	0.679	0.1629	-0.848	-0.429	0.1265	0.001	0.066	0.067	0.114
	North	28	9	0.008	0.78	0.0871	1.014	0.798	0.1671	3.5	0.471	0.328	0.035
	South	14	8	0.005	0.396	0.4136	-0.822	0.050	0.1138	0.001	0.693	0.716	0.231

Table 16: Tests for evidence of *Desmophyllum dianthus* genetic bottlenecks according to the software BOTTLENECK v1.2.02 (Cornuet & Luikart 1996) under the infinite alleles (IAM), two phase model (TPM, allowing 10% SMM), and stepwise mutation model (SMM) assuming mutation-drift equilibrium. Neutral microsatellite markers only were tested (5 loci). He E expected number of loci with heterozygosity excess, H D/E numbers of loci with heterozygosity deficiency / heterozygosity excess. Wilcoxon sign ranked tests show P-value for one tail probability for heterozygote deficiency (HD) and heterozygote excess (HE). Bold P-values represent significance at the 5% level (i.e., showing evidence of a bottleneck) under Sign or Wilcoxon sign ranked tests after 1000 iterations. n/a: prohibitively few individuals from the Macquarie Ridge and Campbell Plateau.

	IAM					TPM					SMM					Mode-shift
Population	He E	H D/E	Sign Test	Wilcoxon HD	Wilcoxon HE	He E	E/D	Sign Test	Wilcoxon test	Wilcoxon test (1 tail H excess)	He E	E/D	Sign Test	Wilcoxon HD	Wilcoxon HE	
North	3	1/4	0.337	0.891	0.3125	2.9	4/1	0.103	**0.031**	0.984	2.96	5/0	**0.011**	**0.016**	1.000	L-shaped
Central	3.01	5/0	**0.010**	**0.016**	1.000	2.94	5/0	**0.012**	**0.016**	1	2.87	5/0	**0.014**	**0.016**	1.000	L-shaped
South	2.97	1/4	0.326	0.891	0.3125	2.97	4/1	0.091	0.109	0.922	2.93	4/1	0.098	**0.031**	0.984	L-shaped
Louisville Seamount Chain	3.01	1/4	0.342	0.891	0.3125	3.02	2/3	0.657	0.500	0.594	3.06	5/0	**0.009**	**0.016**	1.000	L-shaped
Kermadec Ridge region	3.05	2/3	0.647	0.406	0.6875	3.03	2/3	0.654	0.406	0.688	2.96	5/0	**0.011**	**0.016**	1.000	L-shaped
Chatham Rise	3.07	5/0	**0.009**	**0.016**	1.000	2.99	5/0	**0.011**	**0.016**	1.000	2.93	5/0	**0.012**	**0.016**	1.000	L-shaped
Macquarie Ridge	n/a					n/a					n/a					n/a
Campbell Plateau	n/a					n/a					n/a					n/a

Table 17: TOP: Historical gene flow (*M*) and effective population size (N_e) estimates for *Desmophyllum dianthus* using Migrate-n (Beerli & Felsenstein 2001). Historical N_e was calculated using the equation: N_e = theta/4μ, assuming a mutation rate (μ) of 5×10^{-4} per locus per generation (Garza & Williamson 2001). Left hand column in the matrix represents a source population whereas the row represents a sink. BOTTOM: Contemporary gene flow (m) and effective population size (N_e) estimates for *D. dianthus* calculated by BayesAss (Wilson & Rannala 2003) and NeEstimator respectively (Do et al. 2014).

		Historical gene flow (*M*)					Theta	*Ne*
	Geomorphic Feature	Louisville Seamount Chain	Kermadec Ridge region	Chatham Rise	Macquarie Ridge	Campbell Plateau		
Neutral Loci dataset	Louisville Seamount Chain	–	6128.890	86.428	49.322	24.264	1.703	851.5
	Kermadec Ridge region	31.070	–	33.950	322.600	24.460	6.738	3368.8
	Chatham Rise	28.560	44.368	–	69.323	22.031	0.041	20.3
	Macquarie Ridge	25.305	37.662	38.117	–	23.184	5.740	2870.4
	Campbell Plateau	36.612	51.119	48.687	61.888	–	9.514	4756.9
All Loci dataset	Louisville Seamount Chain	–	63.107	35.446	23.771	21.172	0.324	161.8
	Kermadec Ridge region	41.473	–	26.538	21.475	20.742	9.462	4731.1
	Chatham Rise	28.300	29.448	–	29.975	22.253	0.373	186.4
	Macquarie Ridge	23.412	30.588	31.981	–	19.972	13.090	6545.1
	Campbell Plateau	30.405	38.283	21.759	22.242	–	18.636	9317.9
		Contemporary gene flow (m)						*Ne*
Neutral Loci dataset	Louisville Seamount Chain	0.984	0.003	0.007	0.003	0.003		∞
	Kermadec Ridge region	0.277	0.677	0.025	0.011	0.011		∞
	Chatham Rise	0.016	0.002	0.980	0.002	0.002		∞
	Macquarie Ridge	0.039	0.030	0.204	0.697	0.030		∞
	Campbell Plateau	0.141	0.026	0.115	0.026	0.692		∞
All Loci dataset	Louisville Seamount Chain	0.985	0.003	0.006	0.003	0.003		∞
	Kermadec Ridge region	0.271	0.677	0.031	0.010	0.010		∞
	Chatham Rise	0.013	0.002	0.982	0.002	0.002		∞
	Macquarie Ridge	0.031	0.030	0.212	0.697	0.030		∞
	Campbell Plateau	0.145	0.026	0.111	0.026	0.692		∞

Table 18: *Desmophyllum dianthus* effective population size *Ne* calculations, based upon two Pcrit values and two datasets (neutral and all loci) for populations associated with regions and geomorphic features. Values are derived from NeEstimator (Do et al. 2014).

Population	*Ne* Estimator Locus dataset		N	Pcrit 0.05 *Ne*	Cis for *Ne*		Pcrit 0.02 *Ne*	Cis for *Ne*	
					Parametric			Parametric	
Geomorphic features	All	Louisville Seamount Chain	107	780.2	188	∞	766.8	262.5	∞
	All	Kermadec Ridge region	27	179.2	34.3	∞	∞	76.3	∞
	All	Chatham Rise	216	∞	458.6	∞	∞	1422.3	∞
	All	Macquarie Ridge	6	∞	1.6	∞	∞	1.6	∞
	All	Campbell Plateau	8	∞	1.2	∞	∞	1.2	∞
	Neutral	Louisville Seamount Chain	106	6304.7	134.7	∞	363.4	131	∞
	Neutral	Kermadec Ridge region	27	27.4	10.5	∞	∞	38.8	∞
	Neutral	Chatham Rise	205	∞	351.2	∞	∞	389.3	∞
	Neutral	Macquarie Ridge	6	∞	0.6	∞	∞	0.6	∞
	Neutral	Campbell Plateau	8	21.7	0.8	∞	21.7	0.8	∞
Region	All	North	134	416.4	170.7	∞	995.8	321	∞
	All	Central	216	∞	458.6	∞	∞	1422.3	∞
	All	South	26	13.0	5.5	47.7	16.7	9.2	39.2
	Neutral	North	133	537.5	124.4	∞	12204.8	255.8	∞
	Neutral	Central	203	∞	351	∞	∞	389.5	∞
	Neutral	South	26	7.4	2.1	112.3	14.2	3.9	1671.8

Table 19: Seascape genetics GLM results for *D. dianthus*, based upon mean F_{ST} values and 11 environmental variables and for *E. rostrata* on mean Φ_{ST} values and eight environmental variables.

	Variable	Log-Likelihood*	χ^2	*p* value
Desmophyllum dianthus F_{ST}	bpi-fine	31.56	16.428	<0.001
	stdev-slope	32.42	14.712	<0.001
	slope-percent	36.13	7.282	0.007
Enallopsammia rostrata Φ_{ST}	bpi-fine	7.312	4.947	0.026

*The Maximum likelihood Type III test (incremental χ^2 statistic) was used for DDI and the ML Type 1 was used for ERO.

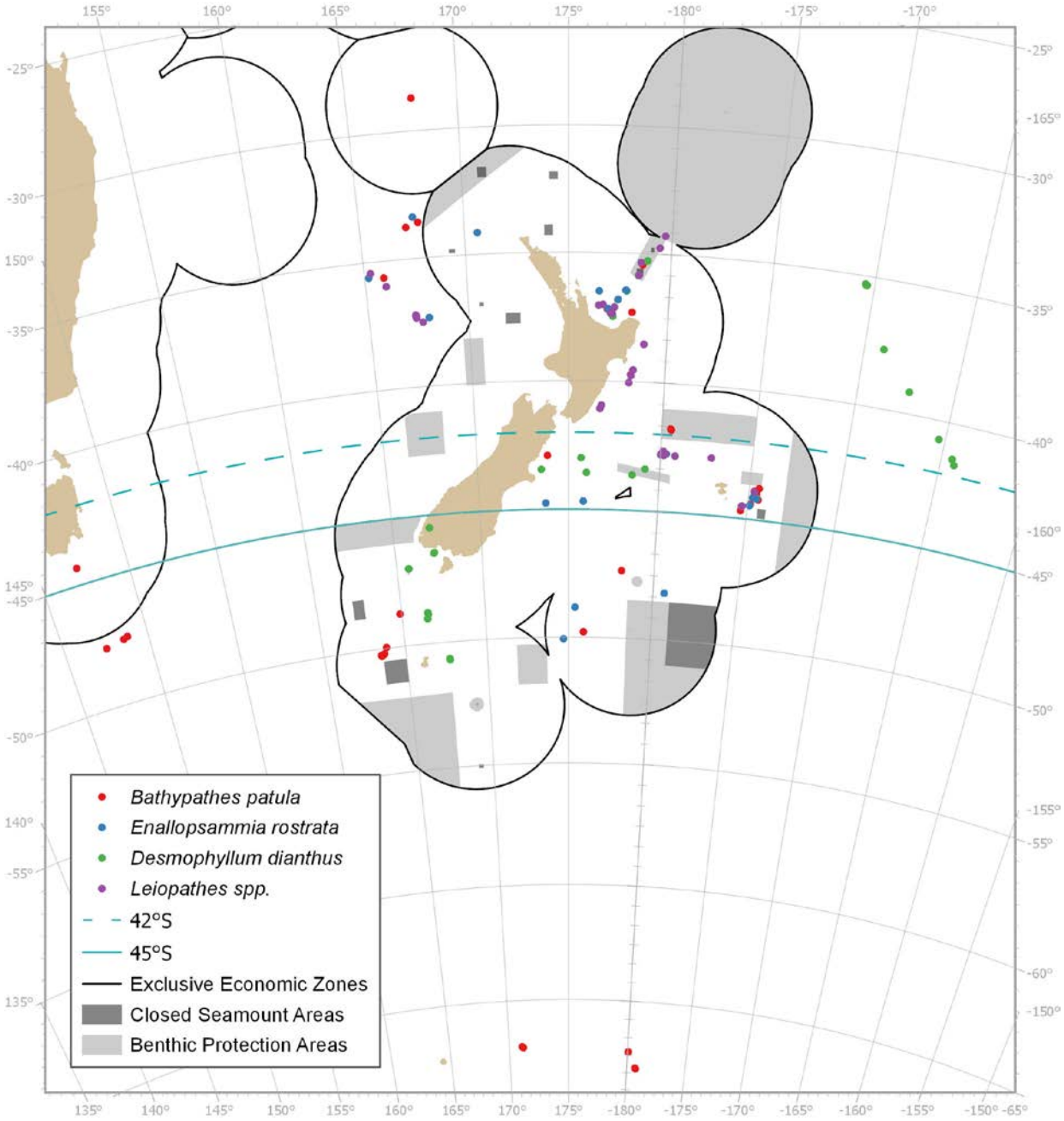

Figure 1: Map showing sample collections of all species, relative to current Benthic Protection Areas and seamount closures within New Zealand's EEZ (outlined in black). Solid blue line denotes boundary between the bioprovionces BY6 (New Zealand-Kermadec) and BY10 (Sub-Antarctic) *sensu* Watling et al. (2013), delineating bioprovinces in this study (45° S, south of the Chatham Rise). Dashed blue line denotes boundary between north and central region at 42° S (with solid line forming lower boundary of the central region with the south region) for the regional scale analysis. Individual species maps (Figure 2) clarify sample locations where points here overlap. Map generated in NABIS (http://nabis.network.maf.govt.nz/NabisHome).

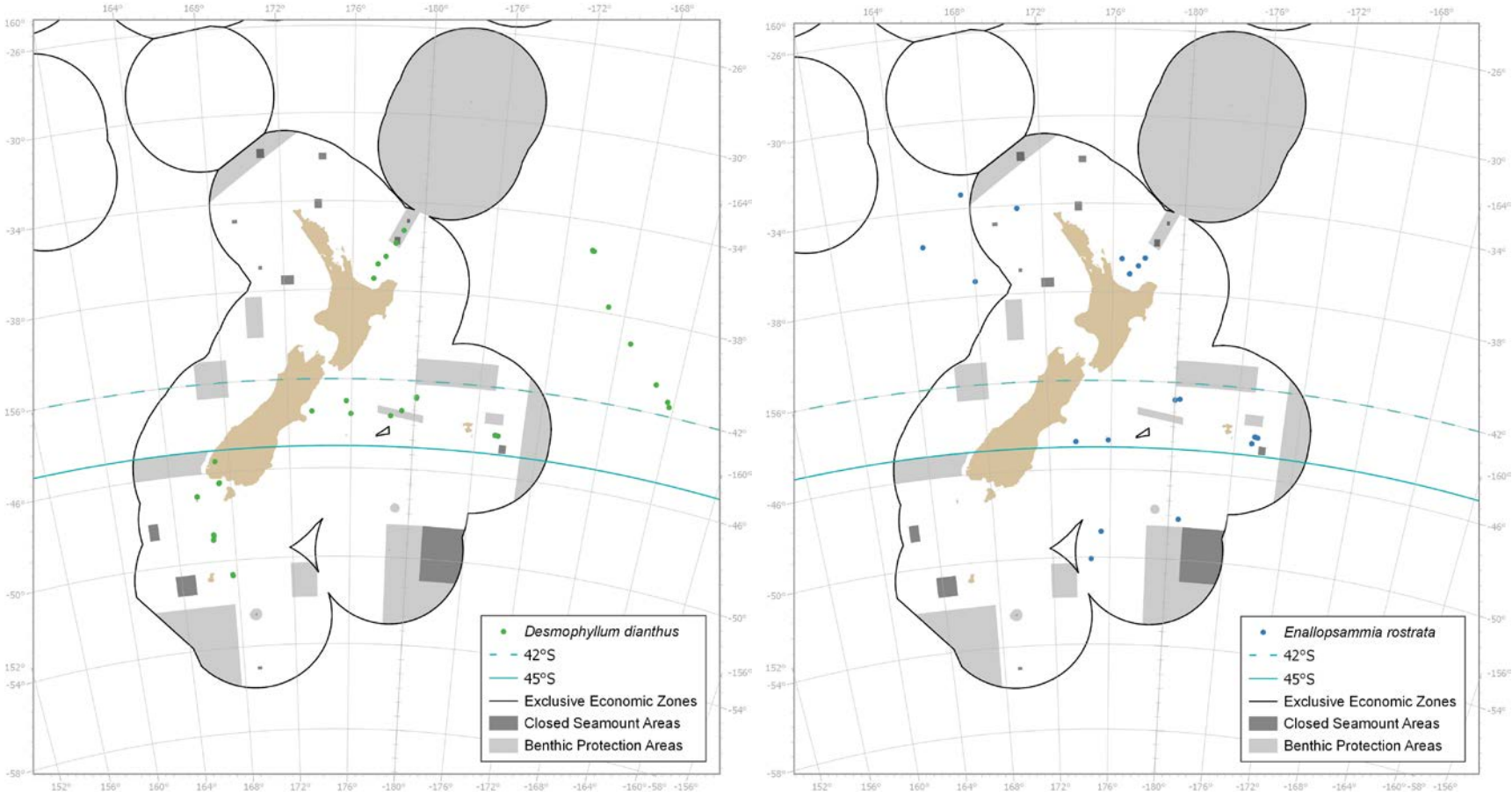

Figure 2: Maps showing the distribution of *Desmophyllum dianthus* (left) and *Enallopsammia rostrata* sampling locations (right) relative to Benthic Protection Areas, seamount closures, and the limits of the EEZ. Maps generated in NABIS (http://nabis.network.maf.govt.nz/NabisHome).

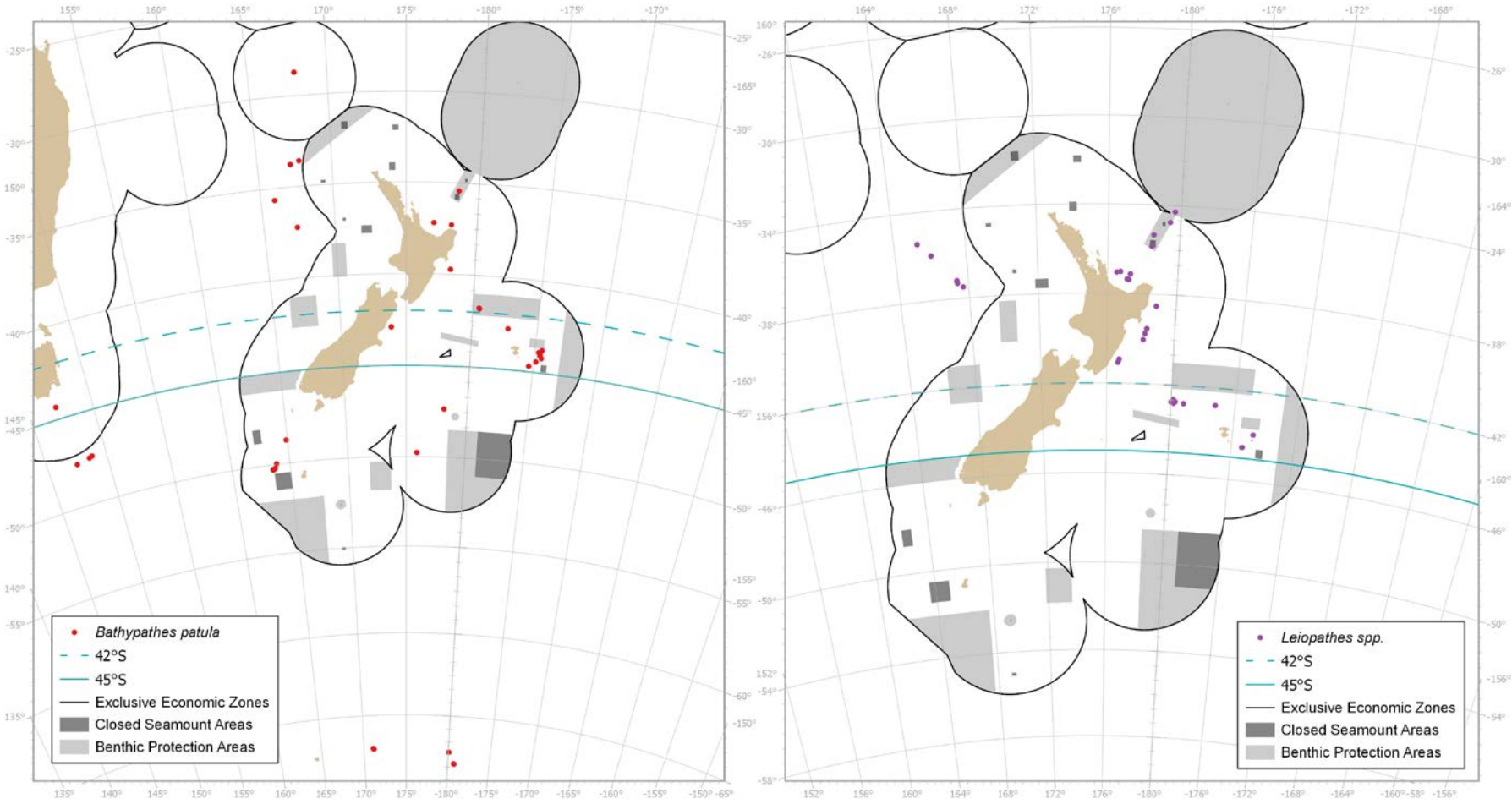

Figure 2 (cont.): Maps showing the distribution of *Leiopathes* spp. (left) and *Bathypathes patula* sampling locations (right) relative to Benthic Protection Areas, seamount closures, and the limits of the EEZ (note: *B. patula* was also sampled from outside of the NZ EEZ in the Southern Ocean and south of Tasmania, both of which are not shown on this map, but see Figure 1). Maps generated in NABIS (http://nabis.network.maf.govt.nz/NabisHome).

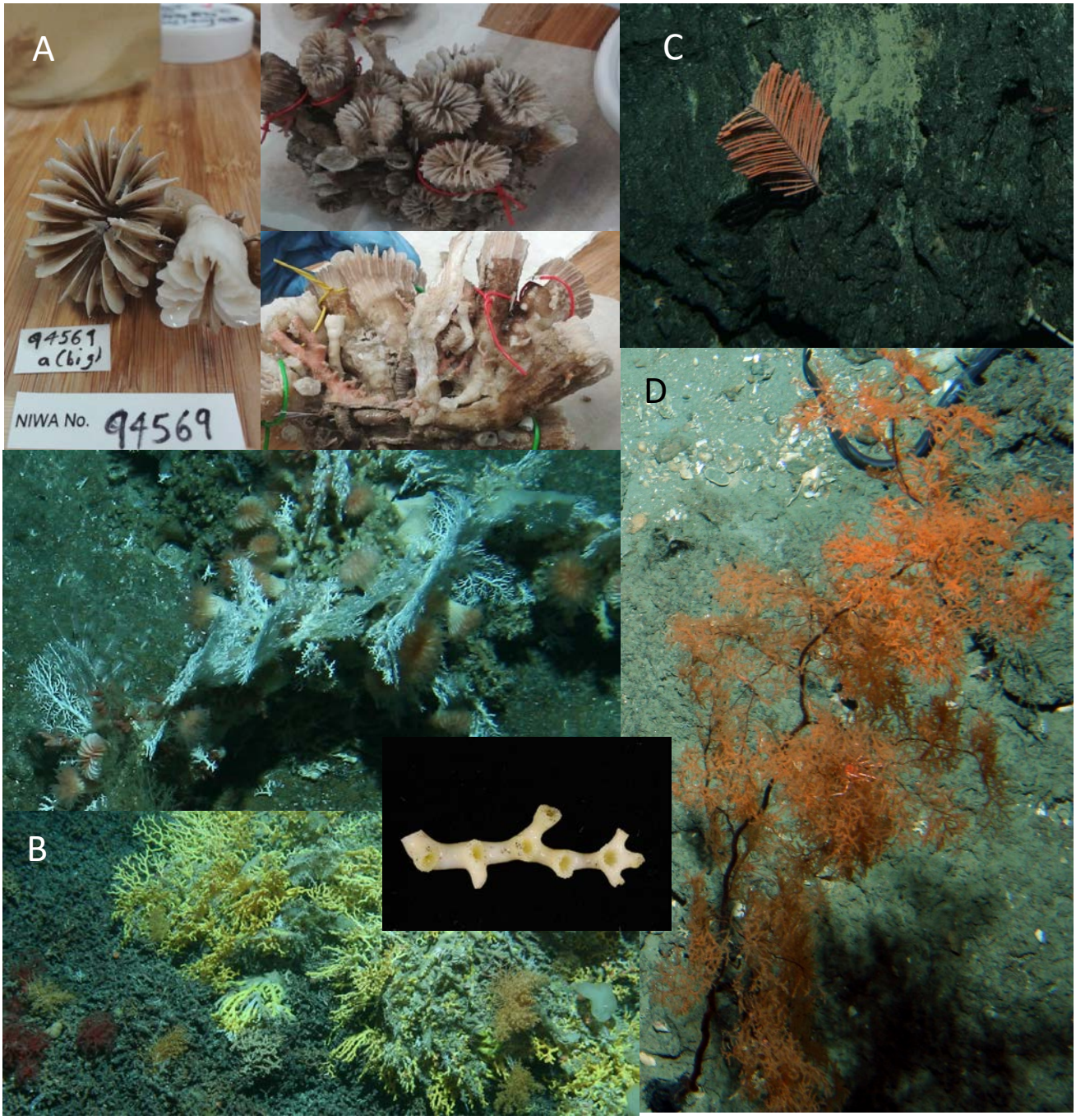

Figure 3: Images of specimens and study species *in vivo*. A: *Desmophyllum dianthus*, a stony coral, showing examples of clusters of tagged individuals (top) and associated macrofauna (bottom) and *in situ* association with stylasterids. B: *Enallopsammia rostrata*, a stony coral, *in situ* and branch, inset, C: *Bathypathes patula*, a black coral, *in situ*, D: *Leiopathes* spp., a black coral, *in situ*. Photo credits: A - L. Holland; B, C, and D - NIWA (DTIS images from voyages TAN1206, TAN1503, TAN1007).

a) Regional (North, Central and South K1-5)

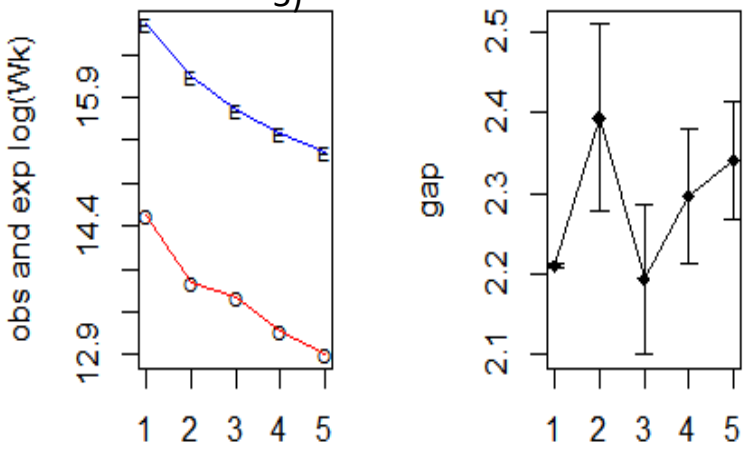

b) Geomorphic features Regional (K1-12)

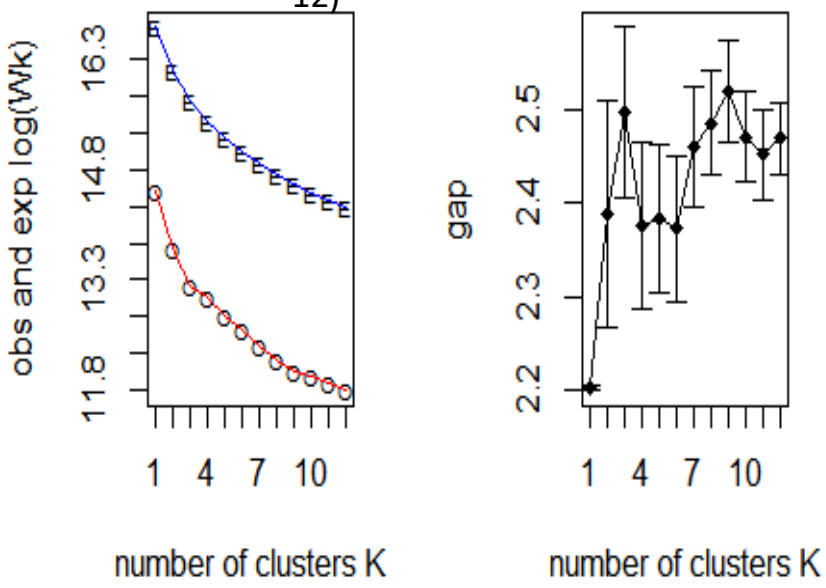

Figure 4: Gap analysis results from AWclust analyses for *Desmophyllum dianthus* a) regional and b) geomorphic features datasets. LHS: plot of the log of the expected (E) and observed (O) pooled within cluster sum of squares plotted against the number of clusters. RHS: shows the gap statistics between the observed and expected values. The biggest gap with the lowest variation indicates the most likely number of clusters.

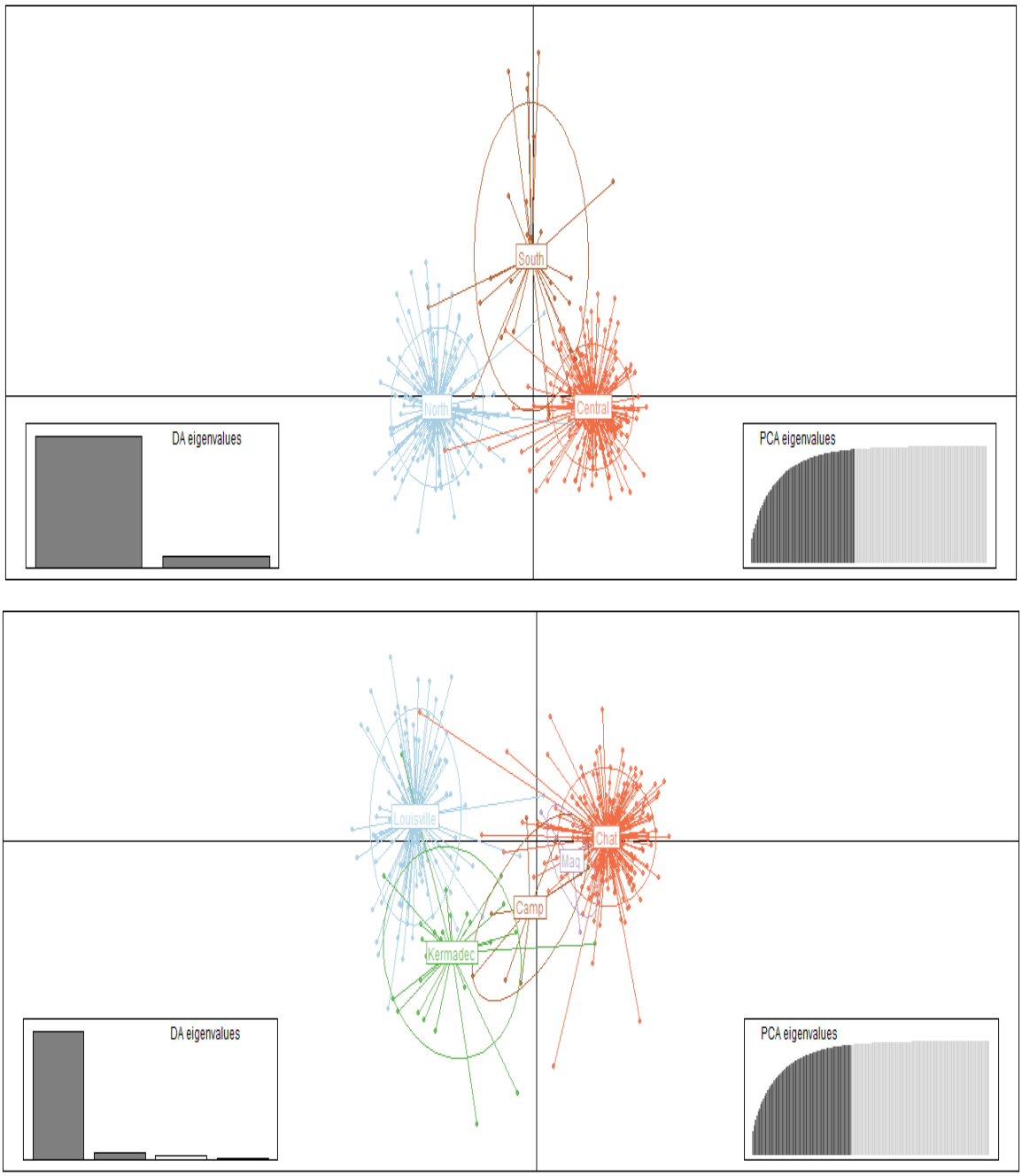

Figure 5: Discriminant analysis of principle components (DAPC) scatter plots of *D. dianthus* at top: regional (North, Central, and South) levels and bottom: by geomorphic features. Each colour represents a population and each dot represents an individual. Eigenvalues correspond to the ratio of the variance between groups over the variance within groups for each discriminant function; left inset shows barplot of discriminant analysis eigenvalues retained and right inset shows cumulative variance explained by the eigenvalues of the PCA.

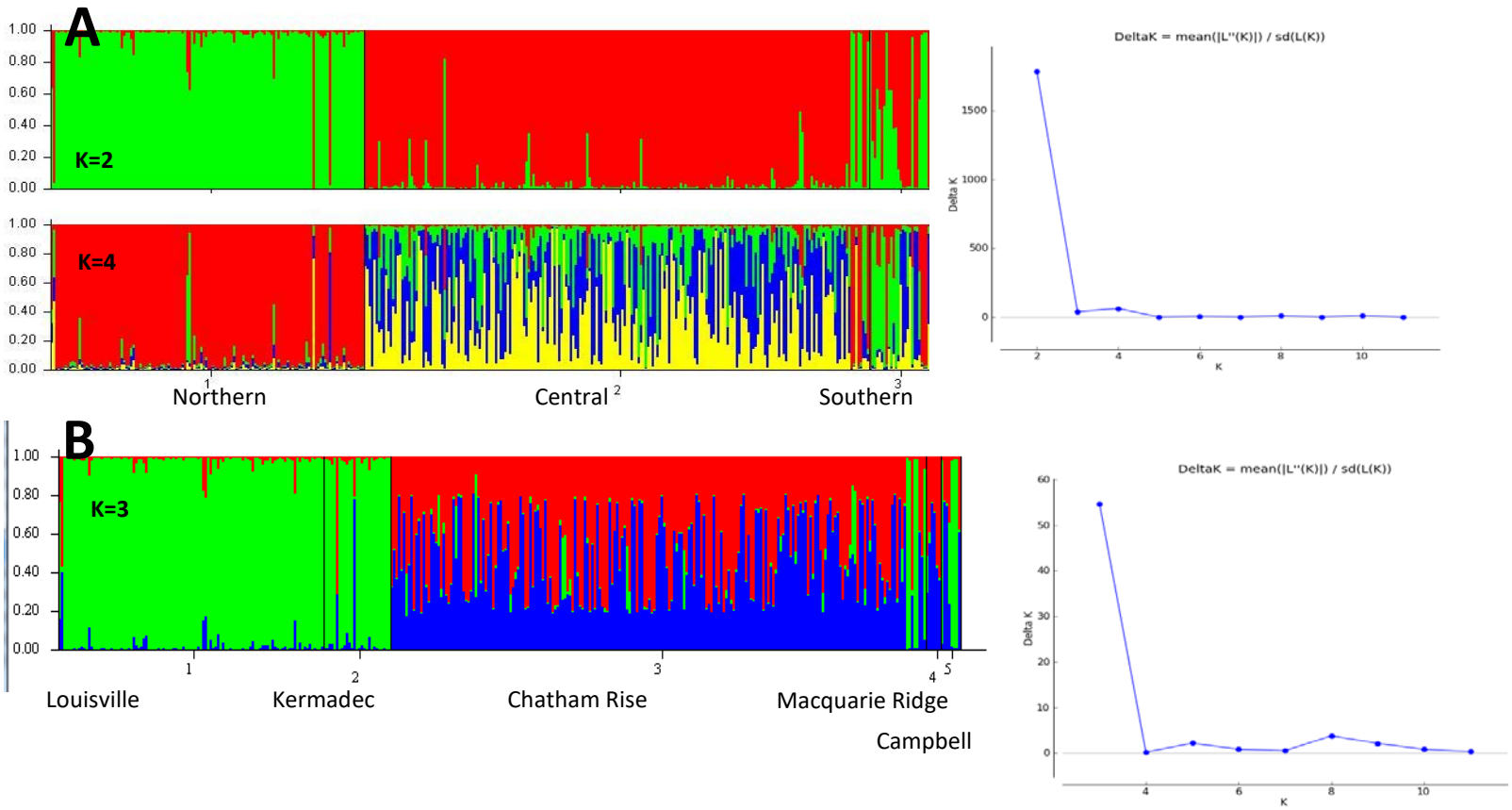

Figure 6: STRUCTURE (Pritchard et al. 2000) results for *Desmophyllum dianthus* showing A: regional and B: geomorphic features datasets. Both analyses included all microsatellite loci, and the software settings were admixture ancestry model (populations are not known to have been isolated), correlated alleles (which assumes a level of non-independence and is more conservative than the independent alleles setting), 100K burn-in and 3 replicates of 1 x10^6 steps, no location prior specified and K1-12. Optimal K values (shown to the right of bar plots) were derived with the correction of Evanno et al. (2005), which plots the log probability [L(K)] of the data and compares it to delta K , as implemented in STRUCTURE HARVESTER (Earl & von Holdt 2012); by this method, optimal K was 2 and 3 for the regional and geomorphic features respectively (for comparative purposes K=4 is also shown (regional scale analysis) to illustrate progressive difficulty in assigning some individuals to a particular putative population (represented by a colour)). Samples from the Louisville Seamount Chain and the Kermadec Ridge region ('northern', shown on the left of each bar plot) are indistinguishable.

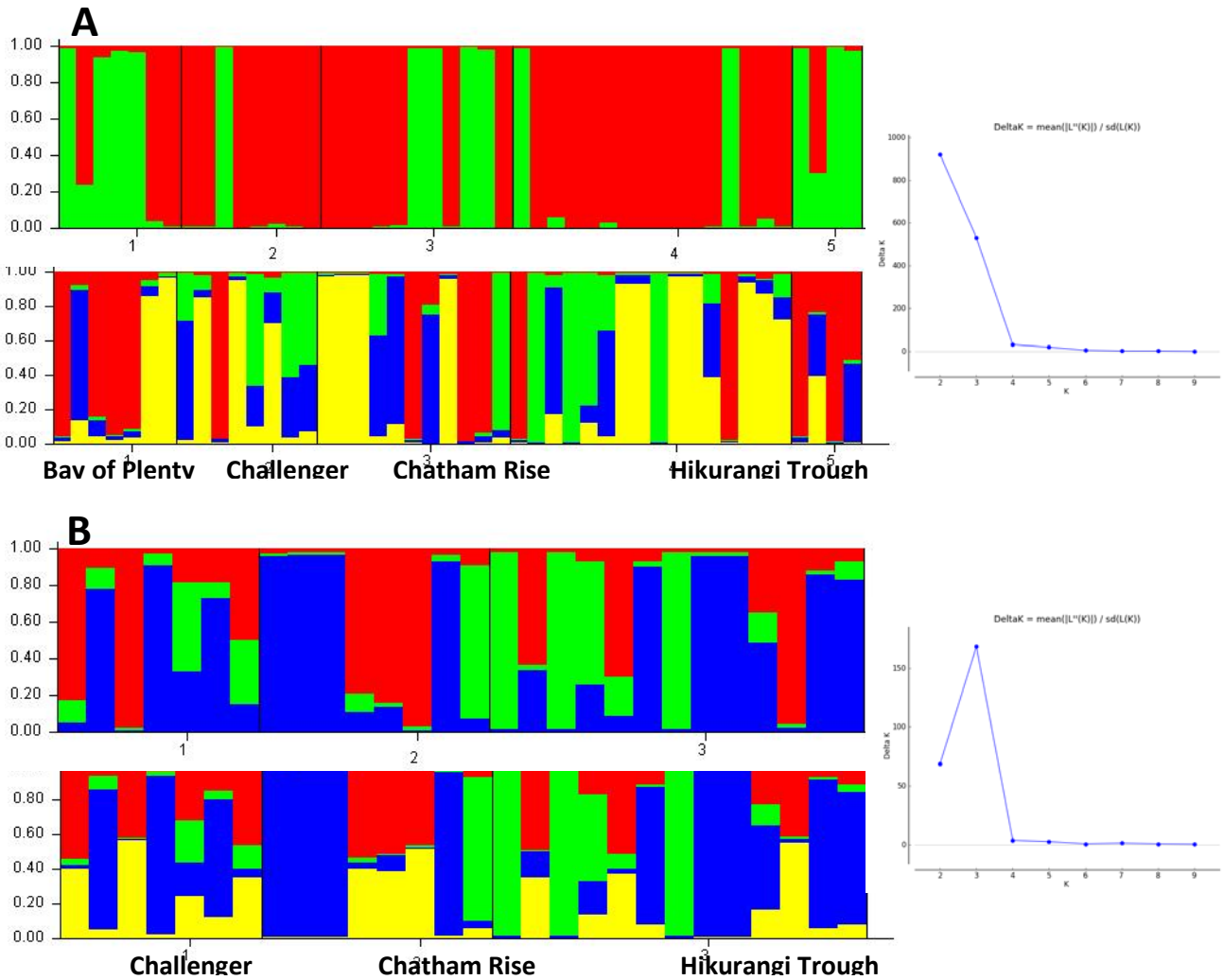

Figure 7: STRUCTURE (Pritchard et al. 2000) results for *Leiopathes* spp. microsatellite data partitioned into geomorphic features showing A: a mixture of *Leiopathes* species (N=46) and B: *Leiopathes secunda* samples only (N=28). Settings for each run were: admixture model, correlated alleles, 100K burn-in and 3 replicates of 1 x10^6 steps, no location prior specified and K1-10. Optimal K values (shown to the right of bar plots) were derived with the correction of Evanno et al. (2005), which plots the log probability [L(K)] of the data and compares it to delta K , as implemented in STRUCTURE HARVESTER (Earl & von Holdt 2012); by this method , optimal K was 2 and 3 for *Leiopathes* spp. and *Leiopathes secunda* respectively (top graphs, for comparative purposes K=4 is also shown for each run to illustrate progressive difficulty of assigning some individuals to a particular putative population).

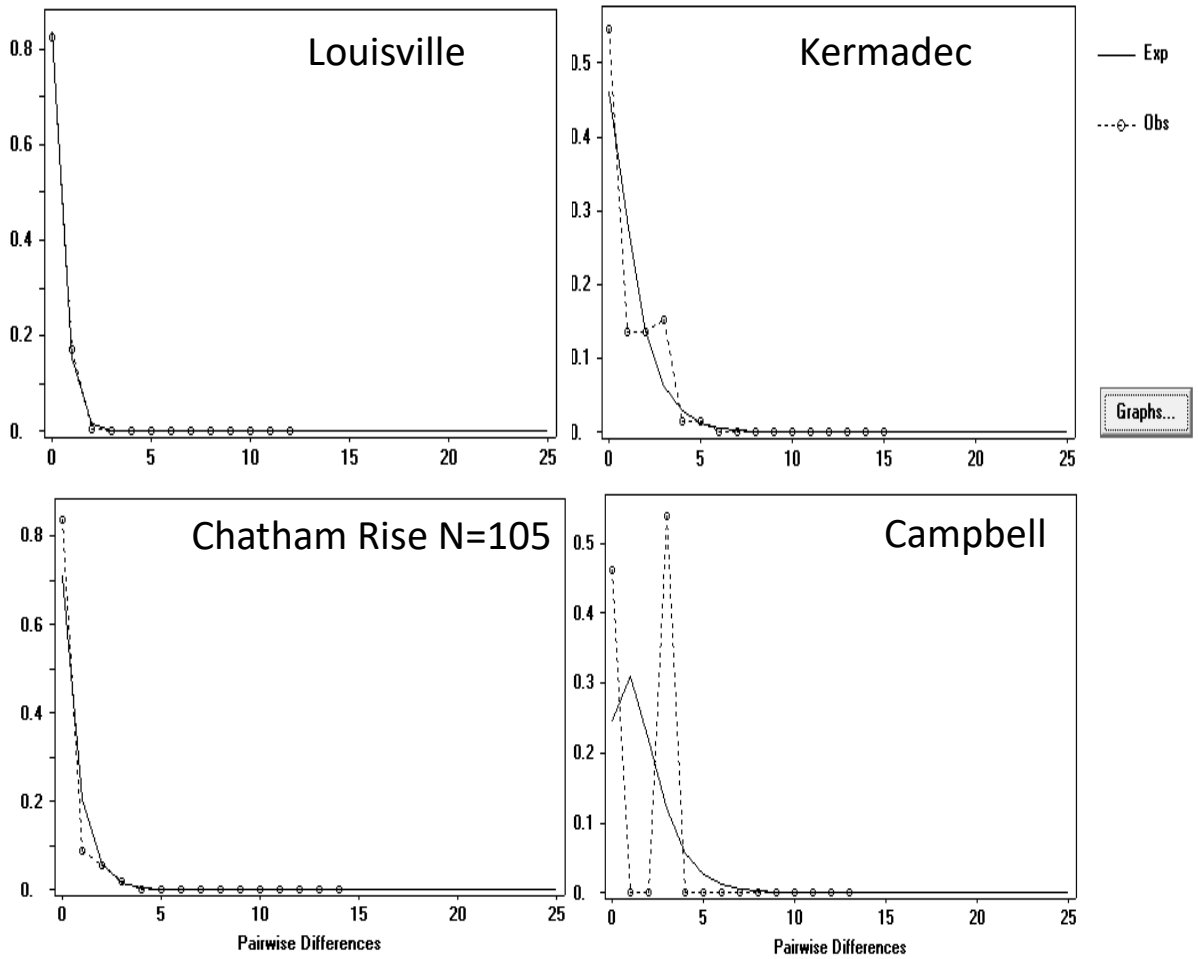

Figure 8: ***Desmophyllum dianthus*** **geomorphic features mismatch distribution (observed vs. expected sequence difference distribution) graphs based upon ITS data (Macquarie Ridge excluded due to low sample sizes).**

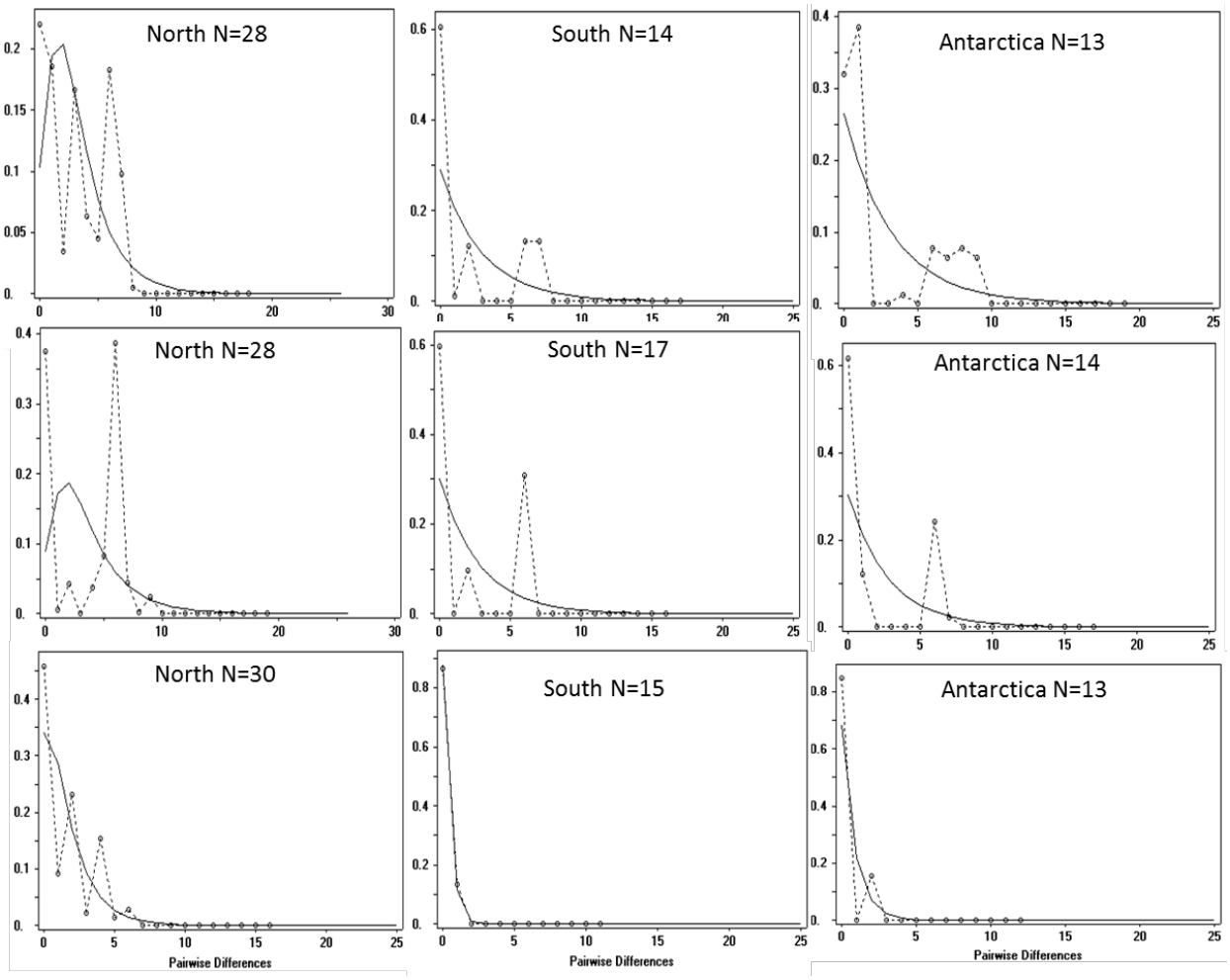

Figure 9: Mismatch distribution (observed vs. expected sequence difference distribution) graphs for the three provincial sample divisions for *Bathypathes patula* using three genes, ND5 (top row), TRP (middle row), and 16S (bottom row). Note: sample size variation between datasets is due to varying amplification success between genes.

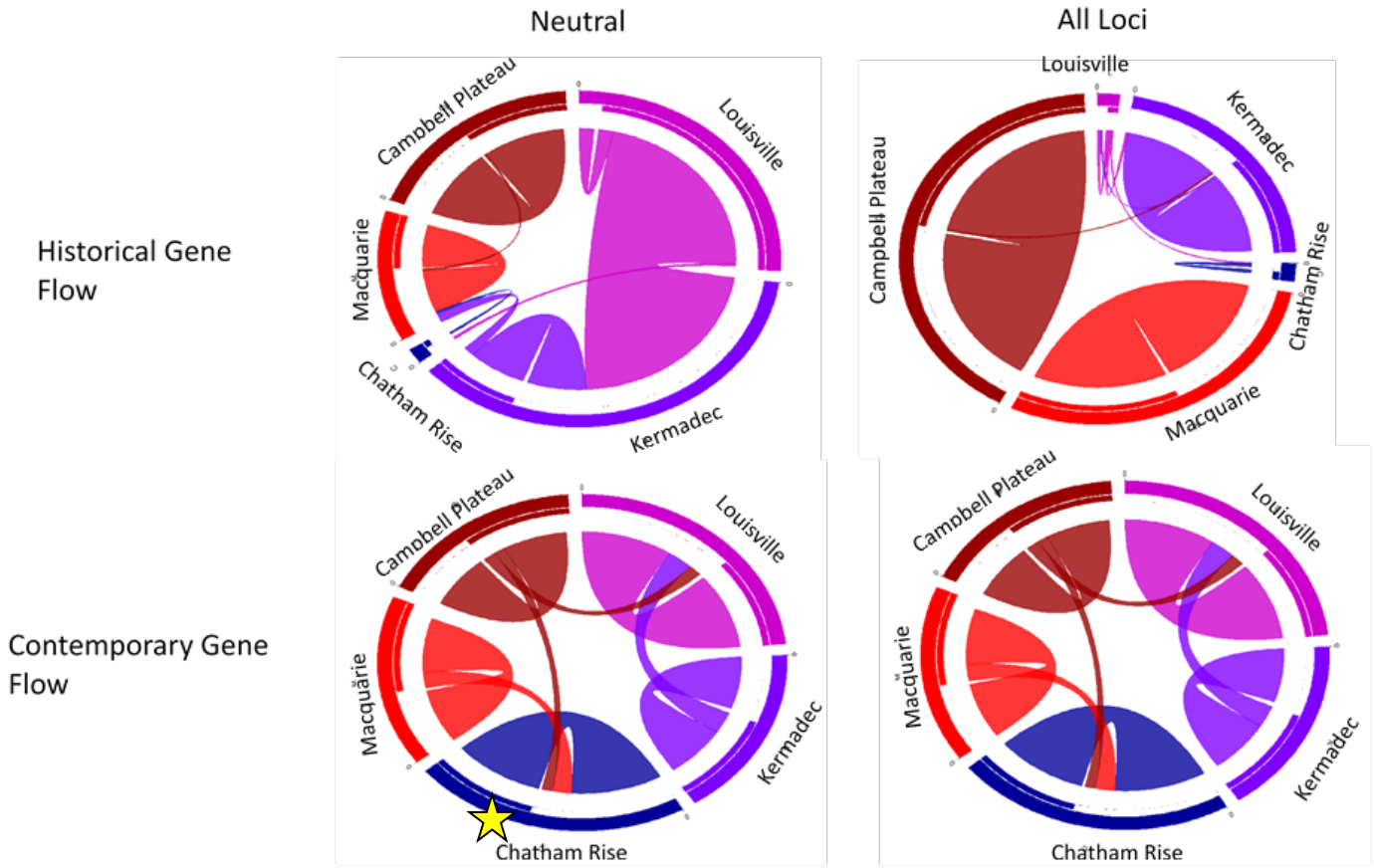

Figure 10: Comparative gene flow diagrams for *D. dianthus* using neutral microsatellite loci (left) or all microsatellite loci (right) Top: Historical gene flow estimates (derived from Migrate-n) and bottom, contemporary gene flow estimates (derived from BayesAss). The colours represent different geomorphic features (i.e., populations). In each diagram, a pathway that moves away from its colour of origin indicates source to sink movement (e.g., in the bottom left diagram, the red pathway going into the Chatham Rise from Macquarie indicates that the former is a source for the latter), whereas a 'hill' represents self-recruitment (e.g., in the bottom left diagram, the dark blue pathway going from the Chatham Rise back to the Chatham Rise). The width of the pathway indicates the relative amount of gene flow (the wider it is, the more gene flow there is). The curved bars to the left of each population (example shown underneath yellow star) indicates the proportion of the population that is a source; as an example, in the top left diagram, the vast majority of Louisville migrants go to the Kermadec area with a small proportion moving back into Louisville (self-recruitment), whereas in the bottom left, all Louisville movement is back to Louisville (i.e., all self-recruitment).

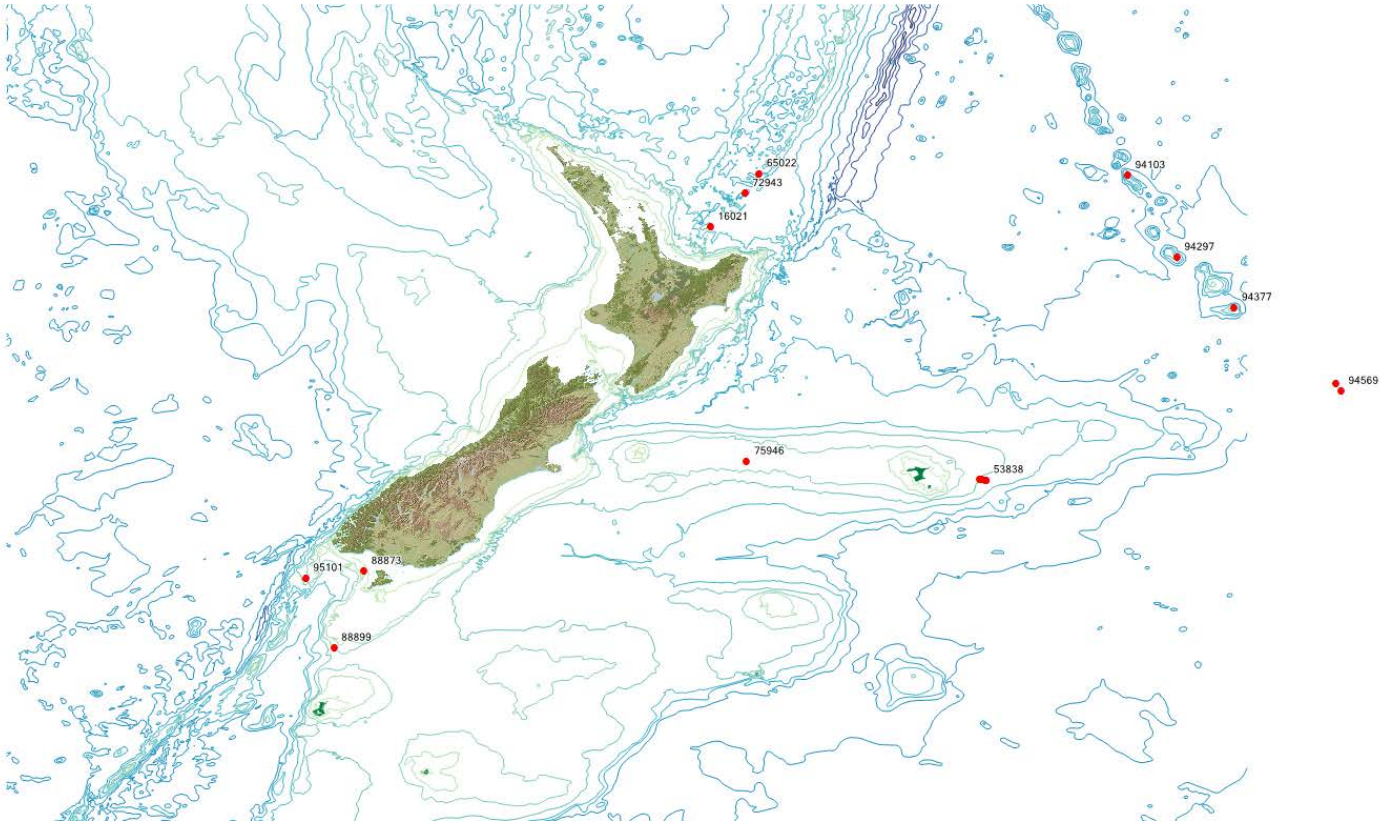

Figure 11: Map showing locations of *Desmophyllum dianthus* putative populations (red dots) comprised of four or more individuals as used in seascape genetic analyses (see Appendix 3 for additional sampling information).

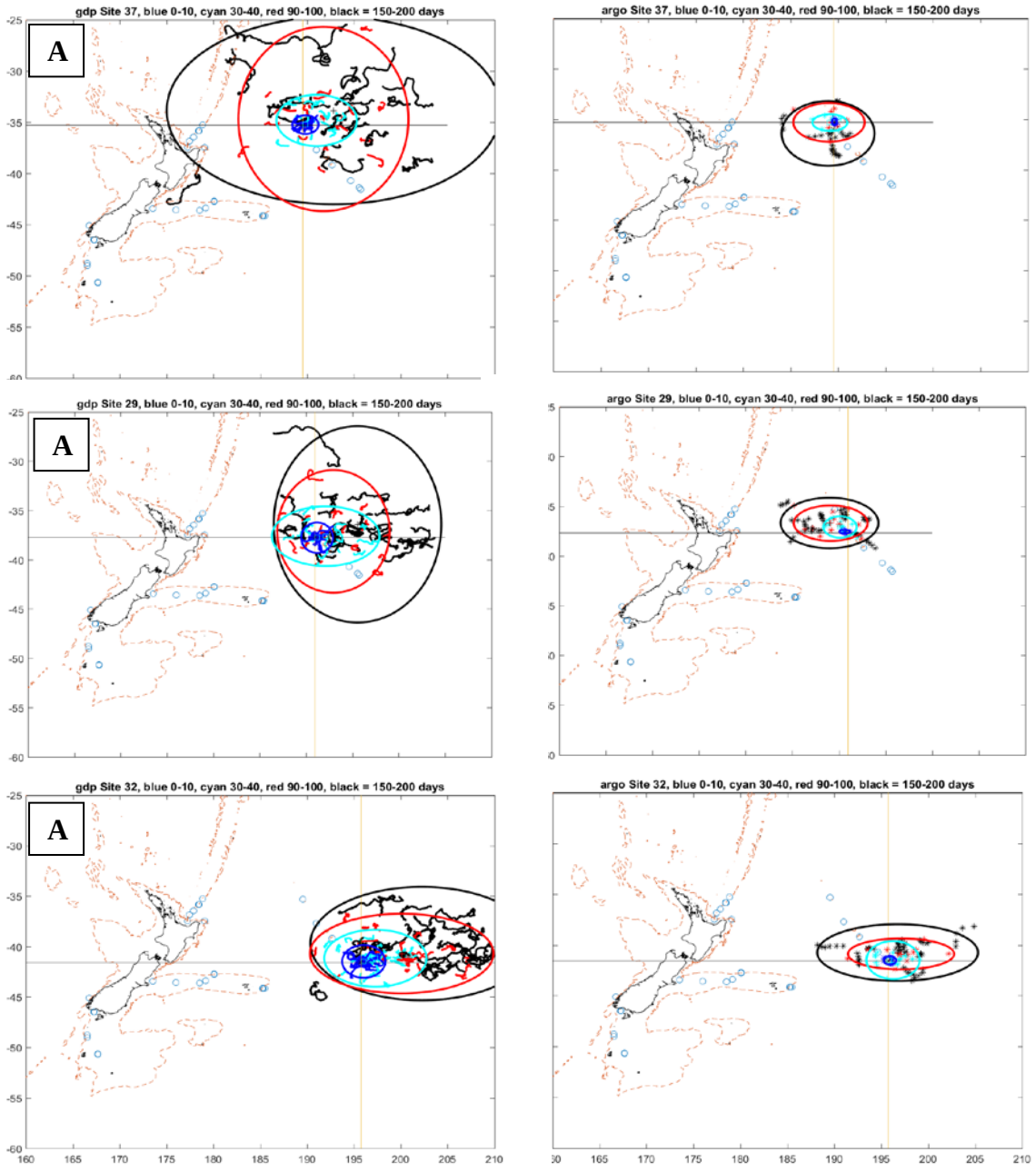

Figure 12: Larval migration trajectories based upon GDP (left) and ARGO floats (right) for pelagic larval durations specified as 0–10, 30–40, 90–120, and 150–200 days (blue, turquoise, red, and black respectively). A: from north, central, and southern sites in the Louisville Seamount Chain, B: from the southern Kermadec Ridge region, C: from the western Campbell Plateau, D: from the Southern Ocean, and E: from sites on the western, mid and eastern Chatham Rise. [Continued on next page.]

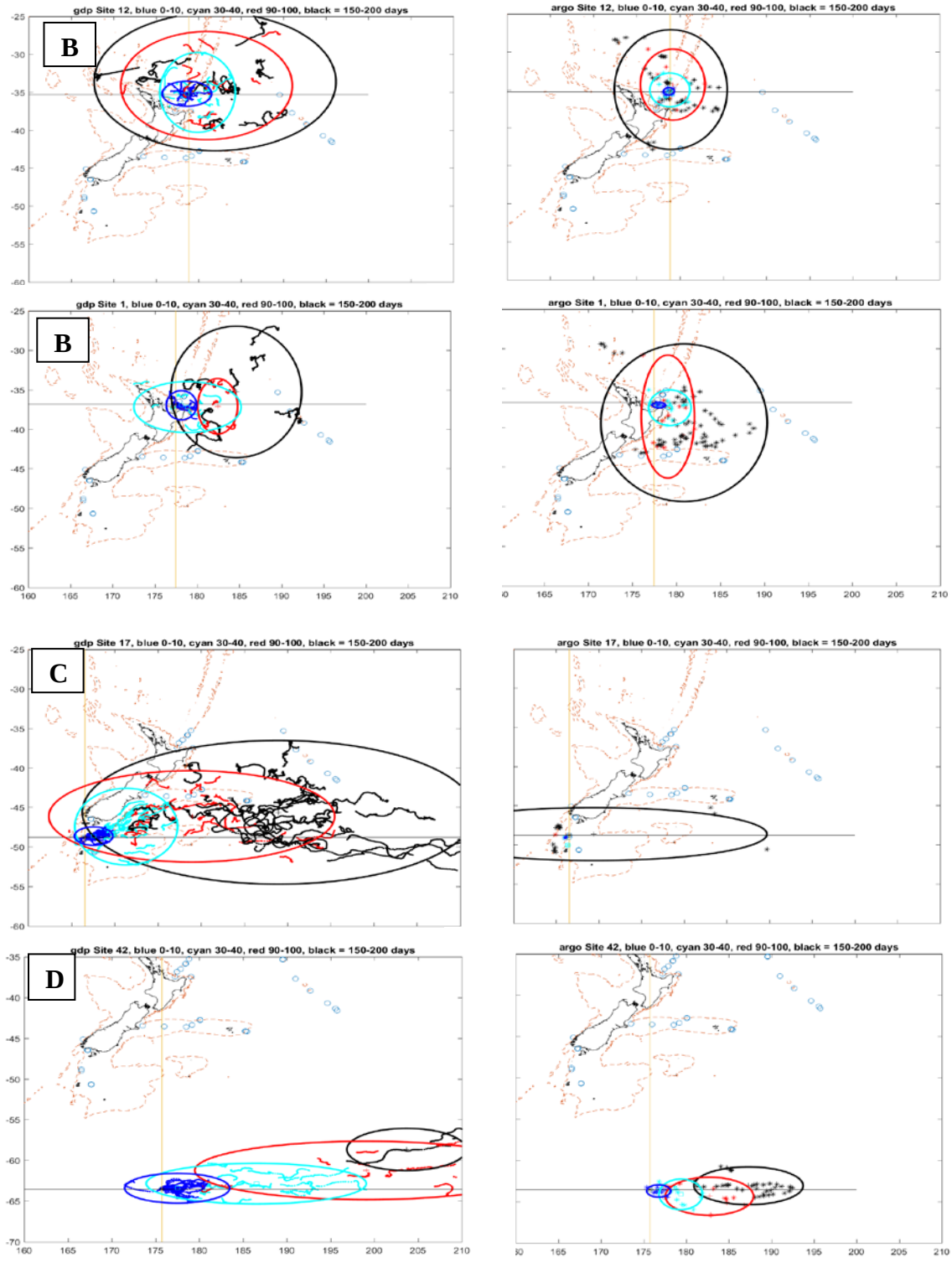

Figure 12: continued. Larval migration trajectories based upon GDP (left) and ARGO floats (right) for pelagic larval durations specified as 0–10, 30–40, 90–120, and 150–200 days (blue, turquoise, red, and black respectively). B: from the southern Kermadec Ridge region, C: from the western Campbell Plateau, and D: from the Southern Ocean. [Continued on next page.]

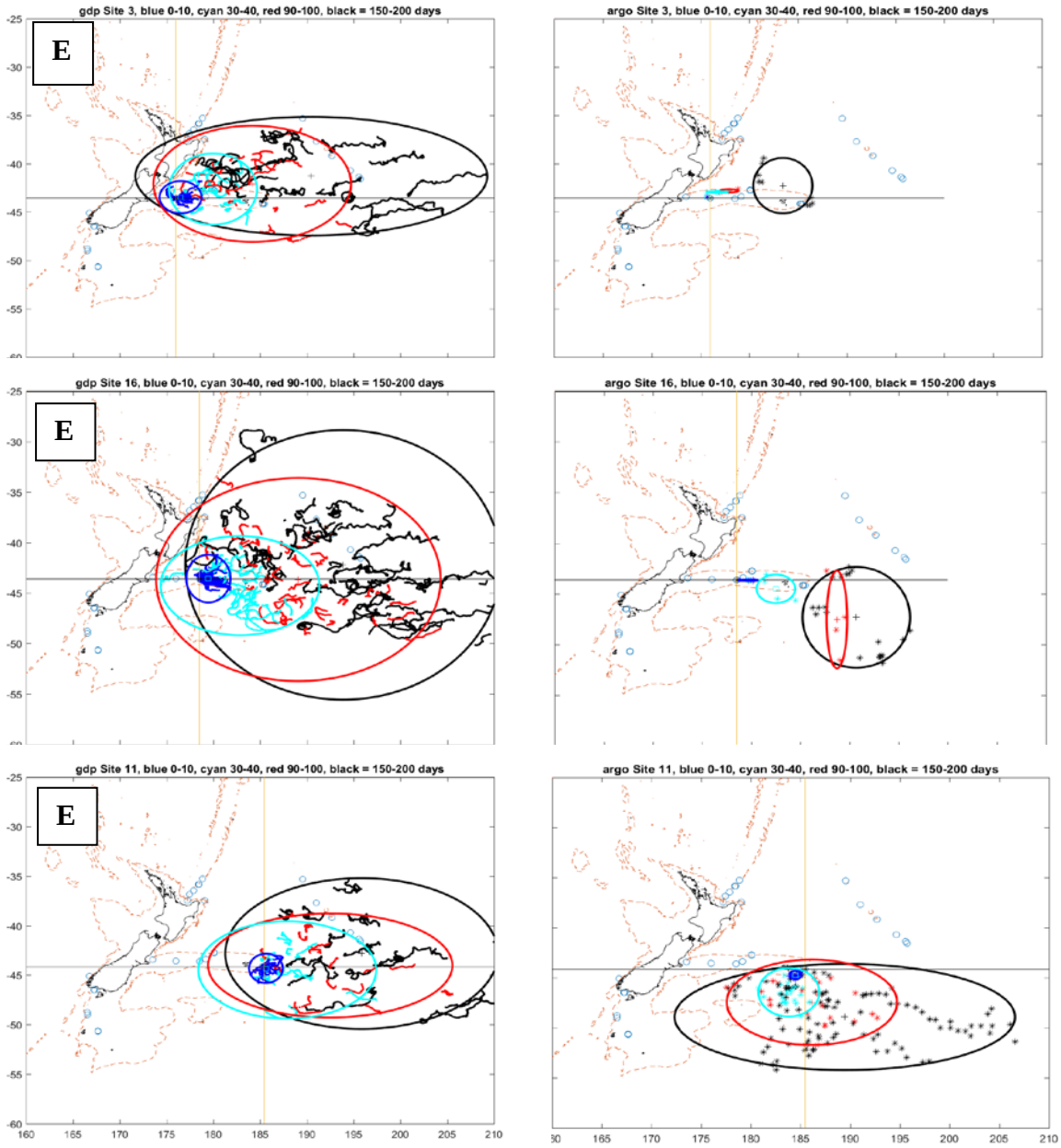

Figure 12: continued. Larval migration trajectories based upon GDP (left) and ARGO floats (right) for pelagic larval durations specified as 0–10, 30–40, 90–120, and 150–200 days (blue, turquoise, red, and black respectively). E: from sites on the western, mid, and eastern Chatham Rise.

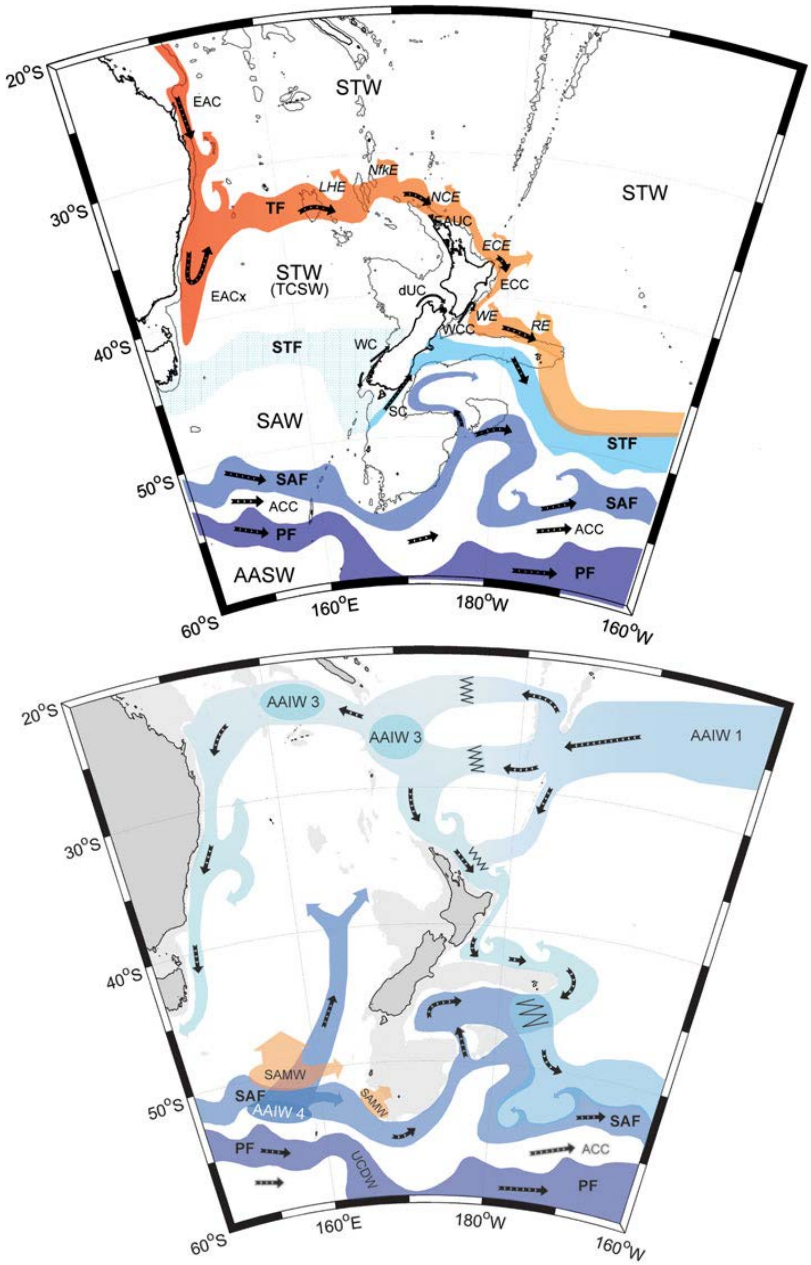

Figure 13: **TOP: Schematic surface circulation around New Zealand based on drifter data and hydrographic data. Water Masses: Subtropical Water (STW), Tasman Sea Central Water (TSCW), Subantarctic Water (SAW), Antarctic Surface Water (AASW). Ocean fronts: Tasman Front (TF), Subtropical Front (STF), Subantarctic Front (SAF), and Polar Front (PF). Ocean currents: East Australia Current (EAC), East Australia Current extension (EACx), East Auckland Current (EAUC), East Cape Current (ECC), d'Urville Current (dUC), Wairarapa Coastal Current (WCC), Westland Current (WC), Southland Current (SC) and Antarctic Circumpolar Current (ACC). Eddies are Lord Howe Eddy (LHE), Norfolk Eddy (NfkE), North Cape Eddy (NCE), East Cape Eddy (ECE), Wairarapa Eddy (WE), and Rekohu Eddy (RE). Colours represent water temperature (red warmest, dark blue coldest) and shading in the STF in the Tasman Sea represents density compensated with little flow.**
BOTTOM: Schematic intermediate (c. 1000 m) circulation around New Zealand based on Argo float and hydrographic data. Antarctic Intermediate Water (AAIW) is thought to form equator-ward of the Polar Front (PF) and subduct under the Subantarctic Front (SAF). Local subtypes (1, 3, and 4) of AAIW are shown and are derived from Bostock et al. (2013a). AAIW circulates around the South Pacific subtropical gyre, mixing with various water masses to form different subtypes as shown. Subantarctic Mode Water (SAMW) forms equator-ward of the SAF and flows north overlying AAIW. Zig-zag lines indicate regions of mixing between the various subtypes of AAIW. Reproduced from Chiswell et al. (2015).

APPENDICES

APPENDIX 1: Sample information for Desmophyllum dianthus microsatellites, *Desmophyllum dianthus* ITS DNA sequences, *Enallopsammia rostrata* ITS DNA sequences, *Bathypathes patula* DNA sequences (concatenated 16S-TRP-ND5), *Leiopathes secunda* microsatellites, and *Leiopathes* spp. microsatellites.

***Desmophyllum dianthus* microsatellite samples**

Bioprovince	Region	Geomorphic feature	NIC#	N	Latitude	Longitude	Average depth (m)
Northern	Central	Chatham Rise	47034	1	-42.78	-179.91	910
Northern	Central	Chatham Rise	48516	1	-43.37	179.19	413
Northern	Central	Chatham Rise	53581	9	-44.15	-174.69	520
Northern	Central	Chatham Rise	53720	6	-44.14	-174.72	700
Northern	Central	Chatham Rise	53838	11	-44.16	-174.55	509
Northern	Central	Chatham Rise	54285	19	-44.16	-174.56	552
Northern	Central	Chatham Rise	75946	1	-43.62	178.50	437
Northern	Central	Chatham Rise	88004	2	-43.44	173.50	392
Northern	Central	Chatham Rise	88075	2	-42.73	-179.90	1033
Northern	Central	Chatham Rise	88660	1	-42.99	175.68	622
Northern	Central	Chatham Rise	102469	48	-44.16	-174.55	497
Northern	Central	Chatham Rise	102485	24	-44.16	-174.55	544
Northern	Central	Chatham Rise	102571	44	-44.14	-174.72	622
Northern	Central	Chatham Rise	102636	47	-44.15	-174.75	570
Northern	North	Kermadec Ridge region	16021	5	-36.83	177.45	1259
Northern	North	Kermadec Ridge region	16022	1	-37.48	177.22	180
Northern	North	Kermadec Ridge region	65022	6	-35.28	178.86	1260
Northern	North	Kermadec Ridge region	72299	2	-36.48	177.89	1300
Northern	North	Kermadec Ridge region	72875	3	-35.87	178.44	1360
Northern	North	Kermadec Ridge region	72943	10	-35.86	178.45	1349
Northern	North	Louisville Seamount Chain	94017	2	-35.35	-170.37	1212
Northern	North	Louisville Seamount Chain	94078	1	-35.33	-170.44	1146
Northern	North	Louisville Seamount Chain	94103	18	-35.34	-170.44	1088
Northern	North	Louisville Seamount Chain	94165	1	-35.32	-170.45	1403
Northern	North	Louisville Seamount Chain	94297	4	-37.71	-169.02	1307
Northern	North	Louisville Seamount Chain	94377	67	-39.16	-167.35	922
Northern	North	Louisville Seamount Chain	94448	1	-40.72	-165.34	863
Northern	North	Louisville Seamount Chain	94569	6	-41.58	-164.26	1232
Northern	North	Louisville Seamount Chain	94570	2	-41.58	-164.26	1232

Northern	North	Louisville Seamount Chain	94613	1	-41.37	-164.42	1251
Northern	North	Louisville Seamount Chain	94623	2	-41.36	-164.42	1235
Northern	North	Louisville Seamount Chain	94629	1	-41.36	-164.42	1235
Northern	North	Louisville Seamount Chain	96623	1	-35.31	-170.46	1403
Southern	South	Campbell Plateau	47033	2	-50.70	167.68	339
Southern	South	Campbell Plateau	75976	3	-48.78	166.56	306
Southern	South	Campbell Plateau	88749	1	-48.85	166.58	341
Southern	South	Campbell Plateau	88899	2	-49.02	166.52	615
Southern	South	Macquarie Ridge	88894	1	-47.00	165.68	452
Southern	South	Macquarie Ridge	95101	5	-47.00	165.70	447
Southern	South	n/a*	88049	1	-45.49	167.09	33
Southern	South	n/a*	88871	2	-46.49	167.23	1000
Southern	South	n/a*	88873	9	-46.46	167.26	2000

Desmophyllum dianthus **ITS DNA samples**

Bioprovince	Region	Geomorphic feature	NIC#	N	Latitude	Longitude	Average depth (m)
Northern	Central	Chatham Rise	25593	1	-43.56	175.98	322.0
Northern	Central	Chatham Rise	48516	2	-43.37	179.19	412.5
Northern	Central	Chatham Rise	53581	27	-44.15	-174.69	520.0
Northern	Central	Chatham Rise	53720	6	-44.14	-174.72	699.5
Northern	Central	Chatham Rise	53838	34	-44.16	-174.55	509
Northern	Central	Chatham Rise	54050	14	-44.15	-174.76	564.0
Northern	Central	Chatham Rise	54285	15	-44.16	-174.56	551.5
Northern	Central	Chatham Rise	75946	1	-43.62	178.50	437.0
Northern	Central	Chatham Rise	88004	2	-43.44	173.50	392.0
Northern	Central	Chatham Rise	88075	3	-42.73	-179.90	1033.0
Northern	North	Kermadec Ridge region	16022	1	-37.48	177.22	179.5
Northern	North	Kermadec Ridge region	72943	11	-35.86	178.45	1348.5
Northern	North	Louisville Seamount Chain	94377	19	-39.16	-167.35	922
Northern	North	Louisville Seamount Chain	94448	1	-40.72	-165.34	863.0
Northern	North	Louisville Seamount Chain	94569	1	-41.58	-164.26	1232
Northern	North	Louisville Seamount Chain	94623	1	-41.36	-164.42	1235
Southern	South	Campbell Plateau	47033	3	-50.70	167.68	339.0
Southern	South	Campbell Plateau	88053	1	-50.65	167.66	400.0
Southern	South	Macquarie Ridge	75976	9	-48.78	166.56	305.5
Southern	South	Macquarie Ridge	88049	1	-45.49	167.09	33

Enallopsammia rostrata **ITS DNA samples**

Bioprovince	Region	Geomorphic feature	NIC#	N	Latitude	Longitude	Average depth (m)
Northern	North	Challenger Plateau	65465	1	-35.60	165.20	902
Northern	North	Challenger Plateau	65910	1	-37.34	168.01	929
Northern	Central	Chatham Rise	42404	1	-44.75	173.72	1010
Northern	Central	Chatham Rise	47924	1	-44.46	-174.89	1048

Northern	Central	Chatham Rise	53483	6	-42.74	-179.69	922
Northern	Central	Chatham Rise	53719	1	-44.14	-174.72	700
Northern	Central	Chatham Rise	53998	14	-44.14	-174.72	791
Northern	Central	Chatham Rise	54169	1	-44.18	-174.55	731
Northern	Central	Chatham Rise	65471	1	-44.47	-174.89	1044
Northern	Central	Chatham Rise	81272	2	-44.68	175.82	621
Northern	Central	Chatham Rise	102305	3	-42.79	-179.99	931
Northern	Central	Chatham Rise	102565	13	-44.14	-174.72	619
Northern	Central	Chatham Rise	102631	17	-44.15	-174.75	585
Northern	North	Kermadec Ridge region	72208	1	-36.45	177.84	838
Northern	North	Kermadec Ridge region	89250	1	-36.50	176.52	956
Northern	North	Norfolk Ridge	88632	1	-33.38	167.57	257
Northern	North	Norfolk Ridge	95552	1	-34.15	170.62	791
Southern	South	Campbell Plateau	47918	1	-50.06	174.69	912
Southern	South	Campbell Plateau	65474	1	-48.82	175.38	716
Southern	South	Campbell Plateau	82309	1	-36.45	177.85	1143
Southern	South	Campbell Plateau	82695	1	-36.81	177.47	895
Southern	South	Campbell Plateau	82752	1	-36.81	177.47	988
Southern	South	Campbell Plateau	82877	1	-36.45	177.84	935
Southern	South	Campbell Plateau	82924	1	-36.45	177.84	889
Southern	South	Campbell Plateau	83296	1	-37.18	176.98	999
Southern	South	Campbell Plateau	83362	1	-37.19	176.98	939
Southern	South	Campbell Plateau	88340	1	-37.19	176.97	770
Southern	South	Campbell Plateau	88999	1	-48.16	-179.33	810

***Bathypathes patula* DNA samples (concatenated 16S-TRP-ND5)**

Bioprovince	NIC#	N	Latitude	Longitude	Average depth (m)
Antarctic	38108	1	-68.089	-179.299	895
Antarctic	38161	1	-68.121	-179.248	876
Antarctic	39236	1	-67.168	171.179	634
Antarctic	41695	1	-67.340	-179.932	1183
Antarctic	47191	1	-67.129	171.091	743
Antarctic	47193	1	-68.089	-179.299	895
Antarctic	47195	1	-67.168	171.179	634
Antarctic	47196	1	-68.121	-179.248	876
Antarctic	49168	1	-67.168	171.179	634
Antarctic	49169	1	-67.129	171.091	743
Northern	14781	1	-39.726	178.220	957
Northern	15044	1	-37.227	167.342	1082
Northern	15057	1	-33.767	167.217	313
Northern	42813	1	-43.913	-174.672	668
Northern	42815	1	-43.893	-174.698	722
Northern	42835	1	-44.208	-174.445	1252
Northern	4294	1	-28.705	167.945	475
Northern	4295	1	-37.300	178.183	1357
Northern	4297	1	-42.900	173.850	1010
Northern	47879	1	-42.773	-177.227	1001
Northern	49468	1	-44.717	184.633	810
Northern	53352	1	-41.766	-179.528	1343
Northern	53374	1	-41.800	-179.492	1263
Northern	64561	1	-35.439	178.625	1323
Northern	66331	1	-35.650	165.933	922
Northern	66337	1	-44.697	-175.362	1195
Northern	66348	1	-44.037	-174.577	998

Northern	66349	1	-43.913	-174.645	820
Northern	66354	1	-43.768	-174.455	875
Northern	69577	1	-33.600	167.812	1049
Northern	69648	1	-43.955	-174.580	840
Northern	69649	1	-44.415	-174.847	1091
Northern	83099	1	-37.199	176.939	1430
Southern	14769	1	-47.451	148.801	890
Southern	14770	1	-47.518	148.551	998
Southern	14771	1	-50.234	163.634	1006
Southern	14773	1	-47.668	147.434	1104
Southern	15339	1	-44.330	147.170	1083
Southern	42814	1	-49.965	163.847	874
Southern	42816	1	-50.205	163.682	1202
Southern	42820	1	-50.292	163.505	1208
Southern	45887	1	-48.723	164.893	970
Southern	45888	1	-47.362	178.098	936
Southern	60355	1	-50.250	163.490	1080
Southern	66344	1	-49.783	175.902	957

***Leiopathes secunda* microsatellite samples**

Geomorphic Feature	NIC#	N	Latitude	Longitude	Average depth (m)
Challenger Plateau	14776	1	-37.30	167.37	876
Challenger Plateau	19735	1	-37.20	167.35	800
Challenger Plateau	19737	1	-37.32	167.37	850
Challenger Plateau	19762	1	-37.50	167.68	943
Challenger Plateau	19766	1	-36.00	166.01	932
Challenger Plateau	19861	1	-37.23	167.34	1081.5
Challenger Plateau	24178	1	-36.00	166.01	932
Chatham Rise	14778	1	-42.80	-179.83	893
Chatham Rise	19759	1	-42.80	-179.21	638
Chatham Rise	19760	1	-42.80	-179.21	638
Chatham Rise	19761	1	-42.74	-179.74	834
Chatham Rise	47185	1	-44.52	-175.32	767
Chatham Rise	47426	1	-44.52	-175.32	873
Chatham Rise	47881	1	-42.64	-179.87	1196
Chatham Rise	85934	1	-42.76	-179.99	874.5
Hikurangi region	26773	1	-40.04	178.14	765
Hikurangi region	26774	1	-40.04	178.14	765
Hikurangi region	26775	1	-40.04	178.14	765
Hikurangi region	26777	1	-40.04	178.14	768
Hikurangi region	26780	1	-39.54	178.34	813.5
Hikurangi region	26790	1	-39.55	178.33	802.5
Hikurangi region	26795	1	-40.04	178.14	765
Hikurangi region	26805	1	-39.54	178.34	817
Hikurangi region	26806	1	-39.54	178.34	817
Hikurangi region	26807	1	-39.54	178.34	817
Hikurangi region	26815	1	-39.55	178.33	798
Hikurangi region	71035	1	-41.07	176.66	934
Hikurangi region	86495	1	-38.53	178.84	885.5

***Leiopathes* spp. microsatellite samples**

Geomorphic Feature	NIC#	N	Taxonomic ID	Latitude	Longitude	Average depth (m)
Bay of Plenty	19733	1	*Leiopathes* spp.	-37.134	177.285	648
Bay of Plenty	19738	1	*Leiopathes* spp.	-37.375	177.195	850
Bay of Plenty	19739	1	*Leiopathes* spp.	-37.134	177.285	341
Bay of Plenty	19743	1	*Leiopathes* spp.	-37.353	177.102	363
Bay of Plenty	19745	1	*L.bullosa*	-37.052	176.502	824
Bay of Plenty	19757	1	*L. secunda*	-37.023	176.718	972
Bay of Plenty	19765	1	*L. secunda*	-37.118	177.287	636
Challenger Plateau	14776	1	*L. secunda*	-37.302	167.367	876
Challenger Plateau	19735	1	*L. secunda*	-37.203	167.352	800
Challenger Plateau	19737	1	*L. secunda*	-37.318	167.367	1204
Challenger Plateau	19762	1	*L. secunda*	-37.500	167.683	943
Challenger Plateau	19766	1	*L. secunda*	-35.995	166.012	932
Challenger Plateau	19861	1	*L. secunda*	-37.227	167.342	1082
Challenger Plateau	24178	1	*L. secunda*	-35.995	166.012	932
Challenger Plateau	65561	1	*Leiopathes* spp.	-35.430	165.303	936
Chatham Rise	14778	1	*L. secunda*	-42.804	-179.827	893
Chatham Rise	19759	1	*L. secunda*	-42.803	-179.208	638
Chatham Rise	19760	1	*L. secunda*	-42.803	-179.208	638
Chatham Rise	19761	1	*L. secunda*	-42.738	-179.740	834
Chatham Rise	47185	1	*L. secunda*	-44.517	-175.320	767
Chatham Rise	47187	1	*Leiopathes* spp.	-44.515	-175.290	855
Chatham Rise	47881	1	*L. secunda*	-42.637	-179.867	1196
Chatham Rise	65558	1	*Leiopathes* spp.	-42.772	-177.230	960
Chatham Rise	65559	1	*Leiopathes* spp.	-43.918	-174.687	711
Chatham Rise	85934	1	*L. secunda*	-42.760	-179.988	875
Chatham Rise	47426	1	*L. secunda*	-44.517	-175.320	795
Hikurangi region	19742	1	*Leiopathes* spp.	-39.763	178.235	648
Hikurangi region	26773	1	*L. secunda*	-40.039	178.144	765
Hikurangi region	26774	1	*L. secunda*	-40.039	178.144	765
Hikurangi region	26775	1	*L. secunda*	-40.039	178.144	765
Hikurangi region	26777	1	*L. secunda*	-40.040	178.145	768
Hikurangi region	26780	1	*L. secunda*	-40.040	178.145	814
Hikurangi region	26789	1	*Leiopathes* spp.	-39.545	178.331	803
Hikurangi region	26790	1	*L. secunda*	-39.545	178.331	803
Hikurangi region	26795	1	*L. secunda*	-40.039	178.144	765
Hikurangi region	26805	1	*L. secunda*	-39.543	178.337	817
Hikurangi region	26806	1	*L. secunda*	-39.543	178.337	817
Hikurangi region	26807	1	*L. secunda*	-39.543	178.337	817
Hikurangi region	26815	1	*L. secunda*	-39.547	178.329	798
Hikurangi region	71035	1	*L. secunda*	-41.070	176.658	934
Hikurangi region	76706	1	*Leiopathes* spp.	-40.935	176.732	920
Hikurangi region	86495	1	*L. secunda*	-38.530	178.844	886
Kermadec Ridge region	19734	1	*Leiopathes* spp.	-34.282	179.670	742
Kermadec Ridge region	64334	1	*L. secunda*	-34.758	179.431	855
Kermadec Ridge region	64839	1	*Leiopathes* spp.	-35.350	178.546	1180
Kermadec Ridge region	72935	1	*Leiopathes* spp.	-35.857	178.448	1349

APPENDIX 2: Detailed methods

Choice of molecular markers

To maximise efficiency, to be sure we would obtain usable results, and to examine several VME indicator species simultaneously, we decided to use pre-existing genetic resources rather than risk time and costs developing techniques *de novo*. We therefore used DNA sequence and microsatellite primers already published from studies of related corals.

Laboratory-based molecular methods

DNA Extraction

Coral tissue was removed from each individual cup (calyx) using forceps (stony corals) or small snippets of colony were removed (black corals) and total DNA was extracted using a Geneaid dnature genomic DNA mini kit (Geneaid Biotech Ltd.) following the manufacturer's instructions. In the case of *D. dianthus*, specimens collected as clusters were labelled individually so that each DNA extract could be traced to an individual coral cup, and for *E. rostrata* the colony fragments were preserved in individual tubes post-extraction.

Marker Amplification

DNA sequences were obtained from the internal transcribed spacer (ITS) regions for *D. dianthus* and *E. rostrata*, and from the 16S mitochondrial and the mitochondrial ND5 and TRP intergenic regions for *B. patula* (primers and PCR profiles outlined in and modified from White et al. 1990, Thoma et al. 2009, and through personal communication with Dr Mercer Brugler at The American Museum of Natural History). DNA sequences were also sequenced by Macrogen Inc. (South Korea). Microsatellite primer sequences and polymerase chain reaction (PCR) amplification profiles are outlined in Zeng et al. (2017) and Miller & Gunasekera (2017) for *D. dianthus*, and in Ruiz-Ramos et al. (2015) for *Leiopathes* spp. Microsatellite PCR products were combined into multiplexes (PCR products from several primer sets with distinguishable fluorescent dyes were mixed in a single tube for analysis) and genotyped via fragment analysis by Macrogen Inc.

Tests of Marker Utility

A variety of different genetic loci (both mitochondrial and nuclear DNA sequences) and polymorphic microsatellites (nuclear DNA) were examined initially for each species. We sought to determine which primers would successfully amplify the DNA of archived material of varying quality and age and then, if successful amplification was achieved, to see which markers had enough variability amongst individuals to prove effective in differentiating amongst populations. We sequenced and tested several genes (Table 1). We also attempted to sequence introns, which are non-coding genomic regions that are not subject to selective constraints and as such have the potential to be highly variable between individuals. Three primer sets from one group of introns, called EPIC (exon-primed intron crossing) loci (loci il, i22 and i34 in Gérard et al. 2013), were selected and tested, given their utility in cnidarians including *Lophelia pertusa*, an Atlantic deep-sea coral closely related to *D. dianthus* (Gérard et al. 2013). Consistently poor amplification resulting in unreadable DNA sequences prevented us from pursuing these loci further. We also tried testing primers targeting the nuclear genes EF1a (elongation factor one alpha - Aurelle et al. 2011), SRP54 (signal recognition particle 54 - Jarman et al. 2002, Concepcion et al. 2007), and the mitochondrial control region (Miller et al. 2010) but consistently poor amplification (and limited population differentiation for the latter as expected given slowly-evolving cnidarian mitochondrial genomes) again resulted in abandonment of these loci. Instead, we sequenced the nuclear internally transcribed spacer (ITS) region based upon its previous utility in differentiating *D. dianthus* populations by depth, its higher amplification success rate relative to mitochondrial genes in preserved coral material, its relatively high haplotypic diversity, and the availability of public data

from the New Zealand region (Miller et al. 2010, Miller et al. 2011). The ITS region amplified reasonably well in both *D. dianthus* and *E. rostrata.* For *D. dianthus*, we sequenced this region first, and obtained data for approximately 150 individuals prior to microsatellite primers becoming available to us part way through our study; therefore for *D. dianthus*, we had two datasets, with the DNA sequence (ITS) dataset being about half of the size of the microsatellite dataset and obtained from different individuals in the same areas. The microsatellites that we used were developed for the confamilial *S. variabilis* (Zeng 2016, Miller & Gunasekera 2017). Following optimisation of these loci and tests for outliers and aberrant markers (see below), 9 of them were used for *D. dianthus*. These microsatellites did not amplify well for *E. rostrata*; data were therefore restricted to nuclear ITS sequence data for this species (Table 1).

For the antipatharians, we were able to use microsatellite primers developed for Atlantic deep-sea *Leiopathes glaberrima* prior to their publication (Ruiz-Ramos et al. 2015). Eight of the ten loci amplified DNA from *L. secunda*, but not in *B. patula*. We therefore used DNA sequence data for the latter species and three markers worked consistently well: the mitochondrial gene 16S, and two mitochondrial intergenic regions, ND5 and TRP (Thoma et al. 2009, Mercer Brugler, pers. comm).

For the octocoral *Thouarella* spp., we tested two mitochondrial and one nuclear loci (mtMutS, 16S and 28S, respectively, following Taylor & Rogers 2015) with 18 subsampled colonies from a 'bulk' sample of *Thouarella* spp. collected from the Ross Sea. The 28S nuclear gene amplified the least successfully (less than 50% success), but the two mitochondrial genes both amplified well (95% for both). Two specimens were genetically unique, differed significantly from the other samples and did not match any publicly available species-identified DNA sequence data, suggesting that Ross Sea samples may reflect diversity in this genus new to science. However, sequences derived from the remaining specimens could not be reliably ascribed to a species. Coupled with the prohibitive cost of the extensive sequencing efforts required (at least three genes/individual), we did not pursue this genus further.

Validating markers

For *D. dianthus* and *Leiopathes* spp., microsatellites were assessed using the Geneious v8.1 (Biomatters Ltd, New Zealand) software with Gene Scan 500LIZ size standards (Applied Biosystems, Inc.). All DNA sequences were aligned using the ClustalW Alignment plugin in Geneious (gap open cost = 15 and a gap extend cost = 6) and were also checked manually. Unreliable data were discarded.

We tested microsatellite method reliability in several ways for *D. dianthus* using a large dataset (more than 350 individuals, Appendix 1). We used Microchecker v2.2.3 (van Oosterhout et al. 2004) to test for deviation from Hardy-Weinberg Equilibrium (HWE), a genetic model in which frequencies of genetic variants, or alleles, will remain constant between generations in the absence of other evolutionary influences such as migration, mutation or selection. Deviations from HWE can indicate that genetic markers are susceptible to genotyping error. Loci showing evidence of null alleles (alleles which do not amplify by PCR) were discarded. For *D. dianthus*, microsatellites with more than 60 alleles per locus were also discarded because highly variable loci may cause downward biases in fixation indices (F_{ST}) estimates (Olsen et al. 2004, O'Reilly et al. 2004). Fixation indices are used to measure population differences, with the basic theoretical premise that an F_{ST} of zero indicates no difference and a value of 1 indicates completely genetically disparate populations.

Duplicate multilocus genotypes, which can be used as a test of clonality and to determine the extent of asexual reproduction (which results in identical genotypes) were tested for in GenAlEx 6.502 (Peakall & Smouse 2012). Next, we tested for linkage disequilibrium (LD, non-random association of alleles which can cause spurious results) using permutation tests implemented in Genepop v4.2 (Raymond & Rousset 1995). No LD was found consistently between pairs of loci in all populations and therefore no loci were discarded on this basis. We then used the software LOSITAN (Antao et al. 2008) and BAYESCAN (Foll & Gaggiotti 2008) to confirm the neutrality of the loci (i.e., to make sure our loci were not under evolutionary selection which can violate some assumptions of neutrality in downstream tests). LOSITAN identifies outlier loci by comparing the expected distribution of Wright's coefficient

of pairwise population differentiation (F_{ST}, Wright 1922) with expected heterozygosity (H_E) under an island model of migration (with neutral markers), identified as those with aberrantly high or low F_{ST} values compared to neutral expectations. LOSITAN settings followed 100 000 simulations, with "Neutral mean F_{ST}" and "Force mean F_{ST}" options selected, a 95% confidence interval and false discovery rate correction set at 0.1 for both infinite alleles (IAM) and stepwise mutation (SMM) models. BAYESCAN is a Bayesian approach in which subpopulation allele frequencies are correlated through a common migrant gene pool from which they differ, assuming that gene frequencies under any neutrally structured population model can be approximated by a multinomial Dirichlet distribution. BAYESCAN parameters were set with a 50 k burn-in period, a thinning interval of 10 with a 100 k sample size, and 20 pilot runs with 50 k iterations each and default model parameters. Based upon these combined results, the *D. dianthus* dataset was split into a putatively 'neutral' dataset (5 loci) and an 'all loci' dataset (9 loci) which also included those loci potentially under selection. We did not discard the possibly-under-selection loci because some software packages are not sensitive to deviations from neutrality and because non-neutral loci may provide additional information (e.g., Wei et al. 2013a;,Gagnaire et al. 2015, Zeng et al. 2017). As such, some analyses were carried out twice, with the neutral and all loci datasets, to determine to what extent the connectivity patterns we observed were a function of the markers considered. Generally, as results were similar between the two, only the all loci dataset results are reported (differences between the results obtained from the two datasets are highlighted).

For *Leiopathes* spp., microsatellite amplification was successful in a total of only 53 individuals. Further validation testing was not continued further.

Data partitioning into spatial frameworks

We employed a spatial hypothesis testing framework and divided samples at three levels according to their collection location prior to genetic analyses. This division scheme was considered to be at spatial scales relevant to marine spatial planners, it can address the effect of various environmental features on connectivity, and it allows us to compare results to complementary research (Zeng et al. 2017). This scheme had three levels; firstly, the lower-bathyal biogeographic provinces (henceforth bioprovinces) identified by Watling et al. (2013), with samples assigned to BY6 (New Zealand-Kermadec, including the Chatham Rise and the Louisville Seamount Chain), BY10 (sub-Antarctic), and in the case of *B. patula*, BY9 (Antarctic); henceforth 'northern', 'southern' or 'Antarctic'. Secondly, we further divided the EEZ into three regions, to recognise the Chatham Rise, an area of mixing and/or high biodiversity. The three regions, namely 'north' (north of the Chatham Rise), 'central' (the Chatham Rise) and 'south' (south of the Chatham Rise) with boundaries at latitudes 42° S and 45° S. Finally, samples were assigned to various geomorphic features that comprise parts of the seascape of the New Zealand EEZ (Appendix 1).

Following Zeng et al. (2017) we defined a 'population' as a minimum of four individuals from the same site or from sites within close proximity. For *B. patula*, the distribution of our samples meant that this definition could not be met under any scheme except the provincial level, so the data were analysed as northern, (including the Chatham Rise), southern (Campbell Plateau, Macquarie Ridge, Tasmania) and Antarctic provincial scales, as outlined above (south of mainland New Zealand but north of the Ross Sea). For the *Leiopathes* dataset, microsatellite amplification was successful for only 53 individuals, which comprised a mix of *L. secunda, L. bullosa*, and some specimens identified only to genus level. *Leiopathes* specimens were collected from waters around the North Island only, prohibiting the division of them into provincial or regional scales, and as such analyses of these species were based on populations on geomorphic features only. To meet the minimum population size threshold of four individuals after assigning samples to a geomorphic feature, the dataset was further reduced to 46 individuals when all *Leiopathes* species were combined, and 28 individuals when considering *L. secunda* alone. We also used our microsatellite data to explore taxonomic division within the genus and to determine whether microsatellite signatures could prove useful to delineate species or MOTUs - genetic entities defined with the intent of representing biological species in the absence of species descriptions (e.g., Niegel et al. 2007).

Population genetics

The *D. dianthus* microsatellite and ITS datasets were by far the largest numerically. Analyses conducted are therefore far more comprehensive for this species, as these data facilitated greater data exploration than the other datasets. Therefore, the following section always refers to *D. dianthus*, and to the other three species only where indicated.

Population differentiation

The most common way to infer the extent of connectivity (and thus gene flow) is to compare variation in allele frequencies amongst populations and then to describe the correlation between two randomly chosen alleles within subpopulations relative to two alleles randomly sampled from the total population. This is calculated using Wright's *F*-statistics and gene flow is summarised by the equation $F_{ST} = 1/(4Nm +1)$, where Nm represents the number of immigrants entering a subpopulation in each generation (N = local subpopulation size, m = the proportion of immigrants), and the expected divergence is a function of the number of immigrants, Nm (Wright 1951, Lowe & Allendorf 2010). If a locus with two alleles (one from each parent) is considered in two subpopulations, F_{ST} (an estimate of genetic difference or distance) will attain a value of one if the subpopulations contain different alleles (e.g., allele *a* in population 1 and allele *b* in population 2), and zero if the allele frequencies in both subpopulations are identical. Put simply, F_{ST} values are estimates of genetic distance and they vary between zero and one, with zero signifying no differentiation and one representing completely disparate populations (Balloux & Lugon-Moulin 2002).

For *D. dianthus*, Analysis of Molecular Variance (AMOVA, Arlequin v3.5, Excoffier & Lischer 2010) was used to test for hierarchical spatial structure and the p-values (significance levels) associated with each spatial scale (bioprovince, region, geomorphic feature) were obtained for the neutral and all loci microsatellite datasets, and from the ITS sequence data. Subsequently, to assess the extent of population differentiation between/amongst populations within this scheme, we calculated conventional pairwise F_{ST} values for microsatellites (Wright 1951, Weir & Cockerham 1984) and its analogue, Φ_{ST}, for ITS sequence data.

For *E. rostrata* and *B. patula*, Φ_{ST} (an analogue of F_{ST} based upon DNA sequence data) was calculated from ITS data and concatenated 16S-ND5-TRP DNA sequence data respectively, whereas *Leiopathes* data were derived from microsatellites (and therefore F_{ST} was calculated). In the case of *E. rostrata*, the patchy distribution of samples resulted in difficulty meeting the minimum population size threshold of four individuals, so to permit analysis of data from this species minimum population sizes less than 4 have been used on some occasions. For example, three geomorphic features were represented by only two individuals (the Kermadec Ridge region, the Norfolk Ridge, and the Challenger Plateau). Therefore, a very cautious interpretation of these data is warranted at the geomorphic features scale.

Genetic diversity

To assess genetic diversity at each of the three spatial scales, we measured allelic richness (the average number of alleles at a given locus) from the microsatellite data, followed by nucleotide and haplotypic diversity (the average number of nucleotide differences per site between any two sequences and the probability that two randomly chosen haplotypes are different, respectively) from the DNA sequence data. Rarefied allelic richness and private allelic richness (the number of unique alleles in a population, Kalinowski 2004) were calculated in HP-Rare (Kalinowski 2005), setting the minimum gene sampling number at 16 and 6 for the regional and geomorphic features data respectively (reflecting values at or close to the minimum number of alleles observed). For geomorphic features, measures of allelic richness were calculated from eight microsatellite loci, because one locus did not amplify in any *D. dianthus* individuals sampled from the Campbell Plateau or the Macquarie Ridge and was therefore removed from this analysis. Nucleotide and haplotypic diversity were calculated in DNASp v.5 (Librado & Rozas 2009).

Identifying genetic clusters

Discriminant analysis of principle components (DAPC) was performed to identify population clusters based on microsatellite variation, as implemented in R 3.0.2 (R Development Core Team 2013) with the ADEGENET software v. 1.3 (Jombart 2008, Jombart et al. 2010). This multivariate analysis first partitions sample variance into between-group and within-group components based upon an initial principal component analysis (PCA), after which a discriminant analysis (DA) identifies clusters using the PCA factors as variables to maximise the intergroup component of variation, making no assumptions about the evolutionary structure of the samples.

To identify clusters at spatial levels deemed significant in AMOVA analyses (i.e., at regional scales and between geomorphic features), microsatellite data were tested using STRUCTURE v2.3.4 (Pritchard et al. 2000), a model-based Bayesian clustering approach in which individuals are probabilistically assigned to a known or unknown population (K) based upon shared allele frequencies. Convergence was verified by graphing MCMC progress *a posteriori* (log alpha) and optimal K values from all simulations were derived with the correction of Evanno et al. (2005), which plots the log probability [L(K)] of the data and compares it to delta K, as implemented in STRUCTURE HARVESTER (Earl & von Holdt 2012). STRUCTURE assumes HWE, but not linkage disequilibrium (LD), and works best when population sample sizes are approximately equal. Adjustment for different population sample sizes is possible (Wang 2017), and has been employed here, where appropriate. For comparison, cluster analyses were also performed using AWclust v3.0 (Gao & Starmer 2008), a non-parametric approach without any prior assumptions about HWE or LD. Because this software (implemented in RStudio open source software v1.0.13) is a platform for the analysis of SNP datasets, microsatellite alleles were coded as either homozygotes (the same copy from both parents), heterozygotes (different copies from each parent) or absent following Wei et al. (2013a). Gap statistics were calculated from K=1–10.

Inferring demographic population changes

We used several approaches to test for population growth. We compared observed pairwise sequence difference distributions in ITS sequence data to expected values (the mismatch distribution) under both constant population size (at equilibrium) and growing/declining population models, using DNASp v.5 (Librado & Rozas 2009). In both scenarios, no recombination was specified, and for the latter scenario, initial and final Θ (theta - before and after the growth or decline respectively) and T (tau) values were determined according to Rogers & Harpending (1992). The Ramos-Onsins and Rozas R2 test, which detects recent pronounced population growth based upon the number of singleton mutations and the average number of nucleotide differences, was also calculated (Ramos-Onsins & Rozas 2002). Its significance was estimated using coalescent methods for no recombination, recombination rates estimated from the data and free recombination models. The raggedness statistic r (Harpending 1994), which relates to the shape of the mismatch distribution and differs between constant size and growing populations, was also calculated. Fu's F (Fu 1997) Fu and Li's F test (Fu & Li 1993) and Tajima's D (Tajima 1989) tests were used to assess neutrality, based upon the haplotype (gene) frequency distribution conditional upon the value of the population size parameter Θ, and upon the differences between the number of segregating sites and the average number of nucleotide differences, respectively.

The neutral microsatellite loci were tested for genetic bottlenecks using the program BOTTLENECK v1.2.02 (Cornuet & Luikart 1996). This software tests whether heterozygosity is temporarily increased relative to the number of alleles at mutation-drift equilibrium (Cornuet & Luikart 1996). The Campbell Plateau and Macquarie Ridge samples were not analysed in the geomorphic features dataset because the program requires at least 10 individuals per population. The data were tested with three mutation models, the infinite alleles (IAM), the stepwise mutation (SMM) and the two-phase models (TPM) with the latter allowing a 10% proportion of SMM following the authors' recommendations for microsatellites. Sign tests and one-tailed Wilcoxon sign rank tests (heterozygote excess and deficiency calculations) determined P (significance) values from 1000 iterations for the likelihood of a bottleneck for each population. Finally, the relative distribution of allele frequencies (mode-shift indicator) was tested, because a reduction in alleles at low frequencies distorts allele frequency distributions in recently bottlenecked populations (Luikart et al. 1998).

Assessing contemporary and historical connectivity, and effective population size

We used two approaches to determine the extent and direction of gene flow between populations associated with geomorphic features, using the *D. dianthus* microsatellite neutral (n=5) and all loci (n=9) datasets. We focussed on these datasets only for these analyses, due to their increased robustness (in terms of sample sizes obtained from each feature) relative to the other species and to permit exploration in more depth of the temporal and directional patterns of migration between the Kermadec Ridge region and the Louisville Seamount Chain indicated in prior analyses (note that where AMOVA results revealed no significant difference at the bioprovince and/or at the regional spatial scales, these same spatial scales were not tested in the analyses described below). Contemporary gene flow (i.e., over the last few generations) was assessed using BayesAss v3.0.4 (Wilson & Rannala 2003), which employs a Bayesian approach to estimate the fraction of migration between populations without assuming HWE (Excoffier & Heckel 2006). Historical gene flow was determined using Migrate-n v3.6.11 (Beerli & Felsenstein 2001, Beerli 2008), which uses a coalescent approach to determine the population size parameter θ (*theta* = 4*Ne* μ, where *Ne* is the effective population size and μ is a constant per-locus mutation rate per site) and migration rate (*M* / μ, where *M* is the immigration rate per generation). The parameter m, the proportion of each population consisting of migrants per generation, can be generated and compared between the software package outputs. We estimated m directly in BayesAss and subsequently derived it from Migrate-n *M* values following Chiucchi & Gibbs (2010) with a mutation rate of 5×10^{-4} (Garza & Williamson 2001). Both the neutral and all loci microsatellite *D. dianthus* datasets were analysed with BayesAss and Migrate-n. Subsequently, θ values derived from Migrate-n were converted into effective population size values (*Ne* = θ/4 μ) assuming several hypothetical microsatellite mutation rates; actual mutation rates for each locus used in this study are unknown and generally microsatellite mutation rates vary between 10^{-2} and 10^{-6} (Li et al. 2002). Results were plotted into chord diagrams to facilitate visualisation of migration pathways using the 'circlize' package in R (Gu et al. 2014). We also estimated contemporary effective population sizes (i.e., estimates applying to the time-period encompassed by the sampling period, *Ne*) at the regional and geomorphic features scales (but not at the bioprovince scale because the AMOVA was not statistically significant) as implemented in NeEstimator V2 (Do et al. 2014, following Waples & Do 2010). Parametric confidence intervals were estimated.

Seascape genetics

To determine the effect of environmental factors (Table 2) on genetic differentiation, we examined correlations between environmental variables at sample sites and F_{ST} estimates derived from microsatellite data for *D. dianthus* and Φ_{ST} for *E. rostrata.* The spatial testing framework employed in prior genetic analyses was not used for seascape analyses, primarily because the geographic extent of sampling at bioprovince and region scales was larger than the scale of differences between environmental variables (and thus could lead to confounding results). Instead, samples were assigned to a population if collected from the same site or from sites in close proximity, with a minimum sample size set at four individuals, and samples were not pooled as before. For the black corals, no more than one specimen was collected at any site or from sites in close proximity and the minimum threshold of four individuals could not be met (Appendix 1). Furthermore, sample sizes were small for each dataset and there was an overall lack of significant genetic structure in the *Leiopathes* dataset. Therefore, seascape genetics analyses focussed on the two scleractinians only. For *D. dianthus,* twenty putative populations were obtained across the sampled range (i.e., from the EEZ to the Louisville Seamount Chain, Appendix 3). For *E. rostrata,* only four putative populations met the minimum sample size threshold and these were all on the Chatham Rise, although each had different environmental variable values (see Table 2 and Appendix 3 for environmental variables for each dataset).

We used a generalised linear model (GLM) as implemented via the GLZ routine in STATISTICA v7.1 (StatSoft, Inc). This approach is a multiple regression analysis between a dependent variable (in this case the mean multilocus F_{ST} or Φ_{ST} for each population which we derived from all pairwise values per population following Wei et al. (2013a) and a combined set of biological, topographical and physicochemical environmental variables (Appendix 3). GLM analyses employed a stepwise approach to build models that were then ranked according to the Akaike Information Criterion (AIC, with the

best fit model having the lowest AIC penalty score at a significance level of $p < 0.05$). We then used maximum likelihood ratio tests to assess the contribution of each variable to the model and to test the significance of a particular effect with all the other effects in the model (i.e., incrementally). The resulting χ^2 statistic indicates change in the log-likelihood attributable to each individual effect.

Larval dispersal models

To compare genetic connectivity patterns revealed by the genetic analyses, and to better understand the environmental factors potentially contributing to these patterns revealed by the seascape genetics analyses, we predicted likely larval trajectories using current modelling. Predicting potential routes of larval movement on a site-by-site basis is a useful approach to determine potential connectivity pathways between or amongst specific regions or geomorphic features. We modelled float trajectories from the Global Drifter Program (GDP) (http://www.aoml.noaa.gov/phod/dac/gdp_information.php) and from the ARGO program (http://www.argo.ucsd.edu/), to predict (respectively) potential distances that larvae may move via surface and deep (1000 m) currents for a range of user-defined PLDs specified for 'virtual' larvae (in this approach, coral larvae are treated as passive particles for dispersal, with no ability to influence the direction or rate of dispersal). We initially used seven PLD periods between 0–70 days (in ten-day increments), but after preliminary runs, we changed this to four PLDs of 0–10 days, 30–40, 90–100 days and 150–200 days, given the high connectivity observed in our preliminary genetic data and the possibility that scleractinian larvae may survive for as long as 195–244 days (Graham et al. 2008).

APPENDIX 3: *Desmophyllum dianthus* microsatellite data exploration.

Left: heat maps illustrating the extent of missing data by locus and population for regional scale (top) and geomorphic features (bottom) analysis. Right: Genotype accumulation curve box and whisper plot showing the minimum number of loci necessary to discriminate between individuals in a population given a random sample of *n* loci as calculated with the R package poppr (Kamvar et al. 2014).

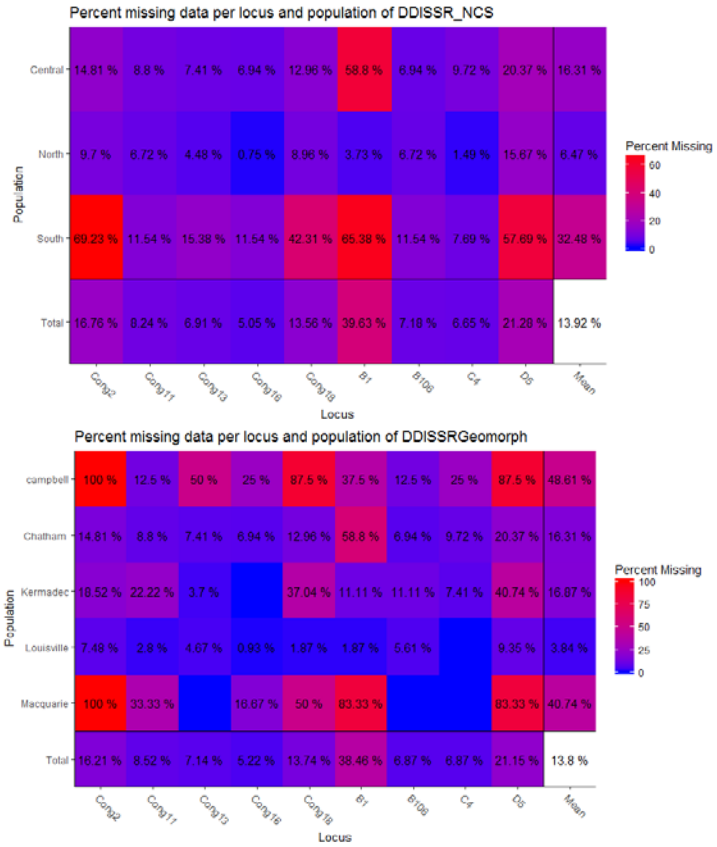

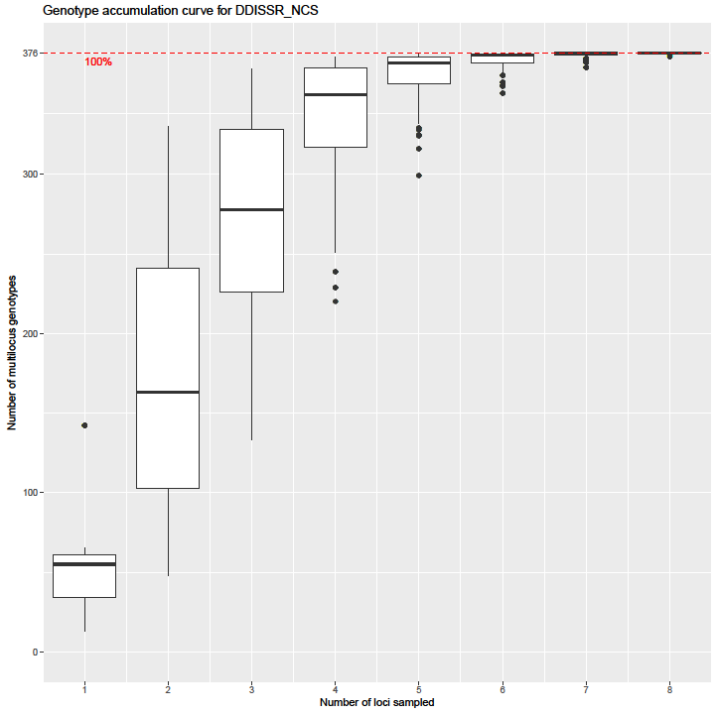

APPENDIX 4: Sample information, F_{ST} matrix and environmental correlates for *Desmophylum dianthus* seascape genetics analyses and sample information, Φ_{ST} matrix and environmental correlates for *Enallopsammia rostrata* seascape genetics analyses.

Desmophylum dianthus

						bpi-broad	bpi-fine	depth	aragonite	calcite	oxygen	POC	salinity	sigma-theta	silicate	slope-percent
Population	**NIC Cat. #**	**N**	**Lat**	**Lon**	**Fst**											
Forde	94103	23	-35.337	-170.443	0.05	669.00	380.00	-1335.00	0.98	1.52	3.98	5.81	34.50	31.98	57.99	26.60
Anvil	94297	4	-37.707	-169.015	0.07	237.00	202.00	-626.00	1.49	2.34	5.15	11.88	34.47	31.44	10.30	3.10
39south	94377	67	-39.164	-167.350	0.13	168.00	126.00	-678.00	1.44	2.26	5.09	12.22	34.46	31.47	10.30	4.48
ValerieSouth	94569	10	-41.582	-164.255	-0.02	371.00	242.00	-723.00	1.40	2.19	5.00	11.02	34.45	31.49	12.88	4.38
ValerieNorth	94623	4	-41.365	-164.419	-0.08	371.00	242.00	-723.00	1.40	2.19	5.00	11.02	34.45	31.49	12.88	4.38
Kermadec_south	16021	8	-36.828	177.448	0.21	751.00	514.00	-1378.00	0.97	1.52	4.03	5.00	34.47	31.94	58.40	5.50
Kermadec_top	65022	6	-35.284	178.863	0.02	808.00	489.00	-1448.00	0.94	1.46	3.91	4.70	34.50	32.02	68.04	10.89
Kermadec_mid	72943	14	-35.857	178.448	0.04	14.00	2.00	-365.00	1.71	2.69	5.67	37.04	34.49	31.38	7.46	0.11
Iceberg_119	54285	19	-44.158	-174.555	0.09	-65.00	-73.00	-274.00	2.08	3.25	5.58	39.22	34.86	31.24	4.97	3.97
Iceberg_102469	102469	48	-44.160	-174.555	0.17	54.00	9.00	-629.00	1.56	2.45	5.45	14.04	34.49	31.45	8.69	1.78
Iceberg_102485	102485	24	-44.160	-174.555	0.24	2641.00	316.00	-1070.00	1.11	1.73	4.56	2.05	34.37	31.75	30.77	6.36
Iceberg105	53838	11	-44.157	-174.554	0.15	1792.00	278.00	-1309.00	0.93	1.45	4.00	2.70	34.43	31.99	59.73	22.73
Diamond C	53581	9	-44.147	-174.690	0.27	1438.00	52.00	-921.00	1.21	1.90	4.82	3.63	34.37	31.62	25.49	2.86
Diamond a	53720	6	-44.140	-174.720	0.01	1767.00	540.00	-1253.00	1.00	1.57	4.41	2.96	34.37	31.88	44.78	13.00
Diamond A	102571	44	-44.136	-174.720	0.29	1282.00	121.00	-1391.00	0.95	1.48	4.17	3.38	34.40	31.96	53.01	10.97
Diamond B	102636	47	-44.148	-174.748	0.24	556.00	43.00	-460.00	1.75	2.74	5.45	18.11	34.63	31.38	7.00	2.80
N&W Chatham	75946	8	-43.617	178.500	0.01	393.00	241.00	-657.00	1.45	2.27	5.08	10.96	34.46	31.46	10.27	3.22
South_mid	88873	12	-46.797	167.388	0.09	393.00	241.00	-657.00	1.45	2.27	5.08	10.96	34.46	31.46	10.27	3.22
Macquarie Ridge	95101	6	-47.000	165.700	0.04	168.00	126.00	-678.00	1.44	2.26	5.09	12.22	34.46	31.47	10.30	4.48
South_south	88899	8	-49.017	166.517	0.01	189.00	168.00	-660.00	1.44	2.26	5.09	12.54	34.46	31.47	10.31	5.10

	seamount	stdev-slope	temperature	woanitc	woaphosc	bathy1km	arag1km	botspd1km	calc1km	cdom1km	disorg1km	dynoc1km	smt1km	sstgrd1km	sst1km	tempbot1km	tempres1km	tidcurr1km	vgpm1km
Population																			
Forde	1.00	5.43	4.16	34.65	2.37	1419.15	0.98	0.07	1.53	1.79	0.02	0.66	1.00	0.00	0.00	0.27	0.25	0.07	545.53
Anvil	1.00	3.02	7.59	30.74	2.07	738.56	1.07	0.05	1.67	2.21	0.04	0.53	1.00	0.01	0.01	0.27	0.26	0.14	530.89
39south	1.00	2.54	7.38	30.73	2.07	739.51	1.07	0.05	1.67	2.16	0.04	0.53	1.00	0.01	0.01	0.26	0.26	0.14	533.49
ValerieSouth	1.00	2.98	7.20	29.36	1.97	722.59	1.14	0.07	1.79	2.19	0.04	0.53	1.00	0.01	0.01	0.28	0.29	0.13	523.97
ValerieNorth	1.00	2.98	7.20	29.36	1.97	722.59	1.14	0.07	1.79	2.19	0.04	0.53	1.00	0.01	0.01	0.28	0.29	0.13	523.97
Kermadec_south	1.00	4.97	4.25	35.97	2.55	1489.71	0.78	0.10	1.20	1.80	0.02	0.72	1.00	0.00	0.00	0.24	0.24	0.11	478.42
Kermadec_top	1.00	5.10	3.89	34.75	2.41	1530.09	0.81	0.08	1.25	1.82	0.02	0.74	1.00	0.00	0.00	0.35	0.35	0.10	494.04
Kermadec_mid	0.00	0.05	8.02	14.66	1.07	416.15	1.73	0.05	2.72	2.23	0.09	0.46	0.00	0.01	0.03	-1.00	-1.00	0.51	725.74
Iceberg_119	0.00	1.78	10.33	11.49	0.78	152.71	2.22	0.05	3.48	2.57	0.07	0.43	0.00	0.01	0.01	0.74	0.68	0.16	744.06
Iceberg_102469	0.00	0.29	7.62	14.57	1.21	527.30	1.75	0.06	2.75	1.50	0.04	0.45	0.00	0.02	0.04	-0.19	-0.21	0.53	380.65
Iceberg_102485	1.00	6.43	5.10	30.05	2.04	-9999.00	-9999.00	-9999.00	-9999.00	-9999.00	-9999.00	-9999.00	-9999.00	-9999.00	-9999.00	-9999.00	-9999.00	-9999.00	-9999.00
Iceberg105	1.00	9.48	3.66	31.71	2.08	-9999.00	-9999.00	-9999.00	-9999.00	-9999.00	-9999.00	-9999.00	-9999.00	-9999.00	-9999.00	-9999.00	-9999.00	-9999.00	-9999.00
Diamond C	1.00	0.85	5.96	28.31	1.79	-9999.00	-9999.00	-9999.00	-9999.00	-9999.00	-9999.00	-9999.00	-9999.00	-9999.00	-9999.00	-9999.00	-9999.00	-9999.00	-9999.00
Diamond a	1.00	5.61	4.17	34.32	2.38	-9999.00	-9999.00	-9999.00	-9999.00	-9999.00	-9999.00	-9999.00	-9999.00	-9999.00	-9999.00	-9999.00	-9999.00	-9999.00	-9999.00
Diamond A	1.00	2.96	3.73	34.04	2.30	-9999.00	-9999.00	-9999.00	-9999.00	-9999.00	-9999.00	-9999.00	-9999.00	-9999.00	-9999.00	-9999.00	-9999.00	-9999.00	-9999.00
Diamond B	0.00	0.87	8.63	16.80	1.35	489.49	1.74	0.05	2.72	1.81	0.06	0.46	0.00	0.01	0.02	0.08	0.08	0.26	554.23
N&W Chatham	1.00	3.28	7.40	29.36	1.97	722.59	1.14	0.07	1.79	2.19	0.04	0.53	1.00	0.01	0.01	0.28	0.29	0.13	523.97
South_mid	1.00	3.28	7.40	29.36	1.97	722.59	1.14	0.07	1.79	2.19	0.04	0.53	1.00	0.01	0.01	0.28	0.29	0.13	523.97
Macquarie Ridge	1.00	2.54	7.38	30.73	2.07	877.48	1.07	0.05	1.67	2.15	0.04	0.53	1.00	0.01	0.01	0.27	0.28	0.14	533.81
South_south	1.00	2.35	7.38	30.73	2.07	741.61	1.06	0.05	1.66	2.13	0.04	0.53	1.00	0.01	0.01	0.23	0.22	0.15	537.57

	Forde	Anvil	39south	ValerieS	ValerieN	Kerm_So	Kerm_to	Kermade	Iceberg11	I116_102	I116_102	Iceberg1(	Diamond	Diam_a	Daim_A	Diamond	N&Wcha	MidSoutl	Macquari	SouthSou
Forde	0.000																			
Anvil	0.043	0.000																		
39south	0.014	0.039	0.000																	
ValerieSouth	0.018	0.063	0.019	0.000																
ValerieNorth	0.038	0.069	0.027	0.039	0.000															
Kerm_South	0.059	0.079	0.036	0.066	0.078	0.000														
Kerm_top	0.060	0.068	0.030	0.065	0.066	0.035	0.000													
Kermadec	0.017	0.045	0.010	0.023	0.026	0.047	0.047	0.000												
Iceberg119	0.211	0.231	0.177	0.218	0.219	0.188	0.193	0.196	0.000											
I116_102469	0.171	0.188	0.140	0.174	0.178	0.147	0.157	0.157	0.015	0.000										
I116_102485	0.159	0.180	0.132	0.161	0.158	0.149	0.156	0.146	0.031	0.015	0.000									
Iceberg105	0.190	0.212	0.159	0.196	0.195	0.174	0.182	0.176	0.025	0.018	0.023	0.000								
DiamondC	0.175	0.201	0.145	0.177	0.176	0.160	0.163	0.159	0.054	0.041	0.047	0.060	0.000							
Diamond_a	0.241	0.292	0.206	0.273	0.261	0.251	0.233	0.225	0.163	0.128	0.116	0.150	0.171	0.000						
Daimond_A	0.173	0.199	0.144	0.177	0.178	0.157	0.164	0.161	0.022	0.009	0.013	0.019	0.037	0.125	0.000					
Diamond_B	0.163	0.184	0.134	0.164	0.165	0.142	0.153	0.149	0.025	0.007	0.018	0.022	0.040	0.117	0.008	0.000				
N&Wchatham	0.102	0.144	0.086	0.123	0.124	0.130	0.136	0.093	0.157	0.116	0.116	0.137	0.144	0.171	0.114	0.103	0.000			
MidSouth	0.100	0.117	0.091	0.104	0.109	0.130	0.122	0.110	0.159	0.129	0.104	0.146	0.145	0.200	0.128	0.128	0.144	0.000		
Macquarie	0.308	0.370	0.275	0.353	0.349	0.334	0.311	0.292	0.129	0.124	0.123	0.124	0.159	0.331	0.129	0.133	0.320	0.264	0.000	
SouthSouth	0.222	0.240	0.187	0.222	0.224	0.208	0.210	0.208	0.143	0.128	0.121	0.129	0.167	0.201	0.132	0.130	0.212	0.184	0.226	0.000

Pairwise F_{ST} matrix from which mean values per population were derived for seascape genetics analysis (generated in GenAlEx, Peakall & Smouse 2012).

Enallopsammia rostrata

NIC cat#.	N	Lat	Lon	Mean Φ_{ST}	bpi-broad	bpi-fine	depth	aragonite	calcite	oxygen	POC	salinity	sigma-theta	silicate	slope-perce	seamount	stdev-slope
102565	13	-44.136	-174.720	0.62	168	126	-678	1.444	2.264	5.085	12.219	34.457	31.467	10.301	4.475	1.000	2.538
102631	17	-44.148	-174.748	0.83	189	168	-660	1.444	2.264	5.085	12.544	34.457	31.467	10.305	5.096	1.000	2.345
53483	6	-42.740	-179.690	0.69	11	2	-1098	1.109	1.736	4.344	14.507	34.438	31.796	35.151	1.951	0.000	0.171
53998	14	-44.140	-174.720	0.73	168	126	-678	1.444	2.264	5.085	12.219	34.457	31.467	10.301	4.475	1.000	2.538
NIC cat#.	temperat	woanitc	woaphosc	bathy1km	arag1km	botspd1km	calc1km	cdom1km	disorg1km	dynoc1km	smt1km	sstgrd1km	sst1km	tempbot1kr	tempres1kı	tidcurr1kn	vgpm1km
102565	7.376	30.732	2.066	877.484	1.066	0.050	1.668	2.151	0.041	0.527	1.000	0.006	0.010	0.269	0.285	0.144	533.808
102631	7.376	30.732	2.066	741.608	1.063	0.052	1.663	2.135	0.043	0.525	1.000	0.006	0.010	0.227	0.223	0.145	537.575
53483	5.158	31.575	2.264	1133.835	0.995	0.123	1.556	2.660	0.051	0.532	1.000	0.009	0.018	-0.207	-0.206	0.181	677.839
53998	7.376	30.732	2.066	739.509	1.066	0.051	1.668	2.155	0.042	0.527	1.000	0.006	0.010	0.261	0.261	0.143	533.490

Pairwise Φ_{ST} matrix from which mean values by population were derived for seascape genetics analysis (generated in Arlequin v3.5, Excoffier & Lischer 2010)

	53483	53998	102565	102631
53483	0			
53998	0.68	0		
102565	0.48	0.66	0	
102631	0.91	0.86	0.72	0

APPENDIX 5: *Desmophyllum dianthus* PCA plot of variation in 17 environmental parameters and *Enallopsammia rostrata* PCA plot of variation in 30 environmental parameters.

Desmophyllum dianthus

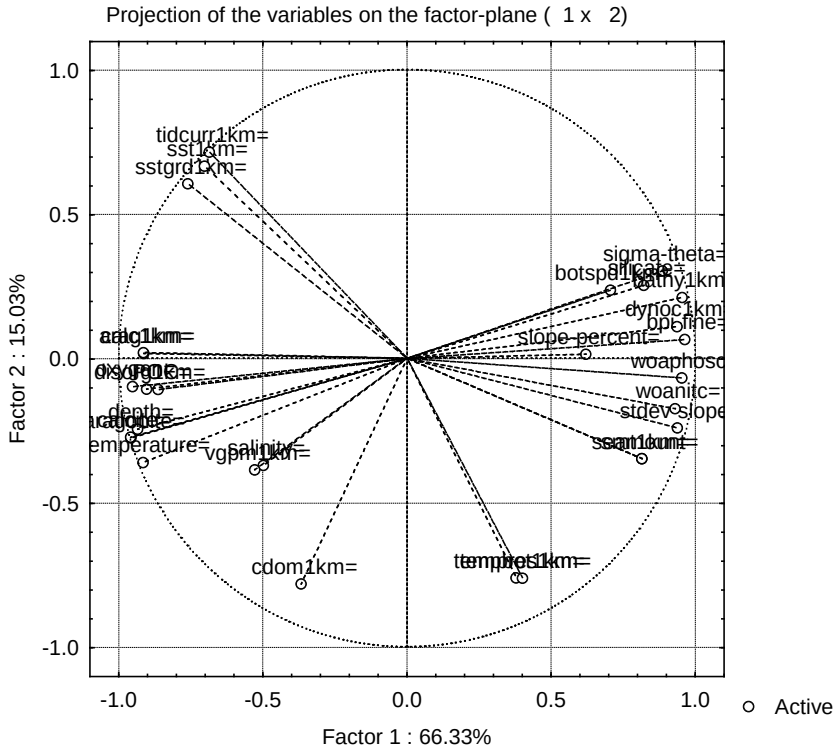

Enallopsammia rostrata

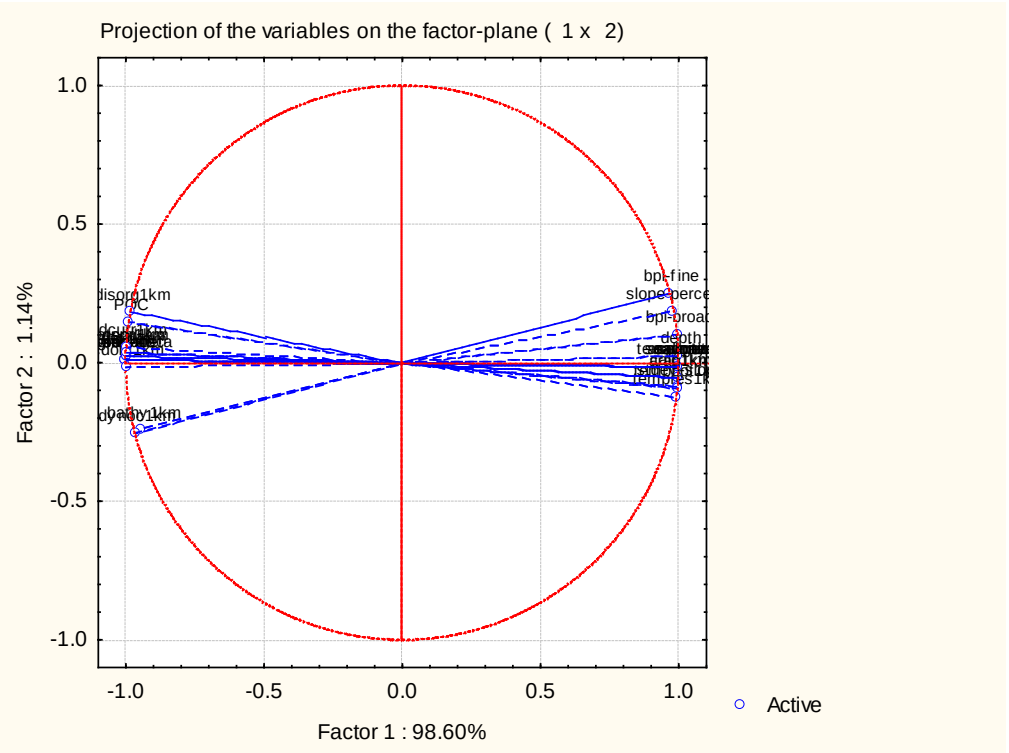

APPENDIX 6: Top 20 best fit GLM models for *Desmophyllum dianthus* based upon 4 individuals in a population (microsatellite data) and for *Enallopsammia rostrata* based upon 4 populations from the Chatham Rise (ITS sequence data).

Desmophyllum dianthus

	Var. 1	Var. 2	Var. 3	Var. 4	Var. 5	Var. 6	Var. 7	Var. 8	Var. 9	Var. 10	Var. 11	Deg. Freedon	AIC	L.Ratio Chi²	p value
1	bpi-broad=	bpi-fine=	aragonite=	POC=	salinity=	slope-percent=	stdev-slope=					7	-63.6771	45.74633	0.000000
2	bpi-broad=	bpi-fine=	aragonite=	POC=	salinity=	silicate=	slope-percent=	stdev-slope=				8	-62.7661	46.83534	0.000000
3	bpi-broad=	bpi-fine=	aragonite=	POC=	salinity=	slope-percent=	stdev-slope=	temperature=				8	-62.1678	46.23705	0.000000
4	bpi-broad=	bpi-fine=	aragonite=	POC=	salinity=	slope-percent=	stdev-slope=	woaphosc=				8	-61.9869	46.05616	0.000000
5	bpi-broad=	bpi-fine=	aragonite=	POC=	salinity=	slope-percent=	seamount=	stdev-slope=				8	-61.7835	45.85271	0.000000
6	bpi-broad=	bpi-fine=	aragonite=	POC=	salinity=	silicate=	slope-percent=	stdev-slope=	woaphosc=			9	-61.0145	47.08380	0.000000
7	bpi-broad=	bpi-fine=	aragonite=	POC=	salinity=	silicate=	slope-percent=	seamount=	stdev-slope=			9	-60.8809	46.95013	0.000000
8	bpi-broad=	bpi-fine=	aragonite=	POC=	salinity=	silicate=	slope-percent=	stdev-slope=	temperature=			9	-60.8380	46.90727	0.000000
9	bpi-broad=	bpi-fine=	POC=	salinity=	slope-percent=	seamount=	stdev-slope=	temperature=				8	-60.7939	44.86320	0.000000
10	bpi-broad=	bpi-fine=	aragonite=	POC=	salinity=	slope-percent=	seamount=	stdev-slope=	woaphosc=			9	-60.5374	46.60661	0.000000
11	bpi-broad=	bpi-fine=	aragonite=	POC=	salinity=	slope-percent=	stdev-slope=	temperature=	woaphosc=			9	-60.4673	46.53659	0.000000
12	bpi-broad=	bpi-fine=	POC=	salinity=	slope-percent=	stdev-slope=	temperature=					7	-60.4156	42.48488	0.000000
13	bpi-broad=	bpi-fine=	aragonite=	POC=	salinity=	slope-percent=	seamount=	stdev-slope=	temperature=			9	-60.3548	46.42402	0.000001
14	bpi-broad=	bpi-fine=	POC=	salinity=	silicate=	slope-percent=	stdev-slope=	temperature=				8	-60.0671	44.13639	0.000001
15	bpi-broad=	bpi-fine=	POC=	salinity=	slope-percent=	seamount=	stdev-slope=	temperature=	woaphosc=			9	-59.6916	45.76081	0.000001
16	bpi-broad=	bpi-fine=	POC=	salinity=	silicate=	slope-percent=	seamount=	stdev-slope=	temperature=			9	-59.6160	45.68523	0.000001
17	bpi-broad=	bpi-fine=	POC=	salinity=	silicate=	slope-percent=	stdev-slope=	temperature=	woaphosc=			9	-59.5183	45.58751	0.000001
18	bpi-fine=	POC=	salinity=	silicate=	slope-percent=	seamount=	stdev-slope=	temperature=	woaphosc=			9	-59.3968	45.46609	0.000001
19	bpi-broad=	bpi-fine=	POC=	salinity=	silicate=	slope-percent=	seamount=	stdev-slope=	woaphosc=			9	-59.3581	45.42738	0.000001
20	bpi-broad=	bpi-fine=	aragonite=	POC=	salinity=	silicate=	slope-percent=	seamount=	stdev-slope=	woaphosc=		10	-59.0880	47.15729	0.000001

Enallopsammia rostrata

	Var. 1	Var. 2	Var. 3	Var. 4	Var. 5	Var. 6	Var. 7	Deg. Freedom	AIC	L.Ratio Chi²	p
1	bpi-broad	dynoc	vgpm					3	-4.40E+12	4.40E+12	0.00E+00
2	depth	dynoc	vgpm					3	-2.20E+12	2.20E+12	0.00E+00
3	slope-percent	dynoc	vgpm					3	-5.03E+07	5.03E+07	0.00E+00
4	POC	dynoc	vgpm					3	-4.19E+06	4.19E+06	0.00E+00
5	bpi-broad	dynoc						2	-1.63E+01	1.31E+01	1.46E-03
6	slope-percent	dynoc						2	-1.54E+01	1.21E+01	2.34E-03
7	depth	dynoc						2	-1.28E+01	9.54E+00	8.48E-03
8	dynoc	vgpm						2	-1.16E+01	8.34E+00	1.55E-02
9	POC	dynoc						2	-1.08E+01	7.50E+00	2.35E-02
10	POC	vgpm						2	-8.82E+00	5.55E+00	6.23E-02
11	bpi-fine	depth						2	-8.62E+00	5.35E+00	6.87E-02
12	bpi-fine	depth	POC					2	-8.62E+00	5.35E+00	6.87E-02
13	bpi-fine	depth	slope-percent					2	-8.62E+00	5.35E+00	6.87E-02
14	bpi-fine	depth	POC	slope-percent				2	-8.62E+00	5.35E+00	6.87E-02
15	bpi-fine	depth	dynoc					2	-8.62E+00	5.35E+00	6.87E-02
16	bpi-fine	depth	POC	dynoc				2	-8.62E+00	5.35E+00	6.87E-02
17	bpi-fine	depth	slope-percer	dynoc				2	-8.62E+00	5.35E+00	6.87E-02
18	bpi-fine	depth	POC	slope-percer	dynoc			2	-8.62E+00	5.35E+00	6.87E-02
19	bpi-fine	depth	vgpm					2	-8.62E+00	5.35E+00	6.87E-02
20	bpi-fine	depth	POC	vgpm				2	-8.62E+00	5.35E+00	6.87E-02